Annular Capillary Surfaces:
Properties and Approximation Techniques

by

James Gordon

A thesis

presented to the University of Waterloo

in fulfilment of the degree of

Master of Mathematics

in

Applied Mathematics

Waterloo, Ontario, Canada, 2007

Author's Declaration

I hereby declare that I am the sole author of this thesis. This is a true copy of the thesis, including any required final revisions, as accepted by my examiners.

I understand that my thesis may be made electronically available to the public.

Abstract

The capillary surface formed within a symmetric annular tube is analyzed. Assuming identical contact angles γ along each boundary, we consider surfaces $u(x, y)$ that satisfy

$$\begin{cases} \nabla \cdot Tu = \kappa u, & \text{in } \Omega \\ \hat{\nu} \cdot Tu = \cos\gamma, & \text{on } \partial\Omega \end{cases}$$

where κ is a positive constant, Ω is an open annular region in $\mathbb{R}^2$ and $\hat{\nu}$ is the exterior unit normal on $\partial\Omega$. Tu is defined as the operator

$$Tu = \frac{\nabla u}{\sqrt{1 + |\nabla u|^2}}.$$

Several qualitative properties of u are determined and in particular, the behaviour of u is examined in the limiting cases of Ω approaching a disk as well as a thin ring. The iterative method of Siegel is also applied to the boundary value problem and convergence is demonstrated under conditions which include $\gamma = 0$. Moreover, some geometries still yield interleaving iterates, allowing for upper and lower bounds to be placed on the boundary values of u. However, the interleaving properties no longer hold universally and for other geometries, another more complex behaviour is described. Finally, a numercial method is designed to approximate the iterative scheme.

Acknowledgements

I would like to thank my supervisor, Prof. David Siegel, for his close guidance in my research over the past two years. This paper would not have been possible without his patience, support and numerous helpful suggestions. Additionally, my gratitude is extended to my fellow Masters students, Scott Sitar and Yasunori Aoki, for all their technical expertise.

This research was supported by the University of Waterloo and by an Ontario Graduate Scholarship.

To my parents, to George and to Sarah:

Thank you for your unwavering support throughout my many pursuits—both finished and unfinished.

Contents

List of Tables

List of Figures

Chapter 1

Background

1.1 Introduction to Capillarity: History and Definitions

Examples of capillary surfaces permeate the natural world. Often they can be observed in the most familiar of occurances like the beading of raindrops on a window pane or the uptake of water by a sponge. Such interfaces are frequently generated whenever solid, liquid and gas come into contact with one another. For a more complete definition of the capillary surface, we turn to Finn:

> [A] capillary surface...describe[s] the free interface that occurs when one of the materials is a liquid and the other is a liquid or gas. In physical configurations...interfaces occur also between these materials and rigid solids; these latter interfaces yield in many cases the dominant influence for determining the configuration [5].

The capillary tube presents the most well known capillary phenomenon–surely we have all dipped a narrow tube in liquid and noted the rise in fluid level within, as Fig. 1.1 illustrates. This geometry can be made precise by considering a cylindrical tube of

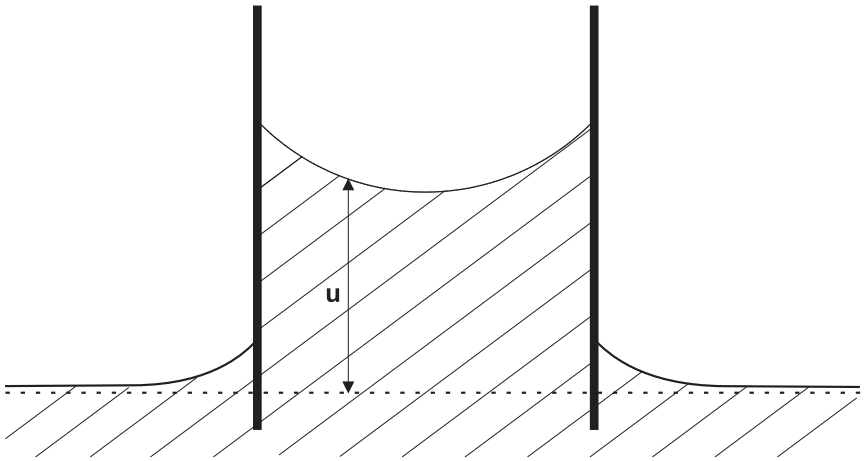

Figure 1.1: Cross section of the capillary tube.

horizontal section Ω immersed vertically in fluid. It was this simple configuration that prompted the first formal mathematical treatment of capillary surfaces to be made by Laplace in 1805 [11]. With contributions by Thomas Young[1], Laplace formalized the idea of mean curvature $H(x, y)$ of a surface $u(x, y)$:

$$H = \frac{(1 + u_y^2)u_{xx} - 2u_x u_y u_{xy} + (1 + u_x^2)u_{yy}}{2(1 + u_x^2 + u_y^2)^{3/2}}. \tag{1.1}$$

He then reasoned that H is proportional to the pressure change across a capillary surface and, using the laws of hydrostatics, this led to

$$2H = \kappa u, \quad \text{in } \Omega \tag{1.2}$$

where u is the height of the surface above the level of atmospheric pressure and κ is a physical constant. In the same year, Young examined the surface tensions arising at capillary interfaces. From this, he devised a force-balancing argument and concluded that, in the absence of frictional forces along a bounding wall, the fluid must meet the wall at a prescribed angle γ, known as the *contact angle* (Fig. 1.2). Young reasoned that γ was dependent on the materials only; the shape of the surface or the boundary

[1]Young is perhaps best known for his work in optics. At the time, he was also a noted Egyptologist.

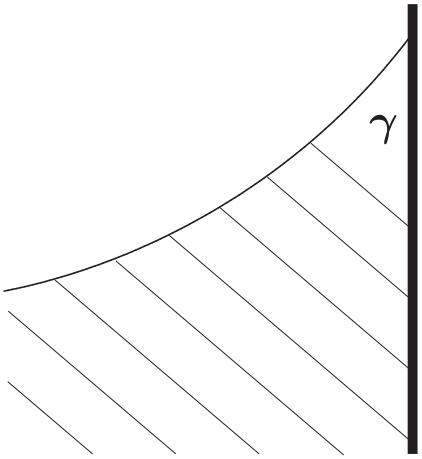

Figure 1.2: Illustration of contact angle.

was not a factor. Consequently, for a cylinder made of a uniform material, Young's requirement leads to the boundary condition

$$\hat{\nu} \cdot Tu = \cos\gamma, \quad \text{on } \partial\Omega; \qquad Tu = \frac{\nabla u}{\sqrt{1+|\nabla u|^2}} \tag{1.3}$$

where $\hat{\nu}$ is the exterior unit normal on the boundary $\partial\Omega$. However, some experts within the field do not view Young's argument as convincing. Very recently, in fact, Finn has created an interesting counterexample [6] and the force-balancing explanation of contact angle remains a disputatious point.

In 1830, Gauss provided an alternate method of describing capillary surfaces by considering the various energies associated with the mechanical system. He postulated that the configured surface must minimize this energy when compared with surfaces that differed by small perturbations. Using a variational argument, Gauss was able to derive both (1.2) and (1.3). Apart from some recent modifications [7], these results have enjoyed wide acceptance, and they found the modern formulation of the capillary surface. It is instructive in our context to present this formulation in terms of the capillary tube; however, Gauss's findings apply to capillary surfaces in general.

Definition 1.1.1 (Capillary Tube) *Consider a cylinder of uniform material and of*

horizontal section Ω *that is immersed vertically in an infinite reservoir of incompressible fluid.* Ω *is defined in the XY–plane and we take the reference level* $Z = 0$ *to be the height of the fluid at a large distance from the cylinder, where perturbations of the liquid within the boundary do not affect the surface height. The capillary surface* $Z = U(X, Y)$ *thus formed over* Ω *can be described by the elliptic boundary value problem*

$$\begin{cases} NU = \kappa U, & \text{in } \Omega \\ \hat{\nu} \cdot TU = \cos\gamma, & \text{on } \partial\Omega \end{cases} \tag{1.4}$$

where $\kappa = \frac{\rho g}{\sigma}$*,* ρ *is the difference in density between the liquid and gas (*$\rho =$ constant *for an incompressible fluid),* g *is the acceleration due to gravity and* σ *is the surface tension. The operator* N *is defined as* $NU := 2H$*, with* $\gamma \in [0, \pi]$ *as the contact angle.*

N.B. NU can also be written as $\nabla \cdot TU$.

1.2 An Overview of Annular Capillary Surfaces

Over the past two hundred years, much progress has been made in describing the nature of the capillary tube. It might seem reasonable that the closely related problem of the annular tube (i.e. Ω is now an annulus) would be the next geometry of study. Amazingly, however, this research is still in its fledgling stage. We begin with a formal exposition of the annular problem. Consider two concentric cylindrical walls possibly made of different materials and having radii R_1 and R_2 ($R_1 < R_2$). These are immersed vertically in an infinite reservoir of fluid. Define $\hat{\Omega}$ in the XY–plane as the cross section between cylinders with $\partial\hat{\Omega}_1$ and $\partial\hat{\Omega}_2$ as the inner and outer boundaries respectively. $\hat{\Omega}$ shall be centred at the origin:

$$\hat{\Omega} = \left\{ (X, Y) \in \mathbb{R}^2 \ : \ 0 < R_1 < \|(X, Y)\| < R_2 < \infty \right\}. \tag{1.5}$$

Extending the results of the previous section, the height of the fluid $U(X,Y)$ between the tubes will satisfy the boundary value problem

$$\begin{cases} NU = \kappa U, & \text{in } \hat{\Omega} \\ \hat{\nu} \cdot TU = \cos\gamma_1, & \text{on } \partial\hat{\Omega}_1 \\ \hat{\nu} \cdot TU = \cos\gamma_2, & \text{on } \partial\hat{\Omega}_2 \end{cases} \tag{1.6}$$

where $0 \leq \gamma_1, \gamma_2 \leq \pi$. Note that we have maintained generality by assuming the contact angle is distinct on each boundary. As will be shown, U can be taken as axisymmetric and hence, the solution can be described in terms of the radial variable only, $U(R)$. (1.6) can now be reduced to a boundary value problem for an ordinary differential equation:

$$\begin{cases} \frac{1}{R}\left(\frac{RU_R}{\sqrt{1+U_R^2}}\right)_R = \kappa U, \quad R_1 < R < R_2 \\ U_R(R_1^+) = -\cot\gamma_1, \quad U_R(R_2^-) = \cot\gamma_2 \end{cases} \tag{1.7}$$

where $(-)_R$ denotes differentiation with respect to R. (1.7) is then non-dimensionalized by introducing the change of variables

$$u = \frac{U}{R_2} \quad \text{and} \quad r = \frac{R}{R_2} \tag{1.8}$$

which gives

$$\begin{cases} \frac{1}{r}\left(\frac{ru_r}{\sqrt{1+u_r^2}}\right)_r = Bu, \quad a < r < 1 \\ u_r(a^+) = -\cot\gamma_1, \quad u_r(1^-) = \cot\gamma_2 \end{cases} \tag{1.9}$$

where $B = \kappa {R_2}^2 > 0$ is known as the *Bond number*. The outer radius of the region is now fixed at 1 with the inner radius $a = \frac{R_1}{R_2}$ such that $0 < a < 1$ (Fig. 1.3). From now on, Ω will be defined as this region:

$$\Omega = \left\{(x,y) \in \mathbb{R}^2 \ : \ a < \|(x,y)\| < 1\right\}. \tag{1.10}$$

As a final step, we define the inclination angle $\psi(r)$ of $u(r)$ as

$$\sin\psi(r) = \frac{u_r(r)}{\sqrt{1+(u_r(r))^2}}. \tag{1.11}$$

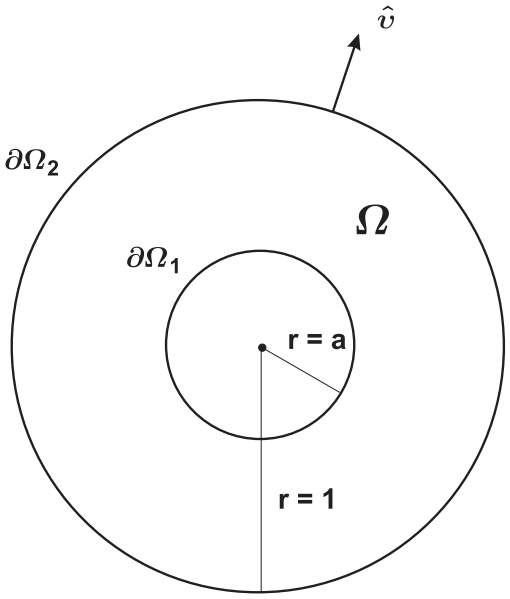

Figure 1.3: Annular region Ω.

Geometrically, $\psi(r)$ is the angle subtended by the tangent of $u(r)$ and the horizontal (see Fig. 1.4). The boundary value problem now attains the form

$$\begin{cases} Nu = \frac{1}{r}(r\sin\psi)_r = Bu, \quad a < r < 1 \\ \sin\psi(a) = -\cos\gamma_1, \quad \sin\psi(1) = \cos\gamma_2 \end{cases} \tag{1.12}$$

For such axisymmetric surfaces, we also note:

$$\begin{aligned} Nu &= \frac{1}{r}(r\sin\psi)_r && (1.13)\\ &= (\sin\psi)_r + \frac{\sin\psi}{r} && (1.14)\\ &= k_m + k_l && (1.15) \end{aligned}$$

where $k_m = (\sin\psi)_r$ is the *meridional curvature* and $k_l = \frac{\sin\psi}{r}$ is the *longitudinal curvature* of the surface. Recalling that $Nu := 2H$, (1.15) takes the more familiar form

$$H = \frac{1}{2}(k_m + k_l). \tag{1.16}$$

To date, the author is aware of only two papers that examine solutions to (1.12). Elcrat et al. [4] provided an introductory survey that included existence theorems as well

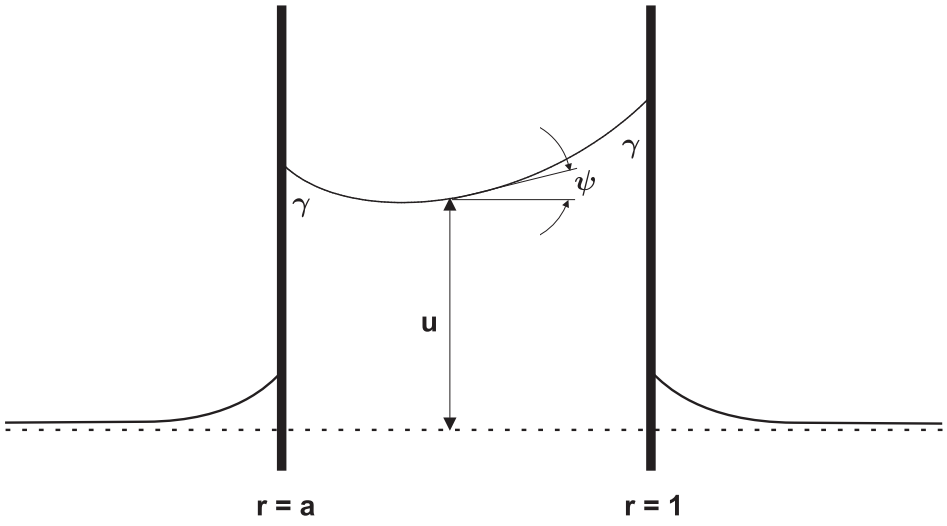

Figure 1.4: Radial cross section of annular capillary surface.

as comparisons of solutions to circular arcs. Siegel [13] then considered the specific case of $\gamma_1 = \frac{\pi}{2}, \gamma_2 \in [0, \pi]$ and developed an iterative procedure that generated increasingly accurate approximate solutions. Certainly, further research is warranted and this paper aims to build upon these existing results.

1.3 Existence and Uniqueness

As mentioned, existence of solutions to (1.12) is provided[2] by [4].

Theorem 1.3.1 (Existence of Annular Surfaces) *There exists a solution to (1.12) for any selection of parameters a, γ_1, γ_2 and B.*

Proof. See [4]. ♦

To demonstrate uniqueness of solutions, we will require the following key result first introduced by Concus and Finn [9].

[2]In actuality, Elcrat et al. demonstrated this result for (1.7); however, the extension to (1.12) is immediate.

Theorem 1.3.2 (Comparison Principle) *Let $u, v \in C^2(\Omega)$ and $\Sigma = \partial\Omega$. Suppose $Nu - Bu \geq Nv - Bv$ in Ω and that Σ admits a decomposition $\Sigma = \Sigma_\alpha \cup \Sigma_\beta \cup \Sigma_0$, such that*

$$\begin{cases} v \geq u, & \text{on } \Sigma_\alpha \\ \hat{\nu} \cdot Tv \geq \hat{\nu} \cdot Tu, & \text{on } \Sigma_\beta \end{cases}$$

Additionally, Σ_0 can be covered, for any $\epsilon > 0$, by a countable number of disks B_{δ_i} of radius δ_i, such that $\sum \delta_i < \epsilon$. It is assumed that $\Sigma_\beta \in C^1$, however, no regularity hypotheses are needed on Σ_α or Σ_0. We conclude:

1. *if $B > 0$ or if $\Sigma_\alpha \neq \emptyset$, then $v \geq u$ in Ω; equality holds at any point if and only if $v \equiv u$.*

2. *if $B = 0$, $\Sigma_\alpha = \emptyset$, then $v(x) \equiv u(x) + \text{const.}$ in Ω.*

N.B. Only case (1) will be considered here.

Proof. See [8]. ♦

The Comparison Principle has proven to be one of the most useful tools in capillarity and it will feature prominently in the next chapter.

Theorem 1.3.3 (Uniqueness of Annular Surfaces) *For any selection of parameters a, γ_1, γ_2 and B, the solution to (1.12) is unique.*

Proof. The proof is taken from [8]; however, its elegance necessitated its inclusion here. Assume there exist two functions $u(r)$ and $v(r)$ that, under the same choice of parameters, are both solutions to (1.12). We have

$$\begin{cases} Nu - Bu = Nv - Bv = 0, & \text{in } \Omega \\ \hat{\nu} \cdot Tu = \hat{\nu} \cdot Tv = \cos\gamma_1, & \text{on } \partial\Omega_1 \\ \hat{\nu} \cdot Tu = \hat{\nu} \cdot Tv = \cos\gamma_2, & \text{on } \partial\Omega_2 \end{cases} \tag{1.17}$$

Using the Comparison Principle, it can be simultaneously argued that

$$v \geq u \quad \text{and} \quad u \geq v \qquad \text{in } \Omega. \tag{1.18}$$

Hence, $u = v$ in Ω. Continuity of u and v implies equality also exists along the boundary so that

$$u(r) = v(r), \quad a \leq r \leq 1. \quad \blacklozenge \tag{1.19}$$

Existence and uniqueness of solutions to (1.12) ensures that all annular surfaces with constant contact angle along each boundary are axisymmetric, and we were justified in restricting our analysis to functions of this form.

1.4 Annular Surfaces Studied

We will narrow our study to surfaces with identical contact angles at either boundary; that is we investigate solutions to

$$\begin{cases} Nu = \frac{1}{r}(r \sin\psi)_r = Bu, & a < r < 1 \\ \sin\psi(a) = -\cos\gamma, \quad \sin\psi(1) = \cos\gamma \end{cases} \tag{1.20}$$

Fig. 1.4 illustrates the surface described in (1.20). This case is of particular significance as it arises when both bounding cylinders are made of the same material. Without loss of generality, we need only consider $\gamma \in [0, \frac{\pi}{2})$. The other possibilities are accounted for as follows:

- if $\gamma = \frac{\pi}{2}$, then $u = 0$ is the unique solution.
- for a solution u with $\gamma \in (\frac{\pi}{2}, \pi]$, let $\bar{u} = -u$. We therefore have $N\bar{u} = B\bar{u}$ with $\bar{\gamma} = \pi - \gamma$ or $\bar{\gamma} \in [0, \frac{\pi}{2})$.

1.4.1 Volume Condition

Under these conditions, the volume of fluid lifted above Ω can be written as follows:

Theorem 1.4.1 (Volume Condition) *Let u be a solution to (1.20). The volume of u above Ω can be determined by*

$$\int_a^1 ru(r)\,dr = \frac{\cos\gamma(1+a)}{B}. \tag{1.21}$$

Proof. We begin by integrating both sides of (1.20a):

$$\iint_\Omega Nu\,dA = \iint_\Omega Bu\,dA. \tag{1.22}$$

The divergence theorem can be applied to the left side of (1.22) so that

$$\begin{aligned} \iint_\Omega Nu\,dA &= \iint_\Omega \nabla\cdot Tu\,dA & (1.23)\\ &= \int_{\partial\Omega_1} \hat{\nu}\cdot Tu\,ds + \int_{\partial\Omega_2} \hat{\nu}\cdot Tu\,ds & (1.24)\end{aligned}$$

and using the boundary condition $\hat{\nu}\cdot Tu = \cos\gamma$ on $\partial\Omega_1 \cup \partial\Omega_2$,

$$\iint_\Omega Nu\,dA = 2\pi\cos\gamma(1+a). \tag{1.25}$$

Symmetry simplifies the right side of (1.22):

$$\iint_\Omega Bu\,dA = 2\pi B\int_a^1 ru(r)\,dr. \tag{1.26}$$

Equating both sides yields

$$\int_a^1 ru(r)\,dr = \frac{\cos\gamma(1+a)}{B}. \quad \blacklozenge \tag{1.27}$$

N.B. We may refer to an arbitrary integrable function $f(r)$ as "satisfying the volume condition" or "having the correct volume." This implies

$$\int_a^1 rf(r)\,dr = \frac{\cos\gamma(1+a)}{B}. \tag{1.28}$$

1.4.2 Integral Equations

The boundary value problem (1.20) may also be expressed in integral form. Multiplying (1.20a) by r,

$$(r\sin\psi)_r = Bru, \tag{1.29}$$

we integrate both sides from a to r,

$$r\sin\psi(r) - a\sin\psi(a) = B\int_a^r su(s)\,ds. \tag{1.30}$$

By requiring $\sin\psi(a) = -\cos\gamma$, the inclination angle $\psi(r)$ can be expressed as

$$\sin\psi(r) = \frac{B}{r}\int_a^r su(s)\,ds - \frac{a}{r}\cos\gamma. \tag{1.31}$$

Note the volume condition provides the correct boundary condition at $r = 1$:

$$\begin{aligned}
\sin\psi(1) &= B\int_a^1 su(s)\,ds - a\cos\gamma && (1.32)\\
&= \cos\gamma(1+a) - a\cos\gamma && (1.33)\\
&= \cos\gamma && (1.34)
\end{aligned}$$

We then use $u_r(r) = \frac{\sin\psi(r)}{\sqrt{1-\sin^2\psi(r)}}$ to write

$$\begin{aligned}
u(r) &= u(a) + \int_a^r u_s(s)\,ds && (1.35)\\
&= u(a) + \int_a^r \frac{\sin\psi(s)}{\sqrt{1-\sin^2\psi(s)}}\,ds && (1.36)
\end{aligned}$$

and, finally, $u(a)$ can be derived from the volume condition:

$$\begin{aligned}
\frac{\cos\gamma\,(1+a)}{B} &= \int_a^1 ru(r)\,dr && (1.37)\\
&= \int_a^1 r\left[u(a) + \int_a^r \frac{\sin\psi(s)}{\sqrt{1-\sin^2\psi(s)}}\,ds\right]dr && (1.38)\\
&= \frac{1-a^2}{2}\,u(a) + \int_a^1\int_a^r r\frac{\sin\psi(s)}{\sqrt{1-\sin^2\psi(s)}}\,ds\,dr && (1.39)
\end{aligned}$$

The order of integration in (1.39) can be changed so that

$$\begin{aligned}
\frac{\cos\gamma\,(1+a)}{B} &= \frac{1-a^2}{2}\,u(a) + \int_a^1\int_s^1 r\frac{\sin\psi(s)}{\sqrt{1-\sin^2\psi(s)}}\,dr\,ds && (1.40)\\
\implies \qquad u(a) &= \frac{2\cos\gamma}{B(1-a)} - \frac{1}{1-a^2}\int_a^1 (1-s^2)\frac{\sin\psi(s)}{\sqrt{1-\sin^2\psi(s)}}\,ds && (1.41)
\end{aligned}$$

The integral equations (1.31), (1.36) and (1.41) provide a useful formulation of the annular problem that will be called upon frequently.

1.5 Outline of Research

This paper is divided into two main sections. The first is contained entirely in Chapter 2 and presents several qualitative properties of solutions to (1.20). The second section spans Chapters 3–5 and extends the iterative procedure introduced by Siegel to the problem considered here. Specifically, Chapter 3 provides conditions under which the approximate functions generated by the procedure converge to the solution of (1.20). Similar to the analysis of Siegel, the behaviour between iterates is examined in Chapter 4, and parallels are drawn with [13]. Finally, Chapter 5 proposes a numerical method as a means of approximating (and visualizing) the iterative procedure.

Chapter 2

Qualitative Properties

2.1 Introduction

As is the case with other boundary value problems, it is possible to comment on the behaviour of capillary surfaces using comparisons with known surfaces. For our purposes, a useful tool will be the Comparison Principle (Theorem 1.3.2). As one of the most important results in capillarity, the Comparison Principle allows for numerous deductions to be made of a qualitative nature, and will be central to the findings of this chapter. We begin in Section 2.2 by illustrating some general properties of the annular surfaces studied; namely, if u is a solution to (1.20), then:

1. $u > 0$ for $r \in [a, 1]$.

2. $u \leq \left(\frac{1-a}{2}\right) \sec\gamma(1 - \sin\gamma) + \frac{\cos\gamma(3-a)}{B(1-a)}$ for $r \in [a, 1]$.

3. there exists a unique radius $r = m$ at which u achieves its minimum value.

4. $u(a) < u(1)$.

5. $m \in (a, \frac{1+a}{2})$.

6. m is monotone increasing with respect to a.

Subsequently, Section 2.3 examines the behaviour of these surfaces in the limiting cases of $a \to 0$ and $a \to 1$.

2.2 General Properties

Theorem 2.2.1 *Let u be a solution to the boundary value problem (1.20). Here, $u > 0$ on $\bar{\Omega}$.*

Proof. Let $\tilde{u} = 0$, which is the unique solution to (1.20) with $\gamma = \frac{\pi}{2}$, and compare this to the solutions u considered here, that is with $\gamma \in [0, \frac{\pi}{2})$:

$$\begin{cases} Nu - Bu = N\tilde{u} - B\tilde{u}\,, & \text{in } \Omega \\ \hat{\nu} \cdot Tu = \cos\gamma > 0 = \hat{\nu} \cdot T\tilde{u}\,, & \text{on } \partial\Omega \end{cases} \tag{2.1}$$

This is a simple application of the Comparison Principle, and we conclude that

$$u > \tilde{u} = 0\,, \quad \text{in } \Omega \tag{2.2}$$

(since the inclination angles of u and $\tilde{u}$ are not equal at $r = a$, the functions must be distinct, leading to the strict inequality in (2.2)). We can also discount the possibility of equality on $\partial\Omega$: if $u = 0$ at $r = a$, the contact angle condition would require $u < 0$ on a neighbourhood immediately inside Ω. This is in contradiction to (2.2) and consequently

$$u > 0\,, \quad \text{on } \bar{\Omega}. \quad \blacklozenge \tag{2.3}$$

A noteworthy consequence of Elcrat's existence theorem [4] requires all solution surfaces to be continuous on $\bar{\Omega}$; hence, u will be bounded on $\bar{\Omega}$. To further this claim, the following theorem presents an explicit upper bound on u.

Theorem 2.2.2 *u is bounded from above on $\bar{\Omega}$ as*

$$u \leq \left(\frac{1-a}{2}\right) \sec\gamma(1 - \sin\gamma) + \frac{\cos\gamma(3-a)}{B(1-a)}$$

Proof. We use the family of functions $\{w_c\}$ defined on $[a,1]$ by

$$w_c(r) = c - \sqrt{\left(\frac{1-a}{2}\right)^2 \sec^2\gamma - \left(r - \frac{1+a}{2}\right)^2} \tag{2.4}$$

with $c \in \mathbb{R}$. Here, each function describes the lower surface of a torus. Furthermore, denote $\omega(r)$ as the inclination angle of $w_c(r)$. Using $\sin\omega(r) = \frac{w_{cr}(r)}{\sqrt{1+{w_{cr}}^2(r)}}$, it can be shown that

$$\sin\omega(r) = \frac{\cos\gamma}{1-a}\left(2r - 1 - a\right). \tag{2.5}$$

Equation (2.5) indicates that w_c will have a contact angle γ at each endpoint, and its minimum (corresponding to $\omega(r) = 0$) will occur at $r = \frac{1+a}{2}$. Each function will also have mean curvature:

$$\begin{aligned} H &= \frac{1}{2}\left(k_m + k_l\right) && (2.6)\\ &= \frac{1}{2}\left((\sin\omega)_r + \frac{\sin\omega}{r}\right) && (2.7)\\ &= \frac{\cos\gamma}{1-a}\left(2 - \frac{1+a}{2r}\right) && (2.8) \end{aligned}$$

Clearly, H achieves its maximum at $r = 1$, with

$$H \le H_{max} = \frac{\cos\gamma(3-a)}{2(1-a)} \tag{2.9}$$

and thus for all w_c,

$$Nw_c = 2H \le \frac{\cos\gamma(3-a)}{1-a}. \tag{2.10}$$

Next, select $\bar{w} \in \{w_c\}$ as the function having

$$\min_{r\in[a,1]}\{\bar{w}(r)\} = \bar{w}\left(\frac{1+a}{2}\right) = \frac{\cos\gamma(3-a)}{B(1-a)} = \frac{2H_{max}}{B} \tag{2.11}$$

so that $N\bar{w} \le \frac{\cos\gamma(3-a)}{1-a} = B\bar{w}\left(\frac{1+a}{2}\right) \le B\bar{w}$. Hence,

$$\begin{cases} Nu - Bu \ge N\bar{w} - B\bar{w}\,, & \text{in } \Omega \\ \hat{\nu}\cdot T\bar{w} = \hat{\nu}\cdot Tu = \cos\gamma\,, & \text{on } \partial\Omega \end{cases} \tag{2.12}$$

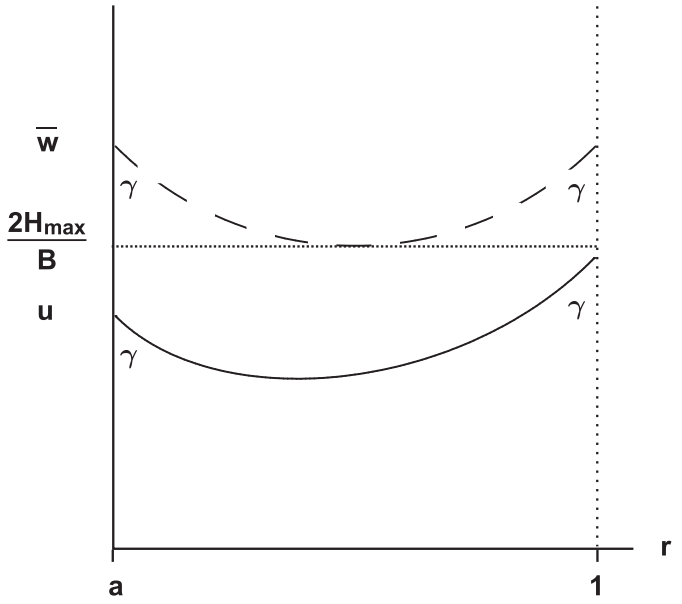

Figure 2.1: Relationship between u and the comparison surface $\bar{w}$.

and the Comparison Principle requires

$$\bar{w} > u\,, \quad \text{in } \Omega \tag{2.13}$$

as Fig. 2.1 illustrates. (2.13) can be extended to the boundary using continuity, and we have

$$\bar{w} \geq u\,, \quad \text{on } \bar{\Omega}. \tag{2.14}$$

A simple geometric argument shows the maximum height of $\bar{w}$ is given by

$$\begin{aligned} \max_{r\in[a,1]}\{\bar{w}(r)\} &= \bar{w}(a) && (2.15)\\ &= \left(\bar{w}(a) - \bar{w}\left(\frac{1+a}{2}\right)\right) + \frac{2H_{max}}{B} && (2.16)\\ &= \left(\frac{1-a}{2}\right)\sec\gamma(1-\sin\gamma) + \frac{2H_{max}}{B} && (2.17) \end{aligned}$$

and thus u is bounded from above as

$$u \leq \left(\frac{1-a}{2}\right)\sec\gamma(1-\sin\gamma) + \frac{\cos\gamma(3-a)}{B(1-a)}, \quad \text{on } \bar{\Omega}. \quad \blacklozenge \tag{2.18}$$

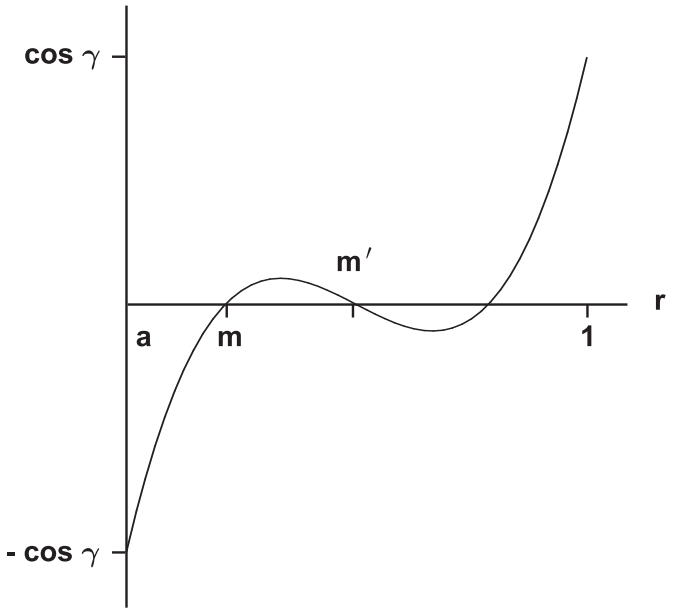

Figure 2.2: Potential configuration of $\sin\psi$, assuming more than one zero for the function.

The boundedness of annular surfaces is a result of $\partial\Omega$ being smooth. Certainly, solutions may be unbounded for domains with non–smooth boundaries, which includes regions containing corners and cusps.

Theorem 2.2.3 *There exists a unique radius $r = m$ at which u achieves its minimum value.*

Proof. Recall that $\psi(r)$ describes the inclination angle of $u(r)$. Since $\sin\psi$ is continuous with

$$\begin{cases} \sin\psi(a) = -\cos\gamma < 0 \\ \sin\psi(1) = \cos\gamma > 0 \end{cases} \tag{2.19}$$

there exists at least one point in $(a, 1)$ where $\sin\psi = 0$, which corresponds to an extremum of u. Define $r = m$ as the first zero of $\sin\psi$. Using (1.29) and Theorem 2.2.1, we note

$$(\sin\psi)_r \;=\; Bu - \frac{\sin\psi}{r} \tag{2.20}$$

$$> \quad 0\,, \quad \text{for } \sin\psi \leq 0 \tag{2.21}$$

and specifically, $\sin\psi$ is increasing at $r = m$. Suppose for the moment there exists more than one point where $\sin\psi = 0$ and let m' be the next zero immediately following m as in Fig. 2.2. Because $\sin\psi$ is increasing at m, it must be nonincreasing as it touches the r–axis at m':

$$(\sin\psi)_r \Big|_{r=m'} \leq 0. \tag{2.22}$$

However, this is in contradiction to (2.21), and m must be the unique extremum point of u. (2.21) also implies this is a minimum. ♦

The next theorem will make use of the following lemma.

Lemma 2.2.4 *$\sin\psi$ is monotone increasing on $[a, 1]$.*

Proof. Given that the zero of $\sin\psi$ is unique, we consider $\sin\psi$ on two subintervals:

- on $[a, m]$, $\sin\psi \leq 0$. (2.20), along with Theorem 2.2.1, ensures that $(\sin\psi)_r > 0$.
- on $(m, 1]$, $\sin\psi > 0$ and thus u is increasing. We integrate (1.29) from m to r:

$$r\sin\psi(r) - m\sin\psi(m) = B\int_m^r su(s)\,ds \tag{2.23}$$

which gives

$$\begin{aligned} \sin\psi(r) &= \frac{B}{r}\int_m^r su(s)\,ds && (2.24)\\ &< \frac{Bu(r)}{r}\left(\frac{r^2 - m^2}{2}\right) && (2.25)\\ &< \frac{Bru(r)}{2} && (2.26) \end{aligned}$$

and therefore, $Bu - \frac{\sin\psi}{r} > 0$. (2.20) confirms that $(\sin\psi)_r > 0$.

Note this lemma implies that u is convex.

Theorem 2.2.5 *$u(a) < u(1)$.*

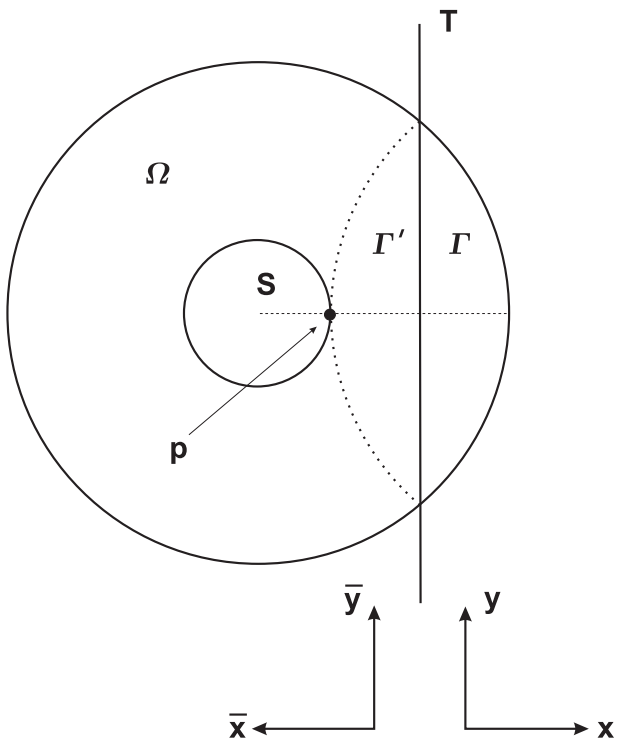

Figure 2.3: Configuration of reflected region Γ' superimposed onto Ω.

Proof. The construction of this proof follows the ideas presented by Serrin [12]. Starting with the annular region Ω, we place a line T that separates from Ω a cap Γ (see Fig. 2.3). Let Γ' be the reflection of Γ with respect to T, and observe that T is positioned so that Γ' is internally tangent to $\partial\Omega$ at p. Finally, let $\hat{n}$ be the exterior unit normal on $\partial\Gamma'$.

With the coordinate system (x, y) re–oriented so that the y–axis is aligned with T, we define a function $\bar{u}$ on Γ' as

$$\bar{u}(x, y) = u(\bar{x}, \bar{y}) = u(-x, y), \quad \text{for } (x, y) \in \Gamma'. \tag{2.27}$$

In other words, $\bar{u}$ is the reflection in T of $u(\Gamma)$. If we let $\bar{N}$ be the operator with respect to the coordinate system $(\bar{x}, \bar{y})$, it is evident that

$$\bar{N}\bar{u} = B\bar{u}. \tag{2.28}$$

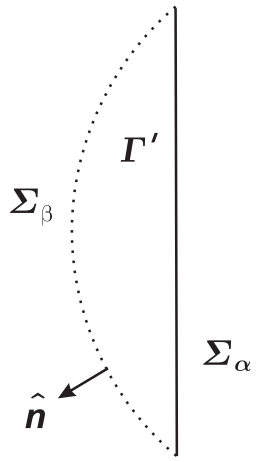

Figure 2.4: Γ' with bounary components labelled.

However, N is invariant under reflections. To see this, we note that

$$\frac{\partial}{\partial x} = -\frac{\partial}{\partial \bar{x}} \quad \text{and} \quad \frac{\partial}{\partial y} = \frac{\partial}{\partial \bar{y}} \tag{2.29}$$

and therefore

$$\begin{aligned} N\bar{u} &= \frac{\left(1+\bar{u}_y^2\right)\bar{u}_{xx} - 2\bar{u}_x\bar{u}_y\bar{u}_{xy} + \left(1+\bar{u}_x^2\right)\bar{u}_{yy}}{\left(1+\bar{u}_x^2+\bar{u}_y^2\right)^{3/2}} && (2.30)\\ &= \frac{\left(1+\bar{u}_{\bar{y}}^2\right)\left(-(-\bar{u}_{\bar{x}})_{\bar{x}}\right) - 2(-\bar{u}_{\bar{x}})\bar{u}_{\bar{y}}(-\bar{u}_{\bar{x}\bar{y}}) + \left(1+(-\bar{u}_{\bar{x}})^2\right)\bar{u}_{\bar{y}\bar{y}}}{\left(1+(-\bar{u}_{\bar{x}})^2+\bar{u}_{\bar{y}}^2\right)^{3/2}} && (2.31)\\ &= \frac{\left(1+\bar{u}_{\bar{y}}^2\right)\bar{u}_{\bar{x}\bar{x}} - 2\bar{u}_{\bar{x}}\bar{u}_{\bar{y}}\bar{u}_{\bar{x}\bar{y}} + \left(1+\bar{u}_{\bar{x}}^2\right)\bar{u}_{\bar{y}\bar{y}}}{\left(1+\bar{u}_{\bar{x}}^2+\bar{u}_{\bar{y}}^2\right)^{3/2}} && (2.32)\\ &= \bar{N}\bar{u} && (2.33) \end{aligned}$$

Thus, $N\bar{u} = \bar{N}\bar{u} = B\bar{u}$ and $\bar{u}$ also satisfies the capillary equation in Γ'. The boundary of Γ' is now decomposed into two pieces, as in Fig. 2.4:

- Σ_α lies along the line of reflection.
- Σ_β will be the remaining curved portion.

We subsequently examine how u and $\bar{u}$ compare on each boundary component. It is immediately clear that

$$u = \bar{u}\,, \quad \text{on } \Sigma_\alpha. \tag{2.34}$$

On Σ_β, we first note

$$\hat{n} \cdot Tu = \frac{u_r}{\sqrt{1+u_r^2}}\ \hat{n} \cdot \hat{r} = \sin\psi\ \hat{n} \cdot \hat{r}\,, \tag{2.35}$$

and thus

$$-|\sin\psi| \le \hat{n} \cdot Tu \le |\sin\psi|. \tag{2.36}$$

Since $\sin\psi$ is increasing, we have $-\cos\gamma \le \sin\psi \le \cos\gamma$ so that

$$-\cos\gamma \le \hat{n} \cdot Tu \le \cos\gamma. \tag{2.37}$$

Of course, $\hat{n} \cdot T\bar{u} = \cos\gamma$ and hence

$$\hat{n} \cdot T\bar{u} \ge \hat{n} \cdot Tu\,, \quad \text{on } \Sigma_\beta. \tag{2.38}$$

As a result, the Comparison Principle requires

$$\bar{u} \ge u\,, \quad \text{in } \Gamma' \tag{2.39}$$

and extending this to the boundary point p,

$$u(p) \le \bar{u}(p) \quad \Longleftrightarrow \quad u(a) \le u(1). \tag{2.40}$$

The possibility of $u(p) = \bar{u}(p)$ can be excluded by contradiction. In this case, we restrict our attention to the dashed line S (Fig. 2.3) and describe both functions in terms of the radial variable only. We begin by assuming $u(a) = u(1)$, which allows the meridional curvature of u at $r = a$ and $r = 1$ to be compared:

$$\begin{aligned} (\sin\psi)_r \Big|_{r=a} &= Bu(a) + \frac{\cos\gamma}{a} \\ &> Bu(1) - \cos\gamma \\ &= (\sin\psi)_r \Big|_{r=1} \end{aligned} \tag{2.41}$$

As a result of (2.41), there exists a $\delta > 0$ such that

$$\min_{r\in[a,a+\delta]} \{(\sin\psi)_r\} > \max_{r\in[1-\delta,1]} \{(\sin\psi)_r\}. \tag{2.42}$$

$(\sin\psi)_r$ can then be integrated over these regions, giving

$$\int_a^{a+r} (\sin\psi)_s \, ds \;>\; \int_{1-r}^{1} (\sin\psi)_s \, ds, \quad \text{for all } r \in (0,\delta] \tag{2.43}$$

$$\Longrightarrow \qquad \sin\psi(a+r) \;>\; -\sin\psi(1-r) \tag{2.44}$$

and since the function $\frac{p}{\sqrt{1-p^2}}$ is increasing on $(-1,1)$, we have

$$\frac{\sin\psi(a+r)}{\sqrt{1-\sin^2\psi(a+r)}} > -\frac{\sin\psi(1-r)}{\sqrt{1-\sin^2\psi(1-r)}}. \tag{2.45}$$

Thus,

$$u(a+\delta) = u(a) + \int_a^{a+\delta} u_s(s)\, ds \tag{2.46}$$

$$= u(a) + \int_a^{a+\delta} \frac{\sin\psi(s)}{\sqrt{1-\sin^2\psi(s)}}\, ds \tag{2.47}$$

$$> u(1) - \int_{1-\delta}^{1} \frac{\sin\psi(s)}{\sqrt{1-\sin^2\psi(s)}}\, ds \tag{2.48}$$

$$= u(1-\delta) \tag{2.49}$$

The above implies that $u(a+\delta) > \bar{u}(a+\delta)$, which is in contradiction to (2.39) and the inequality of (2.40) must be strict. ♦

Theorem 2.2.6 *u achieves its minimum on $(a, \frac{1+a}{2})$.*

Proof. We refer to Fig. 2.3 and again consider u and $\bar{u}$ along S. The proof will be by contradiction, and it is assumed that the minimum occurs on $(\frac{1+a}{2}, 1)$ as in Fig. 2.5. Consider m along with $\bar{m}$, the minimum point of $\bar{u}$. Here, $\bar{m} \in (a, \frac{1+a}{2})$. Since u is convex, it will be monotonically decreasing on $[a, m)$, and thus

$$u(m) < u(\bar{m}) \quad \Longleftrightarrow \quad \bar{u}(\bar{m}) < u(\bar{m}) \tag{2.50}$$

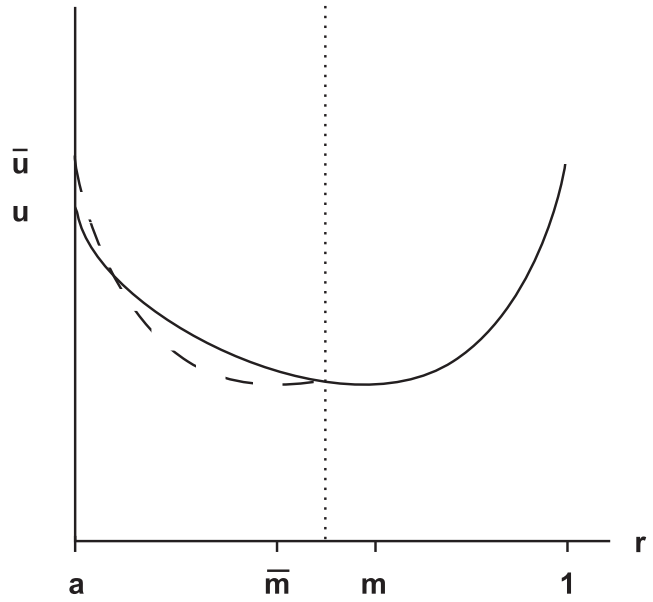

Figure 2.5: Hypothetical configuration of u and $\bar{u}$ along S, assuming $m \in (\frac{1+a}{2}, 1)$.

with $\bar{m} \in \Gamma'$. However, (2.50) is in contradiction to (2.39), making $m \in (a, \frac{1+a}{2}]$. Next, we assume $m = \frac{1+a}{2}$. Differentiating (2.20) with respect to r produces

$$(\sin\psi)_{rr} = u_r - \frac{(\sin\psi)_r}{r} + \frac{\sin\psi}{r^2} \tag{2.51}$$

which, in conjuction with Lemma 2.2.4, gives $(\sin\psi)_{rr}\Big|_{r=m} < 0$. By continuity, there exists a $\delta > 0$ such that

$$(\sin\psi)_{rr} < 0\,, \quad \text{on } [m-\delta, m+\delta]. \tag{2.52}$$

With $(\sin\psi)_r$ decreasing on the interval, we claim

$$\int_{m-r}^{m} (\sin\psi)_s \, ds \;>\; \int_{m}^{m+r} (\sin\psi)_s \, ds\,, \quad \text{for all } r \in (0, \delta] \tag{2.53}$$

$$\Longrightarrow \qquad -\sin\psi(m-r) \;>\; \sin\psi(m+r) \tag{2.54}$$

Finally, an argument similar to the proof of Theorem 2.2.5 yields

$$u(m-\delta) \;=\; u(m) - \int_{m-\delta}^{m} \frac{\sin\psi(s)}{\sqrt{1-\sin^2\psi(s)}}\, ds \tag{2.55}$$

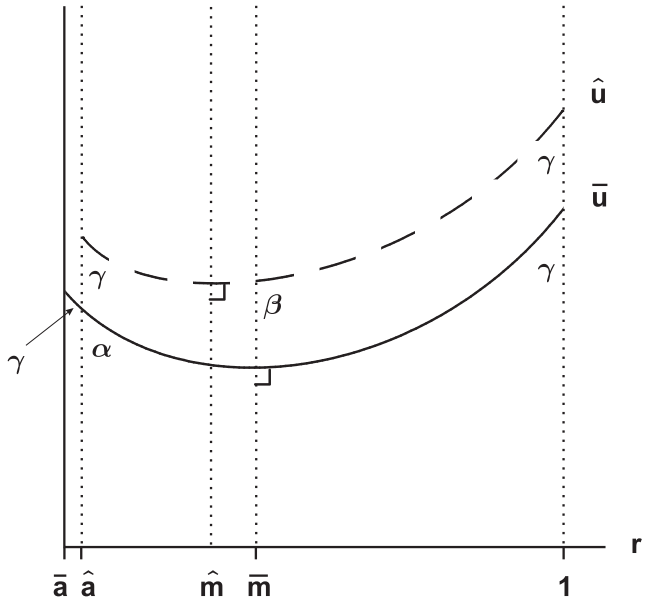

Figure 2.6: Hypothetical configuration assuming m is decreasing with respect to two values of a.

$$> \quad u(m) + \int_m^{m+\delta} \frac{\sin\psi(s)}{\sqrt{1-\sin^2\psi(s)}}\, ds \tag{2.56}$$

$$= \quad u(m+\delta) \tag{2.57}$$

and we conclude $u(m-\delta) > \bar{u}(m-\delta)$. This is again in contradiction with (2.39); therefore the minimum occurs on $(a, \frac{1+a}{2})$. ♦

Theorem 2.2.7 *m is monotone increasing with respect to a.*

Proof. We proceed by contradiction. First, suppose there exist two inner radii $\bar{a}$ and $\hat{a}$ where m decreases with respect to a. This gives rise to the following configuration:

1. $\bar{u}$ is the unique solution over $[\bar{a}, 1]$ with its minimum at $r = \bar{m}$.

2. $\hat{u}$ is the unique solution over $[\hat{a}, 1]$ with its minimum at $r = \hat{m}$.

3. $\bar{a} < \hat{a}$.

4. $\hat{m} < \bar{m}$.

See Fig. 2.6. Consider $\bar{u}$ and $\hat{u}$ on the region $[\hat{a}, 1]$: here, the contact angle of $\bar{u}$ at $r = \hat{a}$ will be $\alpha > \gamma$, and it is clear that

$$\begin{cases} \hat{\nu} \cdot T\bar{u} = \cos\alpha < \cos\gamma = \hat{\nu} \cdot T\hat{u}\,, & \text{at } r = \hat{a} \\ \hat{\nu} \cdot T\bar{u} = \cos\gamma = \hat{\nu} \cdot T\hat{u}\,, & \text{at } r = 1 \end{cases} \tag{2.58}$$

The Comparison Principle therefore implies

$$\bar{u} < \hat{u}\,, \quad \text{in } (\hat{a}, 1). \tag{2.59}$$

We now examine the solutions over $[\bar{m}, 1]$, in which the contact angle of $\hat{u}$ at $r = \bar{m}$ will be $\beta > \frac{\pi}{2}$. Hence,

$$\begin{cases} \hat{\nu} \cdot T\bar{u} = 0 > \cos\beta = \hat{\nu} \cdot T\hat{u}\,, & \text{at } r = \bar{m} \\ \hat{\nu} \cdot T\bar{u} = \cos\gamma = \hat{\nu} \cdot T\hat{u}\,, & \text{at } r = 1 \end{cases} \tag{2.60}$$

and the Comparison Principle would require

$$\bar{u} > \hat{u}\,, \quad \text{in } (\bar{m}, 1) \tag{2.61}$$

which is in disagreement with (2.59). Consequently,

$$\bar{m} \leq \hat{m}\,, \quad \text{for } \bar{a} < \hat{a}. \tag{2.62}$$

Now suppose that m is constant for two increasing values of a. Again, for $\bar{a} < \hat{a}$, $\bar{u}$ and $\hat{u}$ would be configured as before, only with (4) altered as

4. $\bar{u}$ and $\hat{u}$ share the same minimum at $r = m$.

Fig. 2.7 depicts this possibility. In like manner, the Comparison Principle can be applied over $[\hat{a}, 1]$ to reason

$$\bar{u} < \hat{u}\,, \quad \text{in } (\hat{a}, 1). \tag{2.63}$$

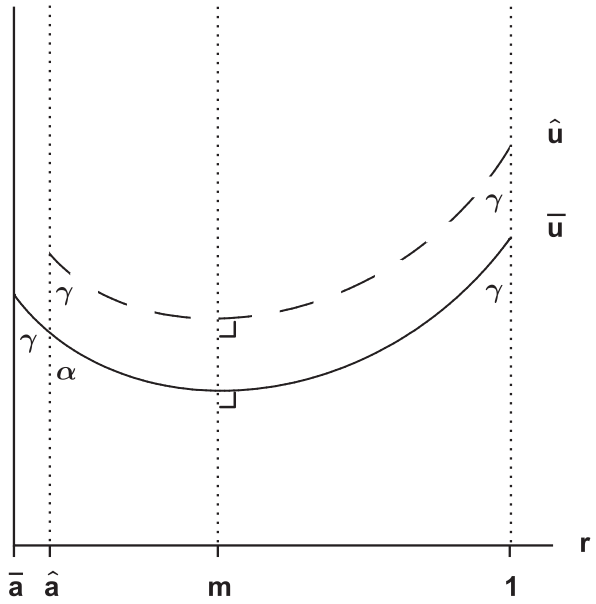

Figure 2.7: Hypothetical configuration assuming m is constant with respect to two values of a.

However, on $[m, 1]$, both $\bar{u}$ and $\hat{u}$ have identical contact angles and uniqueness (Theorem 1.3.3) requires $\bar{u} \equiv \hat{u}$. This is in contradiction to (2.63) and we conclude that

$$\bar{m} < \hat{m}\,, \quad \text{for } \bar{a} < \hat{a}\,, \tag{2.64}$$

thus proving the theorem. ♦

2.3 Solutions In Limiting Cases

We wish to explore the behaviour of solutions to (1.20) in two specific cases: as $a \to 0$ and as $a \to 1$. In preparation, the results of this section will make use of the following lemmas.

2.3.1 Preliminary Lemmas

Lemma 2.3.1 $\frac{\sin\psi}{r}$ *is monotone increasing on* $[a, 1]$.

Proof. We begin by differentiating

$$\left(\frac{\sin\psi}{r}\right)_r = \frac{(\sin\psi)_r}{r} - \frac{\sin\psi}{r^2} \tag{2.65}$$

$$= \frac{2}{r}\left(\frac{Bu}{2} - \frac{\sin\psi}{r}\right) \tag{2.66}$$

with (2.20) used for the last line. Similar to Lemma 2.2.4, $\left(\frac{\sin\psi}{r}\right)_r$ can be examined over two subintervals:

- on $[a, m]$, $\sin\psi \leq 0$ and $\left(\frac{\sin\psi}{r}\right)_r > 0$ by (2.66) and Theorem 2.2.1.
- on $(m, 1]$, $\sin\psi > 0$ and u is monotone increasing. Hence, (2.26) can be used to claim that $\frac{Bu}{2} - \frac{\sin\psi}{r} > 0$, and thus

$$\left(\frac{\sin\psi}{r}\right)_r > 0\,, \quad \text{for } r \in [a, 1]. \quad \blacklozenge \tag{2.67}$$

Lemma 2.3.2 $-\frac{a\cos\gamma}{r} \leq \sin\psi \leq r\cos\gamma$ *on* $[a, 1]$. *Equality occurs exclusively at* $r = a$ *for the lower bound and at* $r = 1$ *for the upper bound.*

Proof. For the lower bound, we observe that (1.29), along with Theorem 2.2.1, provides the differential inequality

$$(r\sin\psi)_r = Bru > 0 \tag{2.68}$$

and thus $r\sin\psi$ is monotone increasing:

$$r\sin\psi(r) \geq a\sin\psi(a) \tag{2.69}$$

$$= -a\cos\gamma \tag{2.70}$$

with equality only at $r = a$. For the upper bound, Lemma 2.3.1 may be used to show

$$\frac{\sin\psi(r)}{r} \leq \sin\psi(1) \tag{2.71}$$

$$= \cos\gamma \tag{2.72}$$

with equality exclusively at $r = 1$. $\blacklozenge$

2.3.2 Main Results

The next theorem will investigate the behaviour of u as $a \to 0$ (i.e. as Ω approaches the disk of radius 1). Here, we will make reference to the interior solution u_{int}, which is the capillary tube surface bounded by a circular wall of radius 1. More precisely, it is the solution to the boundary value problem

$$\begin{cases} (r\sin\psi)_r = Bru_{int}, & r \in (0,1) \\ \sin\psi(0) = 0, \quad \sin\psi(1) = \cos\gamma \end{cases} \tag{2.73}$$

The boundary value problem (2.73), along with the annular problem

$$\begin{cases} (r\sin\psi)_r = Bru, & r \in (a,1) \\ \sin\psi(a) = 0, \quad \sin\psi(1) = \cos\gamma \end{cases} \tag{2.74}$$

was examined by Siegel [13].

First, it will be shown that the solution of (2.74) approaches that of (2.73) as $a \to 0$. For a given $\gamma \in [0, \frac{\pi}{2})$, let $\{v_n\}_{n\geq 2}$ be the sequence of functions such that v_n is the unique solution to (2.74) on the interval $[\frac{1}{n}, 1]$. $\{v_n\}$ is thus defined on an increasing domain; however, it is desirable to define a sequence of extended functions $\{\tilde{v}_n\}_{n\geq 2}$ on $[0,1]$ by continuing each v_n to $r = 0$ as:

$$\tilde{v}_n(r) = \begin{cases} v_n\left(\frac{1}{n}\right), & r \in [0, \frac{1}{n}) \\ v_n(r), & r \in [\frac{1}{n}, 1] \end{cases} \tag{2.75}$$

See Fig. 2.8. Here, $\tilde{v}_n \in C[0,1]$ for all $n \geq 2$. It can be shown from [13] that each function $\tilde{v}_n$, along with the interior solution u_{int}, is increasing and bounded. As well, Siegel demonstrated that each v_n and u_{int} will satisfy the same volume condition:

$$\int_{\frac{1}{n}}^{1} sv_n(s)\,ds = \int_0^1 su_{int}(s)\,ds = \frac{\cos\gamma}{B}. \tag{2.76}$$

Therefore,

$$\int_{\frac{1}{n}}^{1} s\tilde{v}_n(s)\,ds - \int_0^1 su_{int}(s)\,ds \;=\; 0 \tag{2.77}$$

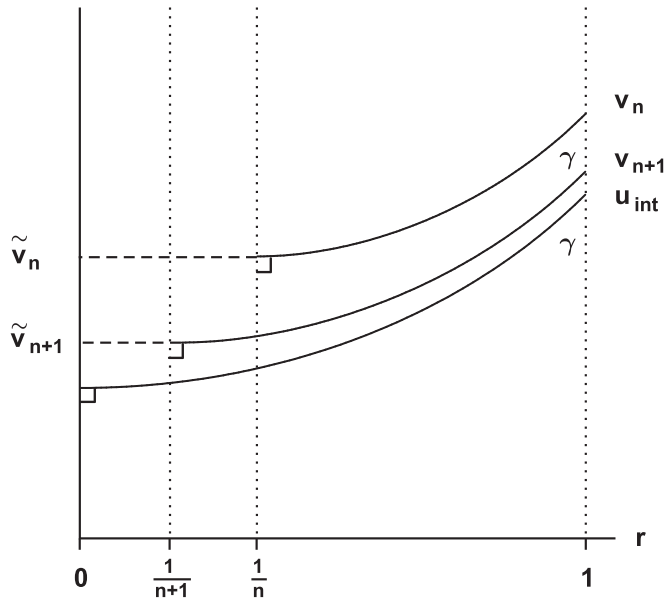

Figure 2.8: Illustration of $\{v_n\}$ and $\{\tilde{v}_n\}$ compared to u_{int}.

$$\Longrightarrow \qquad \int_0^1 s\left(\tilde{v}_n(s) - u_{int}(s)\right)\, ds - \int_0^{\frac{1}{n}} s\tilde{v}_n(s)\, ds \;\; = \;\; 0 \tag{2.78}$$

Additionally, the Comparison Principle provides

$$v_{n+1} \leq v_n \quad \Longleftrightarrow \quad \tilde{v}_{n+1} \leq \tilde{v}_n, \quad \text{for } n \geq 2 \tag{2.79}$$

as well as

$$0 \leq u_{int} \leq v_n \quad \Longleftrightarrow \quad 0 \leq u_{int} \leq \tilde{v}_n, \quad \text{for } n \geq 2. \tag{2.80}$$

Consequently, we are assured that $\tilde{v}_n \to v$ pointwise on $[0,1]$ with

$$v \geq u_{int}\,, \quad \text{on } [0,1]. \tag{2.81}$$

Each integral in (2.78) thus defines a positive, monotone decreasing sequence with a defined limit as $n \to \infty$:

$$\lim_{n\to\infty} \int_0^1 s\left(\tilde{v}_n(s) - u_{int}(s)\right)\, ds - \lim_{n\to\infty} \int_0^{\frac{1}{n}} s\tilde{v}_n(s)\, ds = 0. \tag{2.82}$$

The second limit can be bounded as

$$\begin{aligned} 0 &\leq \lim_{n\to\infty} \int_0^{\frac{1}{n}} s\tilde{v}_n(s)\,ds && (2.83)\\ &\leq \tilde{v}_2(1)\cdot \lim_{n\to\infty} \int_0^{\frac{1}{n}} s\,ds && (2.84)\\ &= 0 && (2.85) \end{aligned}$$

and we conclude $\lim_{n\to\infty} \int_0^{\frac{1}{n}} s\tilde{v}_n(s)\,ds = 0$. The first limit in (2.82) must now be zero and Lebesgue's Dominated Convergence Theorem [1] can be used to claim

$$\begin{aligned} 0 &= \lim_{n\to\infty} \int_0^1 s\left(\tilde{v}_n(s) - u_{int}(s)\right)\,ds && (2.86)\\ &= \int_0^1 s\left(v(s) - u_{int}(s)\right)\,ds && (2.87) \end{aligned}$$

In conjuction with (2.81), this requires

$$v = u_{int}, \quad a.e. \tag{2.88}$$

We further comment that v must be nondecreasing since

$$\begin{aligned} \tilde{v}_n(s_1) &\leq \tilde{v}_n(s_2), \quad \text{for } s_1 < s_2 && (2.89)\\ \implies \quad v(s_1) = \lim_{n\to\infty} \tilde{v}_n(s_1) &\leq \lim_{n\to\infty} \tilde{v}_n(s_2) = v(s_2) && (2.90) \end{aligned}$$

For this reason, inequalities that occur in (2.88) are restricted to jump discontinuities in v. Suppose such a discontinuity of height $\delta > 0$ occurs at a point $c \in [0,1]$. The following two cases will eliminate such a configuration.

1. Suppose $c \in [0,1)$. Here, there will exist a $d > c$ such that u_{int} is continuous on $[c,d]$ with
$$v - u_{int} \geq \frac{\delta}{2}. \tag{2.91}$$
See Fig. 2.9. This is at odds with (2.87) being 0 and $v \equiv u_{int}$ on $[0,1)$.

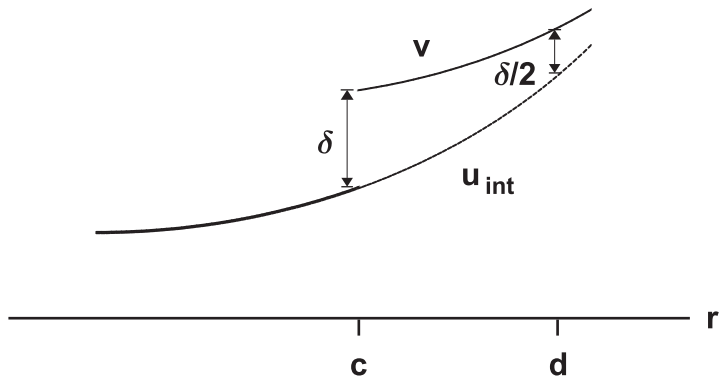

Figure 2.9: Configuration for a jump discontinuity in v at $c \in [0, 1)$.

2. Suppose $c = 1$. For $n \geq 2$, we shift u_{int} upward to the position of $\bar{u}_{int}$ so that $\bar{u}_{int}\left(\frac{1}{n}\right) = v_n\left(\frac{1}{n}\right)$ as in Fig. 2.10. In other words,

$$\bar{u}_{int} = u_{int} + v_n\left(\frac{1}{n}\right) - u_{int}\left(\frac{1}{n}\right). \tag{2.92}$$

The Comparison Principle now requires

$$u_{int} \leq v_n \leq \bar{u}_{int}, \quad \text{for } r \in \left[\frac{1}{n}, 1\right] \tag{2.93}$$

and in particular,

$$u_{int}(1) \leq v_n(1) \leq \bar{u}_{int}(1). \tag{2.94}$$

With Case (1) providing that $\lim_{n\to\infty} v_n\left(\frac{1}{n}\right) = u_{int}(0)$, (2.92) gives

$$\lim_{n\to\infty} \bar{u}_{int}(1) = u_{int}(1), \tag{2.95}$$

and by (2.94),

$$v(1) = u_{int}(1). \tag{2.96}$$

Thus, $v \equiv u_{int}$ as required[1]. Theorem 2.3.3 will rely heavily upon this result.

[1]Dini's Theorem [2] can also be applied at this point to strengthen the convergence claim on $\{\tilde{v}_n\}$ from pointwise to uniform convergence.

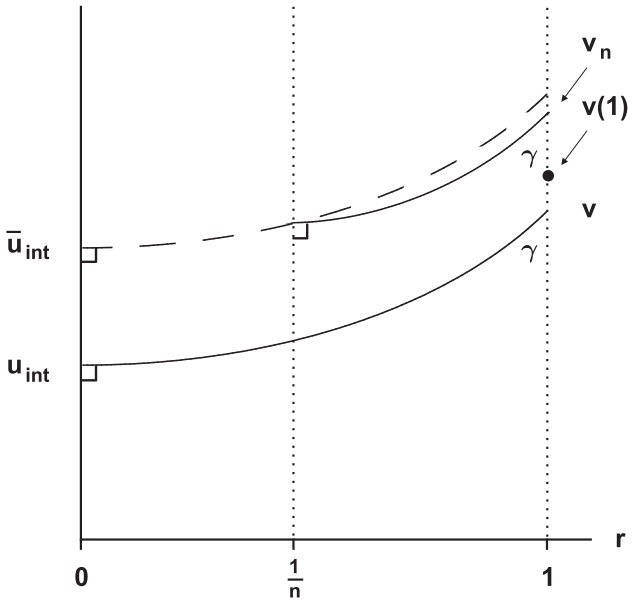

Figure 2.10: Configuration for a jump discontinuity in v at $c = 1$.

Theorem 2.3.3 *For $\gamma \in [0, \frac{\pi}{2})$, consider the interior solution u_{int} defined on $[0,1]$ together with u_a, the solution to (1.20) on $[a,1]$. We have*

$$\lim_{a \to 0} \max_{r \in [a,1]} |u_a(r) - u_{int}(r)| = 0$$

Proof. On $[a,1]$, we compare contact angles of u_a and u_{int} and note that the Comparison Principle compels

$$u_{int} \leq u_a\,, \quad \text{on } [a,1] \tag{2.97}$$

(Fig. 2.11). Additionally, u_{int} may be shifted upward to the position of $\bar{u}_{int}$ such that $\bar{u}_{int}(a) = u_a(a)$. Since the mean curvature remains unchanged, we write $N\bar{u}_{int} = Bu_{int} < B\bar{u}_{int}$ giving

$$\begin{cases} Nu_a - Bu_a > N\bar{u}_{int} - B\bar{u}_{int}\,, & \text{in } (a,1) \\ \bar{u}_{int} = u_a\,, & \text{at } r = a \\ \hat{\nu} \cdot T\bar{u}_{int} = \cos\gamma = \hat{\nu} \cdot Tu_a\,, & \text{at } r = 1 \end{cases} \tag{2.98}$$

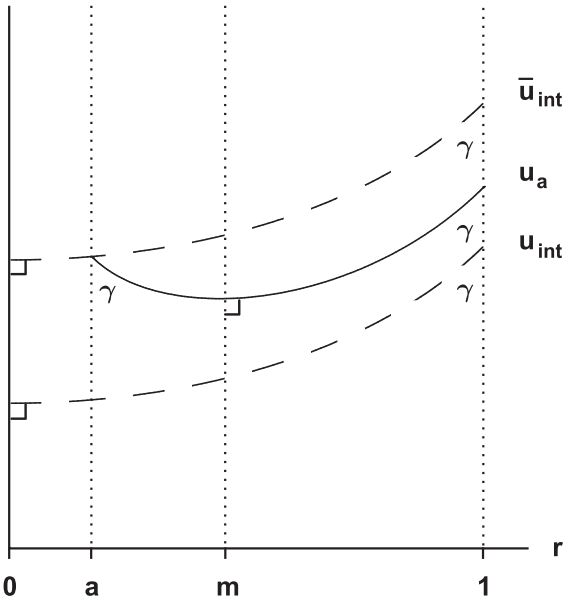

Figure 2.11: Cross section of comparison surfaces for $a \to 0$.

Here again, we use the Comparison Principle to claim that

$$u_a \leq \bar{u}_{int}, \quad \text{on } [a, 1]. \tag{2.99}$$

Consequently, u_a is bounded from above and below with

$$\begin{aligned} \max_{r\in[a,1]} |u_a(r) - u_{int}(r)| &\leq \bar{u}_{int}(a) - u_{int}(a) && (2.100)\\ &= (u_a(a) - u_a(m)) + (u_a(m) - u_{int}(a)) && (2.101)\\ &< (u_a(a) - u_a(m)) + (u_a(m) - u_{int}(0)) && (2.102) \end{aligned}$$

Each bracketed term of (2.102) can be bounded. For the first term,

$$u_a(a) - u_a(m) = -\int_a^m \frac{\sin\psi}{\sqrt{1-\sin^2\psi}}\, ds \tag{2.103}$$

and using Lemma (2.3.2), we have

$$\begin{aligned} u_a(a) - u_a(m) &< a\int_a^m \frac{1}{\sqrt{r^2-a^2}}\, ds && (2.104)\\ &= a\log\left(m + \sqrt{m^2-a^2}\right) - a\log a && (2.105)\\ &< a\log\left(1 + \sqrt{1-a^2}\right) - a\log a && (2.106) \end{aligned}$$

Regardless of m, (2.106) approaches 0 as $a \to 0$. With respect to the second term in (2.102), it is clear that u_a satisifes the boundary value problem (2.74) on $[m, 1]$. Considering m as a function of a, it is thus sufficient to show that $\lim_{a\to 0} m(a) = 0$, as our earlier discussion would then require $\lim_{a\to 0} (u_a(m) - u_{int}(0)) = 0$. This point is developed in the following lemma:

Lemma 2.3.4 *Define u_a and u_{int} identically to the previous theorem and consider m as a function of a. If $\lim_{a\to 0} m(a) = 0$, then*

$$\lim_{a\to 0} u_a(m) = u_{int}(0).$$

Proof. For a given $m(a)$, select the maximum $n \in \mathbb{N}$ such that $m(a) \leq \frac{1}{n}$, which will give

$$\frac{1}{n+1} < m(a) \leq \frac{1}{n}. \tag{2.107}$$

Recalling the sequence of functions $\{v_n\}$, the Comparison Principle produces the following arrangement shown in Fig. 2.12:

$$v_{n+1}\left(\frac{1}{n+1}\right) < u_a(m) \leq v_n\left(\frac{1}{n}\right) \tag{2.108}$$

with

$$\lim_{n\to\infty} v_{n+1}\left(\frac{1}{n+1}\right) = \lim_{n\to\infty} v_n\left(\frac{1}{n}\right) = u_{int}(0). \tag{2.109}$$

For $\lim_{a\to 0} m(a) = 0$, we have $\lim_{a\to 0} n = \infty$ and (2.108) requires

$$\lim_{a\to 0} u_a(m) = u_{int}(0). \quad \blacklozenge \tag{2.110}$$

To show that $\lim_{a\to 0} m(a) = 0$, we proceed by contradiction and assume m does not approach 0. Since m is increasing with respect to a, there must exist a $\sigma > 0$ such that

$$m \geq \sigma, \quad \text{for all } a \in (0, 1). \tag{2.111}$$

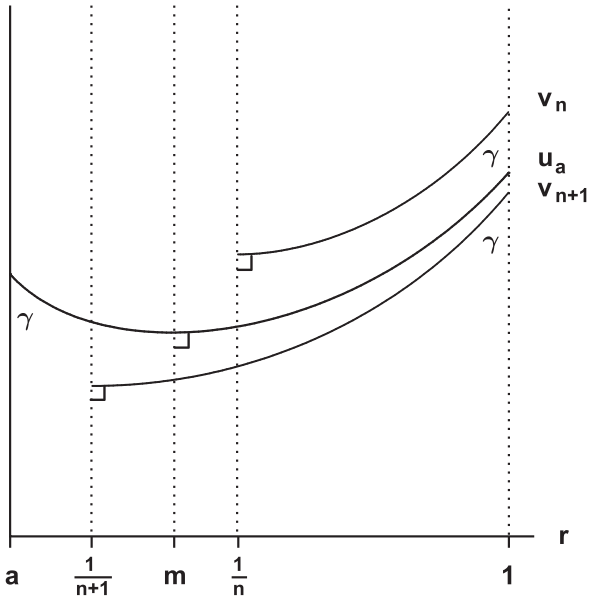

Figure 2.12: n chosen so that $v_{n+1}\left(\frac{1}{n+1}\right) < u_a(m) \leq v_n\left(\frac{1}{n}\right)$

Suppose that $a < \sigma$. By integrating (1.29) from a to m, we have

$$\int_a^m s u_a(s)\, ds = \frac{a\cos\gamma}{B} \tag{2.112}$$

$$\Longrightarrow \qquad \lim_{a\to 0}\int_a^m s u_a(s)\, ds = 0 \tag{2.113}$$

Using (2.111) and that u_a is decreasing on $[a, m)$, the integral could also be bounded as

$$\int_a^m s u_a(s)\, ds \geq u_a(\sigma)\int_a^\sigma s\, ds \tag{2.114}$$

$$= u_a(\sigma)\left(\frac{\sigma^2 - a^2}{2}\right) \tag{2.115}$$

and (2.115) implies that

$$\lim_{a\to 0}\int_a^m s u_a(s)\, ds \geq u_a(\sigma)\frac{\sigma^2}{2} > 0. \tag{2.116}$$

This is an impossible situation and m must approach 0 as $a \to 0$. As a result,

$$\max_{r\in[a,1]} |u_a(r) - u_{int}(r)| \to 0 \quad \text{as } a \to 0. \quad \blacklozenge \tag{2.117}$$

It may also be of interest to examine how u behaves as $a \to 1$ (i.e. as Ω approaches a thin ring with approximate radius 1). For this, we let $u_0 = \frac{2\cos\gamma}{B(1-a)}$ and define the function u_1 as:

$$u_1(r) = u_1(a) + \int_a^r \frac{\sin\psi_1(s)}{\sqrt{1-\sin^2\psi_1(s)}}\,ds \tag{2.118}$$

with

$$\sin\psi_1(r) = \frac{B}{r}\int_a^r su_0\,ds - \frac{a}{r}\cos\gamma \tag{2.119}$$

$$= \frac{\cos\gamma}{1-a}\left(r - \frac{a}{r}\right) \tag{2.120}$$

and

$$u_1(a) = \frac{2\cos\gamma}{B(1-a)} - \frac{1}{1-a^2}\int_a^1 (1-s^2)\frac{\sin\psi_1(s)}{\sqrt{1-\sin^2\psi_1(s)}} \tag{2.121}$$

Here, ψ_1 denotes the inclination angle of u_1. The reader is referred ahead to Chapter 3 where Theorem 3.1.1 ensures that u_1 is defined, continuous and has the correct volume. Addtionally, u_1 is a Delaunay surface[2] satisfying the differential equation

$$Nu_1 = Bu_0 \quad \Longleftrightarrow \quad (r\sin\psi_1(r))_r = Bru_0. \tag{2.122}$$

For $\gamma \neq 0$, it so happens that u_1 will act as a limiting surface as $a \to 1$.

Theorem 2.3.5 *Define u_a identically to the previous theorem and consider the function u_1 described above. For $\gamma \neq 0$,*

$$|u_a - u_1| = O\left((1-a)^3\right), \quad \text{as } a \to 1.$$

Proof. We first bound $|u_a - u_0|$ by referring ahead to equations (3.27)–(3.29) where u_0 is similarly defined:

$$|u_a - u_0| < C(\gamma, m) := \frac{\sqrt{1 - m^2\cos^2\gamma} - \sin\gamma}{\cos\gamma} \tag{2.123}$$

[2]This is a surface of constant mean curvature.

and since $a < m$,

$$|u_a - u_0| < C(\gamma, a). \tag{2.124}$$

Let ψ_a be the inclination angle of u_a. Using (1.31) and (2.119), we write

$$\begin{aligned} |\sin\psi_a - \sin\psi_1| &= \left|\frac{B}{r}\int_a^r s(u_a - u_0)\,ds\right| && (2.125)\\ &\leq \frac{B}{r}\int_a^r s|u_a - u_0|\,ds && (2.126)\\ &\leq \frac{B}{2r}C(\gamma, a)(r^2 - a^2) && (2.127)\end{aligned}$$

Alternatively, (1.29) and (2.122) can be integrated from r to 1 to generate a second bound:

$$\begin{aligned} |\sin\psi_a - \sin\psi_1| &= \left|-\frac{B}{r}\int_r^1 s(u_a - u_0)\,ds\right| && (2.128)\\ &\leq \frac{B}{r}\int_r^1 s|u_a - u_0|\,ds && (2.129)\\ &\leq \frac{B}{2r}C(\gamma, a)(1 - r^2) && (2.130)\end{aligned}$$

Taken together, (2.127) and (2.130) yield

$$|\sin\psi_a - \sin\psi_1| \leq \frac{B}{2r}C(\gamma, a)\min\{r^2 - a^2, 1 - r^2\}, \tag{2.131}$$

and given that $\min\{r^2 - a^2, 1 - r^2\} \leq \frac{2(r^2-a^2)(1-r^2)}{1-a^2}$ (see Appendix, Theorem A.0.5),

$$|\sin\psi_a - \sin\psi_1| \leq \frac{B}{r}C(\gamma, a)\frac{(r^2 - a^2)(1 - r^2)}{1 - a^2}. \tag{2.132}$$

Continuing, we bound $|u_a - u_1|$ by first noting that both u_a and u_1 have the correct volume; therefore they must intersect at least once in $(a, 1)$. Theorem A.0.7 then gives

$$|u_a - u_1| \leq \int_a^1 |(u_a)_r - (u_1)_r|\,dr. \tag{2.133}$$

Using an identical argument to (3.55)–(3.57), the Mean Value Theorem is applied to the integrand so that

$$|u_a - u_1| \leq \int_a^1 \frac{|\sin\psi_a - \sin\psi_1|}{(1 - \xi^2)^{3/2}}\,dr \tag{2.134}$$

where ξ lies between $\sin\psi_a$ and $\sin\psi_1$. By Lemma 2.2.4, we have $\sin\psi_a$ increasing on $[a,1]$, and (2.120) will lead to a similar conclusion for $\sin\psi_1$. Hence, ξ is bounded as $-\cos\gamma < \xi < \cos\gamma$ which implies

$$1-\xi^2 > \sin^2\gamma \tag{2.135}$$

$$> 0, \quad \text{for } \gamma \neq 0 \tag{2.136}$$

Using (2.132) and (2.135), $|u_a - u_1|$ is bounded further:

$$|u_a - u_1| < \int_a^1 \frac{\frac{BC(\gamma,a)}{r}\frac{(r^2-a^2)(1-r^2)}{1-a^2}}{\sin^3\gamma}\,dr \tag{2.137}$$

$$< \frac{B}{a(1-a^2)\sin^3\gamma}\,C(\gamma,a)\int_a^1 (r^2-a^2)(1-r^2)\,dr \tag{2.138}$$

$$< \frac{B}{a(1-a^2)\sin^3\gamma}\,C(\gamma,a)\int_a^1 (1-a^2)^2\,dr \tag{2.139}$$

$$= \frac{B}{a\sin^3\gamma}\,C(\gamma,a)(1-a^2)(1-a) \tag{2.140}$$

Finally, $C(\gamma,a)$ is rewritten as

$$C(\gamma,a) = \frac{\cos\gamma(1-a^2)}{\sqrt{1-a^2\cos^2\gamma}+\sin\gamma} \tag{2.141}$$

$$< \frac{\cos\gamma(1-a^2)}{2\sin\gamma} \tag{2.142}$$

and thus

$$|u_a - u_1| < \frac{B\cos\gamma}{2a\sin^4\gamma}(1-a^2)^2(1-a) \tag{2.143}$$

$$= O\left((1-a)^3\right), \quad \text{as } a\to 1. \quad \blacklozenge \tag{2.144}$$

For $\gamma = 0$, the term $(1-\xi^2)$ can no longer be assigned a positive lower bound, and the above argument does not yield the asymptotic behaviour of u_a as $a \to 1$. Further work is needed to understand this special case.

Finally, we add to Theorem 2.3.5 by showing that for $\gamma \neq 0$, the limiting surface u_1 will in turn approach the lower portion of a torus as $a \to 1$.

Theorem 2.3.6 *Consider the function*

$$t(r) = -\sqrt{\left(\frac{1-a}{2}\right)^2 \sec^2\gamma - \left(r - \frac{1+a}{2}\right)^2} + b(a,\gamma,B)$$

where

$$b(a,\gamma,B) = \frac{2\cos\gamma}{B(1-a)} + \frac{1-a}{8}\sec^2\gamma(\pi - 2\gamma - \sin 2\gamma) + \left(\frac{1-a}{2}\right)\tan\gamma.$$

On $[a,1]$*,* $t(r)$ *describes the lower portion of a torus that satisfies the boundary conditions (1.20b) and the volume condition (Theorem 1.4.1). For* $\gamma \neq 0$*, we have*

$$|u_1 - t| = O\left((1-a)^2\right), \quad \text{as } a \to 1.$$

Proof. From (2.5), the inclination angle of $t(r)$ is given as

$$\sin\omega(r) = \frac{\cos\gamma}{1-a}\left(2r - 1 - a\right), \tag{2.145}$$

and since $\sin\omega \leq \sin\psi_1$ (see the proof of Theorem A.0.13) we write

$$\begin{aligned} |\sin\psi_1 - \sin\omega| &= \sin\psi_1 - \sin\omega & (2.146)\\ &= \frac{\cos\gamma}{1-a}\left(1 + a - r - \frac{a}{r}\right) & (2.147)\end{aligned}$$

It is easily shown that $|\sin\psi_1 - \sin\omega|$ is maximized on $[a,1]$ at $r = \sqrt{a}$ such that

$$|\sin\psi_1 - \sin\omega| \leq \frac{\cos\gamma}{\left(1+\sqrt{a}\right)^2}(1-a). \tag{2.148}$$

Again, Theorem A.0.7 and the Mean Value Theorem may be employed to give

$$|u_1 - t| \leq \int_a^1 \frac{|\sin\psi_1 - \sin\omega|}{(1-\xi^2)^{3/2}}\,dr \tag{2.149}$$

where

$$-\cos\gamma \leq \sin\omega < \xi < \sin\psi_1 \leq \cos\gamma. \tag{2.150}$$

For $\gamma \neq 0$, $|u_1 - t|$ is then bounded as

$$\begin{aligned} |u_1 - t| &< \int_a^1 \frac{\frac{\cos\gamma}{\left(1+\sqrt{a}\right)^2}(1-a)}{\sin^3\gamma} & (2.151)\\ &= \frac{\cos\gamma}{\left(1+\sqrt{a}\right)^2\sin^3\gamma}(1-a)^2 & (2.152)\\ &= O\left((1-a)^2\right), \quad \text{as } a \to 1 \quad \blacklozenge & (2.153)\end{aligned}$$

When considered together, Theorems 2.3.5 and 2.3.6 allow us to conclude that for $\gamma \neq 0$, the solution surface u_a approaches the torus portion $t(r)$ as $O\left((1-a)^2\right)$:

$$\begin{aligned} |u_a - t| &\leq |u_a - u_1| + |u_1 - t| && (2.154) \\ &= O\left((1-a)^2\right), \quad \text{as } a \to 1 && (2.155) \end{aligned}$$

Chapter 3

Iterative Procedure

3.1 Introduction

In many cases, it may be desirable to obtain approximate solutions to the boundary value problem (1.20). As such, we examine the iterative procedure first introduced by Siegel [13]. This scheme was used successfully in [13] to approximate annular surfaces of the related problem (2.74), and it is easily applied here. An outline of the procedure is as follows: consider a function u_1 that satisfies the volume condition (Theorem 1.4.1), and suppose there exists a function u_2 such that $Nu_2 = Bu_1$ or equivalently,

$$(r \sin \psi_2)_r = Bru_1 \tag{3.1}$$

where ψ_2 is the inclination angle of u_2. Requiring $\sin \psi_2(a) = -\cos \gamma$, we use the same techniques found in Section 1.4.2 to arrive at an expression for the inclination angle of u_2:

$$\sin \psi_2(r) = \frac{B}{r} \int_a^r s u_1(s)\, ds - \frac{a}{r} \cos \gamma. \tag{3.2}$$

Furthermore, since u_1 satisfies the volume requirement, u_2 will also have the boundary condition:

$$\sin \psi_2(1) = \cos \gamma. \tag{3.3}$$

We can continue to follow Section 1.4.2 to derive

$$u_2(r) = u_2(a) + \int_a^r \frac{\sin\psi_2(s)}{\sqrt{1-\sin^2\psi_2(s)}}\,ds \tag{3.4}$$

and finally, $u_2(a)$ can be selected so that u_2 has the correct volume:

$$\begin{aligned} \frac{\cos\gamma\,(1+a)}{B} &= \int_a^1 r u_2(r)\,dr & (3.5)\\ &= \int_a^1 r\left[u_2(a) + \int_a^r \frac{\sin\psi_2(s)}{\sqrt{1-\sin^2\psi_2(s)}}\,ds\right]dr & (3.6)\\ \Longrightarrow \qquad u_2(a) &= \frac{2\cos\gamma}{B(1-a)} - \frac{1}{1-a^2}\int_a^1 (1-s^2)\frac{\sin\psi_2(s)}{\sqrt{1-\sin^2\psi_2(s)}}\,ds & (3.7)\end{aligned}$$

The following theorem solidifies the ideas presented.

Theorem 3.1.1 *Let u_1 be a continuous, positive function defined on $[a,1]$ which satisfies the volume condition. Define*

$$\sin\psi_2(r) = \frac{B}{r}\int_a^r s u_1(s)\,ds - \frac{a}{r}\cos\gamma \tag{3.8}$$

and assume $\sin\psi_2 \le r\cos\gamma$. Then:

1. *$-\frac{a\cos\gamma}{r} \le \sin\psi_2$ on $[a,1]$ with equality exclusively at $r=a$.*

2. *There exists a function u_2 defined and continuous on $[a,1]$ given as:*

$$u_2(r) = u_2(a) + \int_a^r \frac{\sin\psi_2(s)}{\sqrt{1-\sin^2\psi_2(s)}}\,ds \tag{3.9}$$

   with

$$u_2(a) = \frac{2\cos\gamma}{B(1-a)} - \frac{1}{1-a^2}\int_a^1 (1-s^2)\frac{\sin\psi_2(s)}{\sqrt{1-\sin^2\psi_2(s)}}\,ds \tag{3.10}$$

   As a result, $Nu_2 = Bu_1$.

3. *u_2 satisfies both the volume condition and the boundary conditions listed in (1.20).*

4. *There exists a unique point $r = m_2$ at which u_2 achieves its minimum value.*

5. *For*

$$B < \frac{2}{(1-a)\left(\frac{1}{3}\sqrt{1-a^2} + a\log\left(1+\sqrt{1-a^2}\right) - a\log a\right)},$$

u_2 will also be positive.

Proof.

1. Using that u_1 is positive, we note

$$(r\sin\psi_2)_r = Bru_1 > 0 \tag{3.11}$$

and the function $r\sin\psi_2$ is monotone increasing. The remainder of the proof mirrors Lemma 2.3.2:

$$\begin{aligned} & a\sin\psi_2(a) \;\leq\; r\sin\psi(r) && (3.12)\\ \Longrightarrow \qquad & -\frac{a\cos\gamma}{r} \;\leq\; \sin\psi_2 && (3.13)\end{aligned}$$

Result 3.13 is a technical point not found in Siegel [13] but will be needed for the proof in Section 3.2.

2. To show u_2 is defined and continuous, it is sufficient to show that u_2 is bounded. With $-\frac{a\cos\gamma}{r} \leq \sin\psi_2 \leq r\cos\gamma$, (3.9) and (3.10) provide that

$$\begin{aligned} u_2(r) &= \frac{2\cos\gamma}{B(1-a)} - \frac{1}{1-a^2}\int_a^1 (1-s^2)\frac{\sin\psi_2}{\sqrt{1-\sin^2\psi_2}}\,ds \\ &\quad + \int_a^r \frac{\sin\psi_2}{\sqrt{1-\sin^2\psi_2}}\,ds && (3.14)\\ &\geq \frac{2\cos\gamma}{B(1-a)} - \frac{1}{1-a^2}\int_a^1 (1-s^2)\frac{s\cos\gamma}{\sqrt{1-s^2\cos^2\gamma}}\,ds \\ &\quad - \int_a^r \frac{a\cos\gamma}{\sqrt{s^2-a^2\cos^2\gamma}}\,ds && (3.15)\\ &\geq \frac{2\cos\gamma}{B(1-a)} - \frac{\cos\gamma}{1-a^2}\int_a^1 (1-s^2)\frac{s}{\sqrt{1-s^2}}\,ds \\ &\quad - a\cos\gamma\int_a^1 \frac{1}{\sqrt{s^2-a^2}}\,ds && (3.16)\end{aligned}$$

$$= \cos\gamma\left[\frac{2}{B(1-a)} - \frac{1}{3}\sqrt{1-a^2} - a\log(1+\sqrt{1-a^2}) + a\log a\right] \tag{3.17}$$

Given that $a\log a \geq -\frac{1}{e}$ on $(0,1]$, u_2 can be bounded below as

$$u_2(r) > \cos\gamma\left[\frac{2}{B} - \frac{1}{3} - \log 2 - \frac{1}{e}\right] \tag{3.18}$$

$$> -\infty \tag{3.19}$$

u_2 can be similarly bounded above:

$$u_2(r) \leq \frac{2\cos\gamma}{B(1-a)} + \frac{1}{1-a^2}\int_a^1 (1-s^2)\frac{a\cos\gamma}{\sqrt{s^2 - a^2\cos^2\gamma}}\,ds + \int_a^r \frac{s\cos\gamma}{\sqrt{1-s^2\cos^2\gamma}}\,ds \tag{3.20}$$

$$< \frac{2\cos\gamma}{B(1-a)} + \frac{a\cos\gamma}{1-a^2}(1-a^2)\int_a^1 \frac{1}{\sqrt{s^2-a^2}}\,ds + \cos\gamma\int_a^1 \frac{s}{\sqrt{1-s^2}}\,ds \tag{3.21}$$

$$= \cos\gamma\left[\frac{2}{B(1-a)} + a\log\left(1+\sqrt{1-a^2}\right) - a\log a + \sqrt{1-a^2}\right] \tag{3.22}$$

$$< \cos\gamma\left[\frac{2}{B(1-a)} + \log 2 + \frac{1}{e} + 1\right] \tag{3.23}$$

$$< \infty \tag{3.24}$$

Finally, the introductory discussion to the chapter confirms that $Nu_2 = Bu_1$.

3. This was also shown in the introductory remarks.

4. This argument progresses indentically to Theorem 2.2.3.

5. The lower bound given in (3.17) is required to be positive:

$$u_2(r) \geq \cos\gamma\left[\frac{2}{B(1-a)} - \frac{1}{3}\sqrt{1-a^2} - a\log(1+\sqrt{1-a^2}) +\right.$$

$$+a\log a\Big]$$
$$> \quad 0$$

Solving for B produces the desired result. Earlier in Chapter 2, it was examined how solutions to the boundary value problem (1.20) approach those considered by Siegel [13] in the limit of $a \to 0$. It may be of interest to note that in this limit, u_2 is positive for $B < 6$. This matches Siegel's result for u_2 analagously defined in his paper. ♦

Theorem 3.1.1 creates the framework needed to generate a sequence of iterates $\{u_n\}$ defined recursively as

$$Nu_{n+1} = Bu_n, \qquad n \geq 0. \tag{3.25}$$

We take the initial function u_0 to be the constant function that satisfies the volume condition:

$$u_0 = \frac{2\cos\gamma}{B(1-a)}. \tag{3.26}$$

It can be shown that for suitable restrictions on B, $\{u_n\}$ constitutes a sequence where:

- (1) through (5) of Theorem 3.1.1 are satisfied for all $n \geq 1$.
- $\{u_n\}$ converges to the solution of the boundary value problem (1.20).

The remainder of the chapter will examine these results.

3.2 The Iterate Convergence Theorem (ICT)

Considering the sequence of iterates $\{u_n\}$ defined by (3.25) and (3.26), it is possible to demonstrate convergence of $\{u_n\}$ to the solution of the boundary value problem (1.20). A benefit of the proof to be developed in Subsection 3.2.1 is its inclusion of the case $\gamma = 0$. Additionally, Subsection 3.2.2 provides motivation for this proof from a geometric context.

3.2.1 Convergence Theorem

Theorem 3.2.1 (Iterate Convergence) *For*

$$B < \frac{2a(1-a^2)\cos\gamma}{2(1+a)(1-a)^2\,C(\gamma,m)+a\pi\cos\gamma}\,,$$

the sequence of iterates $\{u_n\}$ *generated via (3.25) and (3.26) will be continuous and positive. Furthermore,* $B\frac{\pi}{2(1-a^2)} < 1$ *and* $\{u_n\}$ *converges to* u*, the solution of (1.20), with*

$$|u-u_n| < C(\gamma,m)\left(B\frac{\pi}{2(1-a^2)}\right)^n$$

where $C(\gamma,m)=\frac{\sqrt{1-m^2\cos^2\gamma}-\sin\gamma}{\cos\gamma}$ *and* $r=m$ *defines the location of the minimum of* u*.*

Proof[1]**.** We first prove the case for $n=0$ and proceed inductively. It is clear that u_0 is continuous, positive and satisfies the volume condition. Using that u is convex and $u(a)<u(1)$, we have $\max_{r\in[a,1]}\{u(r)\}=u(1)$, and since both u_0 and u satisfy the volume condition, they must intersect at least once in $(a,1)$ with $u(m)<u_0<u(1)$. $|u-u_0|$ is thus bounded as

$$|u-u_0| \le \max\{u(1)-u_0, u_0-u(m)\} < u(1)-u(m) = \int_m^1 \frac{\sin\psi}{\sqrt{1-\sin^2\psi}}\,dr \tag{3.27}$$

Additionally, Lemma 2.3.2 provides that

$$\frac{\sin\psi}{\sqrt{1-\sin^2\psi}} \le \frac{r\cos\gamma}{\sqrt{1-r^2\cos^2\gamma}} \tag{3.28}$$

and consequently

$$|u-u_0| < \int_m^1 \frac{r\cos\gamma}{\sqrt{1-r^2\cos^2\gamma}}\,dr = \frac{\sqrt{1-m^2\cos^2\gamma}-\sin\gamma}{\cos\gamma} := C(\gamma,m) \tag{3.29}$$

[1]The appendix contains some additional results that are omitted from this proof for the sake of brevity.

The case $n = 0$ is thus proved. Next, assume u_n is continuous, positive, and satisfies the volume condition. Also, let $|u - u_n| < \beta_n := C(\gamma, m)\left(B\frac{\pi}{2(1-a^2)}\right)^n$. We write

$$\begin{aligned} |\sin\psi - \sin\psi_{n+1}| &= \left|\frac{B}{r}\int_a^r s\,(u-u_n)\,ds\right| && (3.30)\\ &\le \frac{B}{r}\int_a^r s\,|u-u_n|\,ds && (3.31)\\ &\le \frac{B}{2r}\,\beta_n\,(r^2-a^2) && (3.32)\end{aligned}$$

or alternatively, (1.29) and (3.1) can be integrated from r to 1 to yield

$$\begin{aligned} |\sin\psi - \sin\psi_{n+1}| &= \left|-\frac{B}{r}\int_r^1 s\,(u-u_n)\,ds\right| && (3.33)\\ &\le \frac{B}{r}\int_r^1 s\,|u-u_n|\,ds && (3.34)\\ &\le \frac{B}{2r}\,\beta_n\,(1-r^2) && (3.35)\end{aligned}$$

When used in tandem, (3.32) and (3.35) imply

$$|\sin\psi - \sin\psi_{n+1}| \le \frac{B}{2r}\,\beta_n \min\{r^2-a^2, 1-r^2\}, \tag{3.36}$$

and given that $\min\{r^2-a^2, 1-r^2\} \le \frac{2(r^2-a^2)(1-r^2)}{1-a^2}$ (Theorem A.0.5),

$$|\sin\psi - \sin\psi_{n+1}| \le \frac{\beta_n B}{r}\frac{(r^2-a^2)(1-r^2)}{1-a^2}. \tag{3.37}$$

We can now bound $\sin\psi_{n+1}$. For $n = 0$, $\sin\psi_1$ can be written exactly:

$$\begin{aligned} \sin\psi_1 &= \frac{B}{r}\int_a^r s u_0\,ds - \frac{a}{r}\cos\gamma && (3.38)\\ &= \frac{\cos\gamma}{1-a}\left(r - \frac{a}{r}\right) && (3.39)\end{aligned}$$

and it is easily checked that $-\frac{a\cos\gamma}{r} \le \sin\psi_1 \le r\cos\gamma$. For $n \ge 1$, we do not have the luxury of an explicit function and we proceed as follows: to show $\sin\psi_{n+1} \le r\cos\gamma$, consider the distance between $\sin\psi_1$ and $\sin\psi_{n+1}$:

$$\begin{aligned} |\sin\psi_1 - \sin\psi_{n+1}| &= |\sin\psi_1 - \sin\psi + \sin\psi - \sin\psi_{n+1}| && (3.40)\\ &\le |\sin\psi - \sin\psi_1| + |\sin\psi - \sin\psi_{n+1}| && (3.41)\\ &\le \frac{B}{r}\,C(\gamma,m)\frac{(r^2-a^2)(1-r^2)}{1-a^2}\left[1 + \left(B\frac{\pi}{2(1-a^2)}\right)^n\right] && (3.42)\end{aligned}$$

The bracketed term in (3.42) can be bounded by the geometric series

$$1 + \left(B\frac{\pi}{2(1-a^2)} \right)^n < \sum_{k=0}^{\infty} \left(B\frac{\pi}{2(1-a^2)} \right)^k \tag{3.43}$$

and since

$$B < \frac{2a(1-a^2)\cos\gamma}{2(1+a)(1-a)^2\, C(\gamma,m) + a\pi\cos\gamma} < \frac{2(1-a^2)}{\pi} \tag{3.44}$$

(see Appendix, Theorem A.0.9) the sum is convergent. (3.43) can then be used in (3.42) to give

$$\begin{aligned} |\sin\psi_1 - \sin\psi_{n+1}| &\leq \frac{B}{r}\, C(\gamma,m)\frac{(r^2-a^2)(1-r^2)}{1-a^2}\frac{1}{1-B\frac{\pi}{2(1-a^2)}} && (3.45)\\ &= \frac{B}{r}\, C(\gamma,m)\frac{2(r^2-a^2)(1-r^2)}{2(1-a^2)-B\pi} && (3.46) \end{aligned}$$

The condition on B can be substituted into (3.46) to obtain

$$\begin{aligned} |\sin\psi_1 - \sin\psi_{n+1}| &\leq \frac{a\cos\gamma(r^2-a^2)(1-r^2)}{r(1+a)(1-a)^2} && (3.47)\\ &\leq \frac{a\cos\gamma(1-a^2)(1-r^2)}{r(1+a)(1-a)^2} && (3.48)\\ &= \frac{a\cos\gamma}{1-a}\left(\frac{1}{r} - r\right) && (3.49) \end{aligned}$$

With this in hand, we are able to show that $\sin\psi_{n+1} \leq r\cos\gamma$:

$$\begin{aligned} r\cos\gamma - \sin\psi_{n+1} &= (r\cos\gamma - \sin\psi_1) + (\sin\psi_1 - \sin\psi_{n+1}) && (3.50)\\ &\geq (r\cos\gamma - \sin\psi_1) - |\sin\psi_1 - \sin\psi_{n+1}| && (3.51)\\ &\geq \left[r\cos\gamma - \frac{\cos\gamma}{1-a}\left(r - \frac{a}{r}\right)\right] - \left[\frac{a\cos\gamma}{1-a}\left(\frac{1}{r} - r\right)\right] && (3.52)\\ &= 0 && (3.53) \end{aligned}$$

and properties (1)–(4) of Theorem 3.1.1 apply to u_{n+1}. In addition, the bound on B required here is more restrictive than that in Theorem 3.1.1 (5):

$$\begin{aligned} B &< \frac{2a(1-a^2)\cos\gamma}{2(1+a)(1-a)^2\, C(\gamma,m) + a\pi\cos\gamma} \\ &< \frac{2}{(1-a)\left(\frac{1}{3}\sqrt{1-a^2} + a\log\left(1+\sqrt{1-a^2}\right) - a\log a\right)} \end{aligned}$$

(see the Appendix, Theorem A.0.10) and consequently, u_{n+1} also exhibits property (5) of Theorem 3.1.1. In summary, u_{n+1} will be continuous, positive and will satisfy the volume condition.

Next, we bound $|u - u_{n+1}|$. Noting that both u and u_{n+1} have the correct volume, they must intersect at least once in $(a, 1)$. This allows us to employ Theorem A.0.7:

$$|u - u_{n+1}| \leq \int_a^1 |u_r - (u_{n+1})_r \,| \, dr. \tag{3.54}$$

In order to estimate the integrand of (3.54), we use the Mean Value Theorem on the function $f(p) = \frac{p}{\sqrt{1-p^2}}$ so that

$$\frac{f(\sin\psi) - f(\sin\psi_{n+1})}{\sin\psi - \sin\psi_{n+1}} = f'(\xi), \tag{3.55}$$

where ξ lies between $\sin\psi$ and $\sin\psi_{n+1}$. This can be rewritten as

$$\frac{\sin\psi}{\sqrt{1-\sin^2\psi}} - \frac{\sin\psi_{n+1}}{\sqrt{1-\sin^2\psi_{n+1}}} = \frac{\sin\psi - \sin\psi_{n+1}}{(1-\xi^2)^{3/2}} \tag{3.56}$$

$$\Longrightarrow \qquad |u_r - (u_{n+1})_r \,| = \frac{|\sin\psi - \sin\psi_{n+1}|}{(1-\xi^2)^{3/2}} \tag{3.57}$$

The numerator of (3.57) has an upper bound given in (3.37). For the denominator, Lemma 2.3.2 provides bounds on $\sin\psi$ that are identical to those derived above for $\sin\psi_{n+1}$:

$$-\frac{a\cos\gamma}{r} \leq \sin\psi\,,\ \sin\psi_{n+1} \leq r\cos\gamma \tag{3.58}$$

and ξ is bounded as

$$-\frac{a}{r} \leq -\frac{a\cos\gamma}{r} < \xi < r\cos\gamma \leq r, \tag{3.59}$$

with $\xi^2 < \max\left\{\frac{a^2}{r^2}, r^2\right\}$. The denominator of (3.57) can thus be estimated using

$$1 - \xi^2 > 1 - \max\left\{\frac{a^2}{r^2}, r^2\right\} \tag{3.60}$$

$$= \min\left\{1 - \frac{a^2}{r^2}, 1 - r^2\right\} \tag{3.61}$$

$$\geq \left(1 - \frac{a^2}{r^2}\right)(1 - r^2) \tag{3.62}$$

See the Appendix, Theorem A.0.6 for an explanation of the last line. Returning to (3.54), an upper bound on $|u - u_{n+1}|$ is now possible,

$$\begin{aligned} |u - u_{n+1}| &\leq \int_a^1 \frac{|\sin\psi - \sin\psi_{n+1}|}{(1-\xi^2)^{3/2}}\, dr && (3.63) \\ &< \int_a^1 \frac{\frac{\beta_n B}{r}\frac{(r^2-a^2)(1-r^2)}{1-a^2}}{\left[\left(1-\frac{a^2}{r^2}\right)(1-r^2)\right]^{3/2}}\, dr && (3.64) \\ &= \frac{\beta_n B}{1-a^2}\int_a^1 \frac{r^2}{\sqrt{r^2-a^2}\sqrt{1-r^2}}\, dr && (3.65) \end{aligned}$$

This integral is no greater than $\frac{\pi}{2}$ (Appendix, Theorem A.0.8). Hence,

$$\begin{aligned} |u - u_{n+1}| &< \frac{\beta_n B}{1-a^2}\frac{\pi}{2} && (3.66) \\ &= \beta_{n+1} && (3.67) \end{aligned}$$

and the inductive step is complete. ♦

Fig. 3.1 illustrates a numerical approximation of the iterates $\{u_n\}$, allowing us to visualize the procedure as well as the predicted convergence. Although the first four iterates are plotted, the convergence is rapid enough that the second and third iterates are already barely discernable. Fig. 3.2 plots $\{\sin\psi_n\}$ for the same parameters and, in addition, Table 3.1 lists the maximum difference between adjacent pairs of iterates $\{u_n\}$ and $\{\sin\psi_n\}$, up to $n = 5$. Note that $|u_5 - u_4| \leq 3.0 \times 10^{-8}$ and $|\sin\psi_5 - \sin\psi_4| \leq 4.0 \times 10^{-8}$. The numerical method used here will be examined more fully in Chapter 5.

3.2.2 Geometric Interpretation

The derivation of the bound

$$-\frac{a\cos\gamma}{r} \leq \sin\psi_{n+1} \leq r\cos\gamma$$

was crucial to the proof of the ICT. In order to clarify this point, it may be instructive to provide a geometric explanation of how the result was arrived at. This will speak to

n	$\max \lvert u_n - u_{n-1} \rvert$	$\max \lvert \sin\psi_n - \sin\psi_{n-1} \rvert$
1	3.6×10^{-1}	9.5×10^{-1}
2	3.2×10^{-3}	7.0×10^{-3}
3	8.8×10^{-5}	1.6×10^{-4}
4	1.5×10^{-6}	2.3×10^{-6}
5	3.0×10^{-8}	4.0×10^{-8}

Table 3.1: Maximum distance between adjacent iterates with parameters a, γ and B selected as in Figs. 3.1 and 3.2.

the author's original motivation and ideas, made precise (albeit more abstract) in the above theorem.

With the intent of bounding $\sin\psi_{n+1}$ as

$$-\frac{a\cos\gamma}{r} \leq \sin\psi_{n+1} \leq r\cos\gamma,$$

it may seem reasonable to compare $\sin\psi_{n+1}$ directly with $\sin\psi$, since the latter is known to have these bounds. Indeed, (3.37) provides the estimate

$$|\sin\psi - \sin\psi_{n+1}| < \frac{\beta_n B}{r}\frac{(r^2-a^2)(1-r^2)}{1-a^2}.$$

It is clear that as $B \to 0$, the distance between $\sin\psi$ and $\sin\psi_{n+1}$ can be made arbitrarily small for all $r \in [a,1]$. However, $\sin\psi$ is not known exactly, and it is therefore difficult to determine any condition on B so that $\sin\psi_{n+1}$ will satisfy the required bounds. We thus turn our attention to $\sin\psi_1$ which has the explicit form given in (3.39). Using (3.37), we derive the estimate between $\sin\psi_1$ and $\sin\psi_{n+1}$ as noted in (3.46):

$$|\sin\psi_1 - \sin\psi_{n+1}| < \frac{B}{r}C(\gamma,m)\frac{2(r^2-a^2)(1-r^2)}{2(1-a^2)-B\pi}.$$

Here again, the distance can be made arbitrarily small as $B \to 0$. See Figs. 3.3 and 3.4. With $\sin\psi_1$ known (solid black curve), (3.46) allows for the creation of an envelope

(curves drawn with crosses) that restricts the $(n+1)^{\text{th}}$ iterate within. Reducing B narrows the width of this envelope. As in Fig. 3.4, the goal was to first select a threshold for B so that the envelope's upper portion lay within the bound of $r\cos\gamma$ (top curve drawn with circles). Consequently, B was solved using

$$\frac{B}{r}\,C(\gamma,m)\frac{2(r^2-a^2)(1-r^2)}{2(1-a^2)-B\pi} \leq r\cos\gamma-\sin\psi_1 \tag{3.68}$$

$$= \frac{a\cos\gamma}{1-a}\left(\frac{1}{r}-r\right) \tag{3.69}$$

With B restricted, Theorem 3.1.1 then ensured the envelope's lower portion lay above $-\frac{a\cos\gamma}{r}$ (bottom curve drawn in circles). Of course, in the proof of the ICT, the more systematic approach was to state the restriction on B and work backwards.

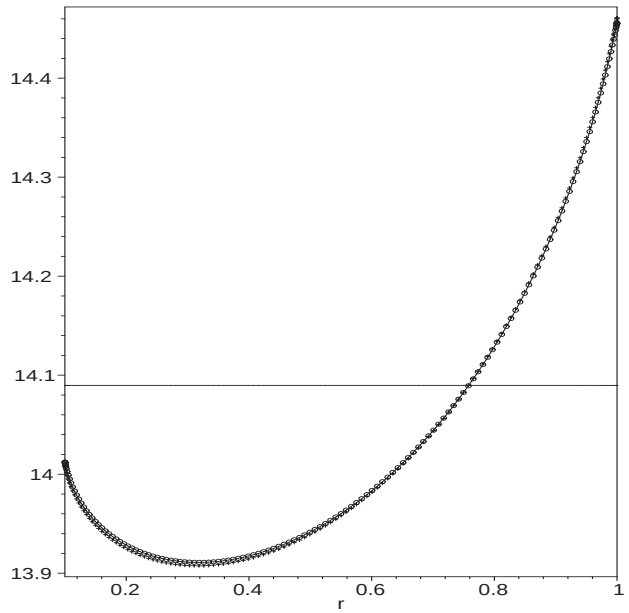

Figure 3.1: Numerical approximation of u_n vs. r for $n = 0, \ldots, 3$ with $a = 0.1$, $\gamma = \frac{\pi}{10}$, $B = 0.15$. Iterates are drawn as {*solid line, cross, circle, solid curve*}.

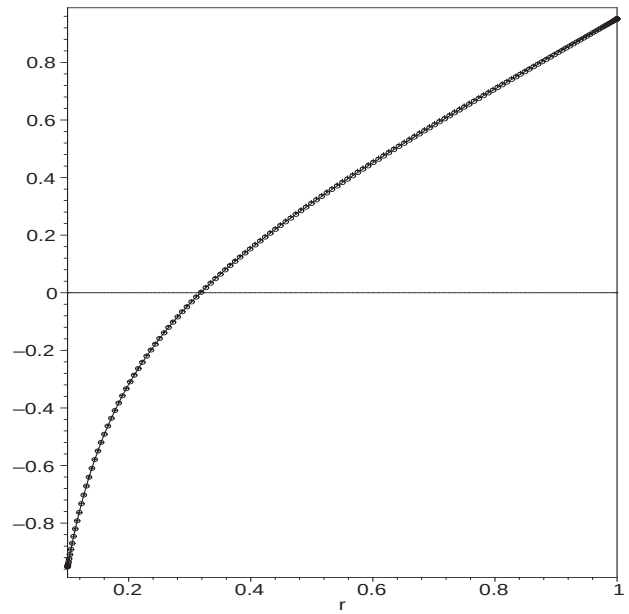

Figure 3.2: Numerical approximation of $\sin\psi_n$ vs. r for $n = 0, \ldots, 3$ with $a = 0.1$, $\gamma = \frac{\pi}{10}$, $B = 0.15$. Iterates are drawn as {*solid line, cross, circle, solid curve*}.

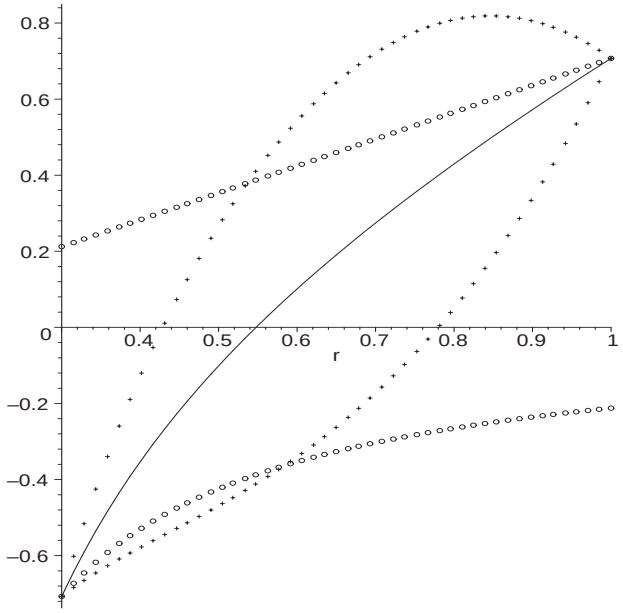

Figure 3.3: Envelope of $\sin\psi_1$ with $a = 0.3, \gamma = \frac{\pi}{4}, B = 0.5$. The envelope exceeds both upper and lower bounds.

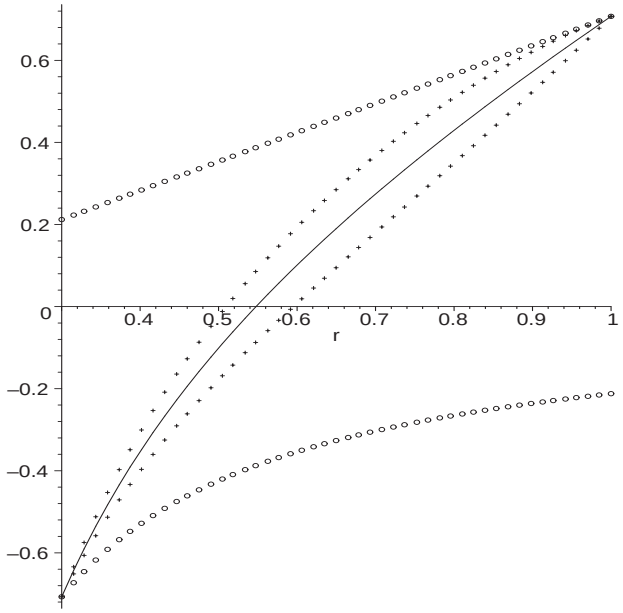

Figure 3.4: Envelope of $\sin\psi_1$ with $a = 0.3, \gamma = \frac{\pi}{4}, B = 0.33$. B was selected to satisfy (3.68), and the envelope now lies within the required bounds.

Chapter 4

Iterate Behaviour

4.1 Single Intersection Case: Interleaving Properties

In [13], the iterates of Siegel were shown to exhibit a highly organized interplay:

1. $\psi_0 < \psi_2 < \cdots < \psi < \cdots < \psi_3 < \psi_1, \quad$ for $r \in (a, 1)$
2. $u_1(a) < u_3(a) < \cdots < u(a) < \cdots < u_2(a) < u_0$
3. $u_0 < u_2(1) < \cdots < u(1) < \cdots < u_3(1) < u_1(1)$

(1) to (3) were defined collectively by Siegel as the *interleaving properties* of the iterates, with (2) and (3) providing guaranteed under– and over–estimates for the boundary values of u. In the case considered here, the behaviour between iterates is slightly more complex, being sensitive to the values of the parameters a, γ and B selected. However, we are able to recover these interleaving properties under certain conditions. It so happens that it will be necessary to find selections of a, γ and B such that u, u_2 and u_0 will be configured as noted in Fig. 4.1. In other words, there exist unique points b_0

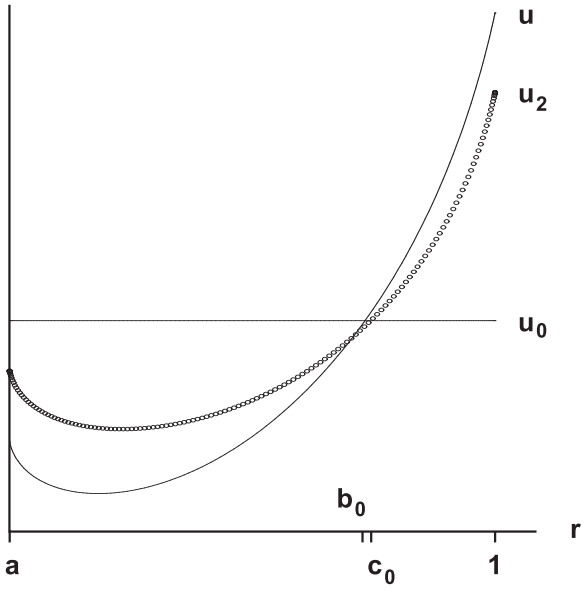

Figure 4.1: Configuration required for interleaving properties. u and u_2 must be oriented as noted with respect to u_0. The orientation between u and u_2 is not important.

and c_0 in $(a, 1)$ such that

$$\begin{cases} u < u_0\,, & r \in [a, b_0) \\ u > u_0\,, & r \in (b_0, 1] \end{cases} \tag{4.1}$$

and

$$\begin{cases} u_2 < u_0\,, & r \in [a, c_0) \\ u_2 > u_0\,, & r \in (c_0, 1] \end{cases} \tag{4.2}$$

The numerical experiment in Fig. 3.1 suggests this may be possible, but we can take a more analytical approach. Should (4.1) and (4.2) occur, it turns out that the interleaving properties are a consequence. We examine the conditions necessary for each configuration below.

4.1.1 Single Intersection of u with u_0

It will be shown that the configuration of (4.1) is a result of

$$u(a) < u_0, \tag{4.3}$$

and it is indeed possible to find conditions under which (4.3) is true through a comparison with $u_1(a)$. We thus begin by investigating the conditions necessary for $u_1(a) < u_0$ (recall that since $\sin\psi_1 \leq r\cos\gamma$, u_1 is defined and continuous without an *a priori* condition on B). Looking at the difference,

$$u_0 - u_1(a) = \frac{1}{1-a^2}\int_a^1 (1-s^2)\frac{\sin\psi_1}{\sqrt{1-\sin^2\psi_1}}\,ds, \tag{4.4}$$

the integrand of (4.4) can be bounded from below by first estimating $\frac{\sin\psi_1}{\sqrt{1-\sin^2\psi_1}}$, treating the domains in which it is positive and negative separately. From (3.39), it is clear that $\sin\psi_1$ changes sign at $r=\sqrt{a}$, and hence, $\frac{\sin\psi_1}{\sqrt{1-\sin^2\psi_1}}$ will do the same. For $a \leq r \leq \sqrt{a}$, we use that $\sin\psi_1$ is concave to create a linear lower bound,

$$\frac{\cos\gamma}{\sqrt{a}-a}(r-\sqrt{a}) \leq \sin\psi_1, \tag{4.5}$$

(see Fig. 4.2) which then gives

$$\frac{\sin\psi_1}{\sqrt{1-\sin^2\psi_1}} \geq \frac{\frac{\cos\gamma}{\sqrt{a}-a}(r-\sqrt{a})}{\sqrt{1-\left[\frac{\cos\gamma}{\sqrt{a}-a}(r-\sqrt{a})\right]^2}} = \frac{r-\sqrt{a}}{\sqrt{\frac{\left(\sqrt{a}-a\right)^2}{\cos^2\gamma}-(r-\sqrt{a})^2}}. \tag{4.6}$$

For $\sqrt{a} \leq r < 1$, it is easily seen that[1]

$$\frac{\sin\psi_1}{\sqrt{1-\sin^2\psi_1}} \geq \sin\psi_1 = \frac{\cos\gamma}{1-a}\left(r-\frac{a}{r}\right). \tag{4.7}$$

Using these bounds in (4.4),

$$u_0 - u_1(a) \;>\; \frac{1}{1-a^2}\left[\int_a^{\sqrt{a}}(1-s^2)\frac{s-\sqrt{a}}{\sqrt{\frac{\left(\sqrt{a}-a\right)^2}{\cos^2\gamma}-(s-\sqrt{a})^2}}\,ds\right.$$

[1]Here, it was initially attempted to use a linear bound similar to above. This, however, proved difficult to integrate later on.

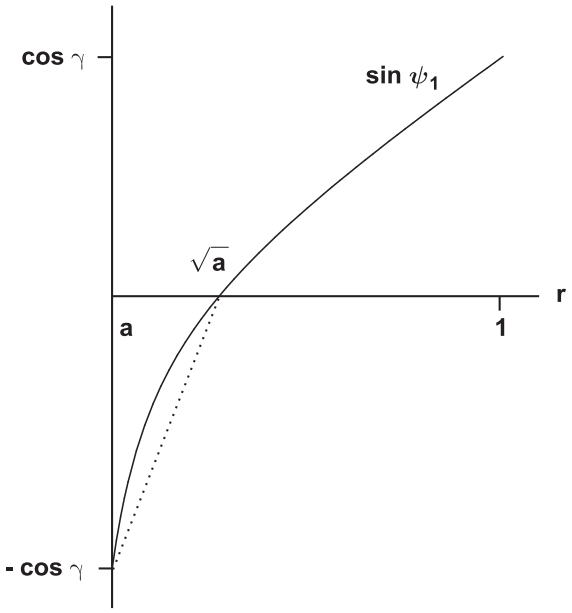

Figure 4.2: Linear lower bound on $\sin\psi_1$ over its negative regime.

$$+\int_{\sqrt{a}}^{1}(1-s^2)\frac{\cos\gamma}{1-a}\left(s-\frac{a}{s}\right)\,ds\Bigg] \tag{4.8}$$

$$> \frac{1}{1-a^2}\Bigg[(1-a^2)\int_a^{\sqrt{a}}\frac{s-\sqrt{a}}{\sqrt{\frac{\left(\sqrt{a}-a\right)^2}{\cos^2\gamma}-\left(s-\sqrt{a}\right)^2}}\,ds$$

$$+\int_{\sqrt{a}}^{1}(1-s^2)\frac{\cos\gamma}{1-a}\left(s-\frac{a}{s}\right)\,ds\Bigg] \tag{4.9}$$

$$= \sqrt{\frac{\left(\sqrt{a}-a\right)^2}{\cos^2\gamma}-\left(\sqrt{a}-a\right)^2}-\frac{\sqrt{a}-a}{\cos\gamma}$$

$$+\frac{\cos\gamma\,(1-a^2+2a\log a)}{4(1-a)(1-a^2)} \tag{4.10}$$

and since $a\log a > (a-1)+\frac{1}{2}(a-1)^2-\frac{1}{6}(a-1)^3$ on $(0,1)$,

$$u_0-u_1(a) > \frac{\sqrt{a}-a}{\cos\gamma}\left(\sin\gamma-1\right)+\frac{\cos\gamma(1-a)}{12(1+a)} \tag{4.11}$$

$$\geq \frac{\sqrt{a}-a}{\cos\gamma}\left(\sin^2\gamma-1\right)+\frac{\cos\gamma(1-a)}{12(1+a)} \tag{4.12}$$

$$= \cos\gamma\left[\frac{1-a}{12(1+a)}-\left(\sqrt{a}-a\right)\right] \tag{4.13}$$

To ensure that $u_0 > u_1(a)$, the expression in square brackets must be nonnegative:

$$\frac{1-a}{12(1+a)} - \left(\sqrt{a} - a\right) \geq 0 \tag{4.14}$$

$$\implies \quad -12\left(\sqrt{a} - a + a^{3/2} - a^2\right) + 1 - a \geq 0 \tag{4.15}$$

Let $x = \sqrt{a}$, making (4.15)

$$(x-1)(12x^3 + 11x - 1) \geq 0. \tag{4.16}$$

The above polynomial has two real roots: one at $x = 1$ and the other at

$$\Lambda := \frac{1}{6}\left(9 + 2\sqrt{353}\right)^{1/3} - \frac{11}{6\left(9 + 2\sqrt{353}\right)^{1/3}} \doteq 0.09. \tag{4.17}$$

It is also nonnegative for $x \in (0, \Lambda]$. Consequently, for $a \in (0, \Lambda^2]$, the polynomial in (4.15) will be nonnegative and $u_0 > u_1(a)$.

To compare $u(a)$ with u_0, we employ the same technique used in the proof of the Iterate Convergence Theorem: find B so that $u(a)$ lies close enough to $u_1(a)$ making $u(a) < u_0$ as well.

Theorem 4.1.1 *For any $\gamma \in [0, \frac{\pi}{2})$, select $a \leq \Lambda^2$ and*

$$B \leq \frac{2(1-a^2)\cos\gamma}{\pi}\left(\frac{1-a}{12(1+a)} - \left(\sqrt{a} - a\right)\right).$$

Under these conditions, there exists a unique $b_0 \in (a, 1)$ such that $u(b_0) = u_0$ with

$$\begin{cases} u < u_0\,, & r \in [a, b_0) \\ u > u_0\,, & r \in (b_0, 1] \end{cases}$$

Proof. We begin by noting

$$u_0 - u(a) = (u_0 - u_1(a)) + (u_1(a) - u(a)) \tag{4.18}$$

$$\geq (u_0 - u_1(a)) - |u(a) - u_1(a)| \tag{4.19}$$

Since $\sin\psi_1 \leq r\cos\gamma$ (see page 42), (1)–(4) of Theorem 3.1.1 applies to u_1. As well, it can be shown that

$$B \leq \frac{2(1-a^2)\cos\gamma}{\pi}\left(\frac{1-a}{12(1+a)} - \left(\sqrt{a}-a\right)\right) < 1 \tag{4.20}$$

(A.0.11) and u_1 also exhibits property (5) of Theorem 3.1.1. The selection of a ensures that the first term of (4.19) has a positive lower bound. For the second term, we go through the proof of the ICT for the specific case of u_1 to argue

$$|u - u_1| < C(\gamma, m)B\frac{\pi}{2(1-a^2)}. \tag{4.21}$$

(4.19) can now be bounded using (4.13) and (4.21):

$$u_0 - u(a) > \cos\gamma\left(\frac{1-a}{12(1+a)} - \left(\sqrt{a}-a\right)\right) - C(\gamma, m)B\frac{\pi}{2(1-a^2)}, \tag{4.22}$$

and since $C(\gamma, m) < 1$,

$$u_0 - u(a) > \cos\gamma\left(\frac{1-a}{12(1+a)} - \left(\sqrt{a}-a\right)\right) - B\frac{\pi}{2(1-a^2)}. \tag{4.23}$$

Finally, substituting the condition on B produces the desired result,

$$u(a) < u_0. \tag{4.24}$$

With both u and u_0 having the correct volume, at least one intersection occurs between these functions. The convexity of u, in conjuction with (4.24), limits this to a unique intersection occuring at a point $b_0 \in (a, 1)$. The functions thus behave as noted in the theorem. ♦

The configuration of u with u_0 in Fig. 4.1 is now possible.

4.1.2 Single Intersection of u_2 with u_0

In like manner, we are able to find conditions for $u_2(a) < u_0$ which will result in (4.2). Before turning to this, it should be verifed that under the hypotheses of the previous

theorem, u_2 is defined and continuous. This will require a lemma also employed in [13]. It is stated here without proof.

Lemma 4.1.2 *Consider two functions v and w defined on $[a,1]$ with inclination angles given by ψ_v and ψ_w respectively. If $\psi_v < \psi_w$ on $(a,1)$ and $\int_a^1 rv\,dr = \int_a^1 rw\,dr$, then there exists a unique $b \in (a,1)$ where $v(b) = w(b)$ and*

$$\begin{cases} w < v\,, & r \in [a,b) \\ w > v\,, & r \in (b,1] \end{cases} \qquad \blacklozenge$$

To show u_2 is defined and continuous, we first write the difference function

$$r\sin\psi - r\sin\psi_1 = B\int_a^r s(u-u_0)\,ds \tag{4.25}$$

which has its derivative given by

$$(r\sin\psi - r\sin\psi_1)_r = Br(u-u_0). \tag{4.26}$$

Clearly, the function (4.25) is zero at $r = a$ and $r = 1$, and has a unique extremum at $r = b_0$. Thus, $r\sin\psi - r\sin\psi_1$ must be either positive or negative on $(a,1)$. The fact that $u(a) < u_0$ implies

$$r\sin\psi - r\sin\psi_1 \;<\; 0 \tag{4.27}$$

$$\Longrightarrow \qquad \psi \;<\; \psi_1, \qquad \text{for } r \in (a,1) \tag{4.28}$$

and Lemma 4.1.2 ensures that there exists a unique $b_1 \in (a,1)$ where $u_1(b_1) = u(b_1)$ and

$$\begin{cases} u_1 < u\,, & r \in [a,b_1) \\ u_1 > u\,, & r \in (b_1,1] \end{cases} \tag{4.29}$$

With this in hand, we can verify that u_2 is defined and continuous by considering the difference

$$r\sin\psi - r\sin\psi_2 = B\int_a^r s(u-u_1)\,ds \tag{4.30}$$

and reason accordingly that

$$\sin\psi_2 < \sin\psi < r\cos\gamma, \qquad \text{for } r \in (a,1). \tag{4.31}$$

With B bounded as in Theorem 4.1.1, u_2 will exhibit all properties of Theorem 3.1.1. Conditions can now be stated so that $u_2(a) < u_0$. Here, B will be restricted further than Theorem 4.1.1.

Theorem 4.1.3 *For any $\gamma \in [0, \frac{\pi}{2})$, select $a \leq \Lambda^2$ and*

$$B \leq \frac{(1-a^2)\cos\gamma}{\pi}\left(\frac{1-a}{12(1+a)} - \left(\sqrt{a}-a\right)\right).$$

Under these conditions, there exists a unique $c_0 \in (a,1)$ such that $u_2(c_0) = u_0$ with

$$\begin{cases} u_2 < u_0\,, & r \in [a, c_0) \\ u_2 > u_0\,, & r \in (c_0, 1] \end{cases}$$

Proof. Similarly, we write

$$\begin{aligned} u_0 - u_2(a) &= (u_0 - u(a)) + (u(a) - u_2(a)) && (4.32)\\ &\geq (u_0 - u(a)) - |u(a) - u_2(a)| && (4.33) \end{aligned}$$

The first term can be bounded as in (4.22), and an identical argument to the proof of the ICT specifically for u_2 estimates the second term. We thus have

$$\begin{aligned} u_0 - u_2(a) &> \cos\gamma\left(\frac{1-a}{12(1+a)} - \left(\sqrt{a}-a\right)\right) - C(\gamma,m)B\frac{\pi}{2(1-a^2)} \\ &\quad -C(\gamma,m)\left(B\frac{\pi}{2(1-a^2)}\right)^2 && (4.34)\\ &> \cos\gamma\left(\frac{1-a}{12(1+a)} - \left(\sqrt{a}-a\right)\right) \\ &\quad -B\frac{\pi}{2(1-a^2)}\left(1 + B\frac{\pi}{2(1-a^2)}\right) && (4.35) \end{aligned}$$

Substituting for B gives

$$u_2(a) < u_0. \tag{4.36}$$

As before, the volume condition guarantees an intersection between the two functions. Theorem 3.1.1 (4) implies that u_2 is monotone decreasing on $[a, m_2)$ and monotone increasing on $(m_2, 1]$. Hence, the intersection is unique and the theorem's result easily follows. ♦

Physically, the single intersection case defined by configurations (4.1) and (4.2) will occur for any fluid/solid combination provided that the boundaries are positioned appropriately. To demonstrate this, let us return to the physical geometry where the annular tube has inner and outer radii R_1 and R_2 respectively. For any $\gamma \in [0, \frac{\pi}{2})$, we select a configuration where

$$R_1 = \Lambda^2 R_2. \tag{4.37}$$

Consequently, $a = \frac{R_1}{R_2} = \Lambda^2$ and the term

$$\frac{(1-a^2)\cos\gamma}{\pi}\left(\frac{1-a}{12(1+a)} - \left(\sqrt{a}-a\right)\right) \tag{4.38}$$

is constant. R_2 can now be chosen sufficiently small so that

$$B = \kappa {R_2}^2 \leq \frac{(1-a^2)\cos\gamma}{\pi}\left(\frac{1-a}{12(1+a)} - \left(\sqrt{a}-a\right)\right). \tag{4.39}$$

In this regime, Theorems 4.1.1 and 4.1.3 apply thus producing the single intersection case.

4.1.3 Interleaving Properties

We are now in a position to prove the interleaving properties for $\{u_n\}$. Here, B is restricted so that the single intersection case is guaranteed to occur.

Theorem 4.1.4 *For any $\gamma \in [0, \frac{\pi}{2})$, select $a \leq \Lambda^2$ and*

$$B \leq \frac{(1-a^2)\cos\gamma}{\pi}\left(\frac{1-a}{12(1+a)} - \left(\sqrt{a}-a\right)\right).$$

Under these conditions, the sequence of iterates $\{u_n\}$ defined by (3.25) and (3.26) satisfy (1) through (5) of Theorem 3.1.1. Furthermore, they exhibit the following properties:

1. $\psi_2 < \psi_4 < \cdots < \psi < \cdots < \psi_3 < \psi_1, \qquad \text{for } r \in (a,1)$

2. $u_1(a) < u_3(a) < \cdots < u(a) < \cdots < u_4(a) < u_2(a)$

3. $u_2(1) < u_4(1) < \cdots < u(1) < \cdots < u_3(1) < u_1(1)$

Proof.

1. We first go through a cycle of recursive arguments and proceed to show that the base case, which is known to be true, sets the cycle in motion. To start, assume that for a certain $k \geq 0$:

   (a) u_{2k}, u_{2k+1}, and u_{2k+2} satisfy (1) through (5) of Theorem 3.1.1[2]

   (b) $\psi < \psi_{2k+1}$ with $\sin\psi_{2k+1} \leq r\cos\gamma, \quad \text{for } r \in (a,1)$

   (c) there exists a unique $c_{2k} \in (a,1)$ such that

   $$\begin{cases} u_{2k+2} < u_{2k}\,, & r \in [a, c_{2k}) \\ u_{2k+2} > u_{2k}\,, & r \in (c_{2k}, 1] \end{cases} \tag{4.40}$$

   From (b), Lemma 4.1.2 requires there to exist a unique $b_{2k+1} \in (a,1)$ with

   $$\begin{cases} u > u_{2k+1}\,, & r \in [a, b_{2k+1}) \\ u < u_{2k+1}\,, & r \in (b_{2k+1}, 1] \end{cases} \tag{4.41}$$

   Using the difference function

   $$r\sin\psi - r\sin\psi_{2k+2} = B\int_a^r s(u - u_{2k+1})\,ds \tag{4.42}$$

   it can be shown

   $$\sin\psi_{2k+2} < \sin\psi < r\cos\gamma, \quad \text{for } r \in (a,1). \tag{4.43}$$

[2] u_{2k} does not have to satisfy the boundary conditions.

(4.43) implies $\psi_{2k+2} < \psi$ on $(a, 1)$. Lemma 4.1.2 can be used again:

$$\begin{cases} u < u_{2k+2}\,, & r \in [a, b_{2k+2}) \\ u > u_{2k+2}\,, & r \in (b_{2k+2}, 1] \end{cases} \tag{4.44}$$

and a new difference function

$$r \sin\psi - r \sin\psi_{2k+3} = B \int_a^r s(u - u_{2k+2})\, ds \tag{4.45}$$

produces $\psi < \psi_{2k+3}$ on $(a, 1)$. It must now be verified that u_{2k+3} is defined. For this, we use

$$r \sin\psi_{2k+1} - r \sin\psi_{2k+3} = B \int_a^r s(u_{2k} - u_{2k+2})\, ds \tag{4.46}$$

along with (c) to reason that

$$\sin\psi_{2k+3} < \sin\psi_{2k+1} < r\cos\gamma, \quad \text{for } r \in (a, 1), \tag{4.47}$$

and with B restricted as hypothesized, u_{2k+3} now obeys (1) through (5) of Theorem 3.1.1. Lemma 4.1.2 ensures

$$\begin{cases} u_{2k+3} > u_{2k+1}\,, & r \in [a, c_{2k+1}) \\ u_{2k+3} < u_{2k+1}\,, & r \in (c_{2k+1}, 1] \end{cases} \tag{4.48}$$

As a final step, we can similarly argue that u_{2k+4} satisfies Theorem 3.1.1 since

$$\sin\psi_{2k+2} < \sin\psi_{2k+4} < \sin\psi < r\cos\gamma \tag{4.49}$$

with

$$\begin{cases} u_{2k+4} < u_{2k+2}\,, & r \in [a, c_{2k+2}) \\ u_{2k+4} > u_{2k+2}\,, & r \in (c_{2k+2}, 1] \end{cases} \tag{4.50}$$

The cycle is now complete as (a), (b) and (c) are proved for the next increment of k. In addition, the above discussion provides the following summary:

$$\psi_{2k+2} < \psi_{2k+4} < \cdots < \psi < \cdots < \psi_{2k+3} < \psi_{2k+1}, \quad \text{for } r \in (a, 1). \tag{4.51}$$

It remains to verify that (a), (b) and (c) are true for the base case $k = 0$. However, these were shown as a result of Theorems 4.1.1 and 4.1.3, making (4.51) true for all $k \geq 0$:

$$\psi_2 < \psi_4 < \cdots < \psi < \cdots < \psi_3 < \psi_1, \quad \text{for } r \in (a, 1) \tag{4.52}$$

2. Apply Lemma 4.1.2 to each adjacent pair of angles in (4.52) to arrive at

$$u_1(a) < u_3(a) < \cdots < u(a) < \cdots < u_4(a) < u_2(a) \tag{4.53}$$

3. The same analysis in (2) will produce

$$u_2(1) < u_4(1) < \cdots < u(1) < \cdots < u_3(1) < u_1(1). \quad \blacklozenge \tag{4.54}$$

Using the numerical procedure, Figs. 4.3 and 4.4 demonstrate the interleaving properties for a specific choice of parameters. Because Theorem 4.1.4 requires values of a, γ and B that cause rapid convergence, it is difficult to identify individual iterates in a plot. Instead, a selection of parameters is used where the configuration of Fig. 4.1 still holds numerically and the resulting interleaving nature is more apparent.

4.2 Double Intersection Case

In contrast to the iterates of Siegel (they consistently intersect once with u_0, resulting in interleaving properties throughout), here it is also possible to find selections of a, γ and B where u and u_2 intersect twice with u_0. In this case, there exist exactly two points b_{01} and b_{02} in $(a, 1)$ such that $u(b_{01}) = u(b_{02}) = u_0$ with

$$\begin{cases} u > u_0\,, & r \in [a, b_{01}) \\ u < u_0\,, & r \in (b_{01}, b_{02}) \\ u > u_0\,, & r \in (b_{02}, 1] \end{cases} \tag{4.55}$$

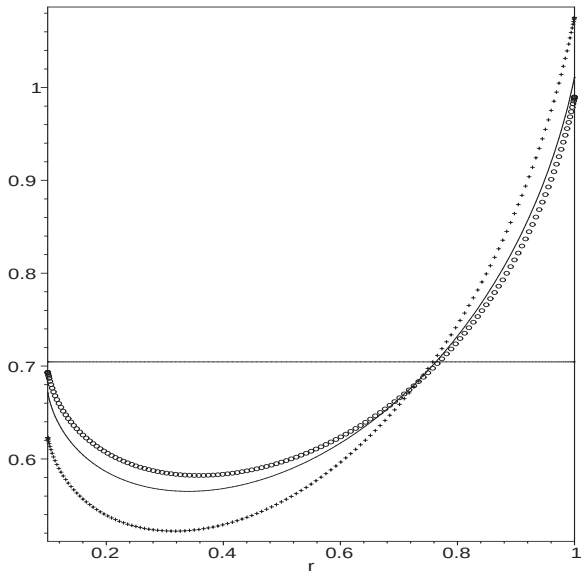

Figure 4.3: Numerical approximation of u_n vs. r $(n = 0, \ldots, 3)$, showing interleaving properties. Here, $a = 0.1$, $\gamma = \frac{\pi}{10}$ and $B = 3$. Iterates are drawn as {*solid line, cross, circle, solid curve*}

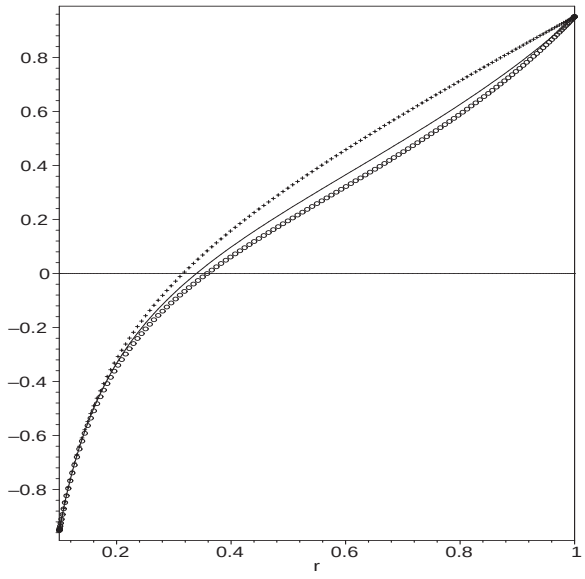

Figure 4.4: Numerical approximation of $\sin\psi_n$ vs. r $(n = 0, \ldots, 3)$, showing interleaving properties. Iterates are drawn as {*solid line, cross, circle, solid curve*} and the parameters are identical to Fig. 4.3.

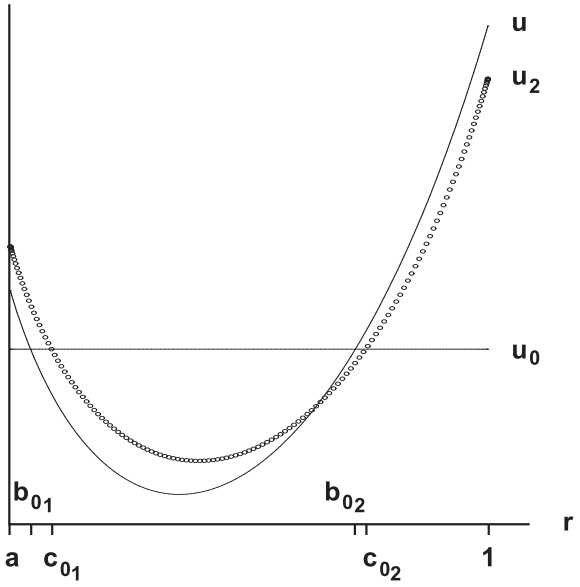

Figure 4.5: Configuration considered for double intersection case. u and u_2 must be arranged as noted with respect to u_0. The orientation between u and u_2 is not important.

As well, there exist exactly two points c_{01} and c_{02} in $(a, 1)$ such that $u_2(c_{01}) = u_2(c_{02}) = u_0$ and

$$\begin{cases} u_2 > u_0\,, & r \in [a, c_{01}) \\ u_2 < u_0\,, & r \in (c_{01}, c_{02}) \\ u_2 > u_0\,, & r \in (c_{02}, 1] \end{cases} \tag{4.56}$$

Fig. 4.5 demonstrates these configurations. The effect of (4.55) and (4.56) on subsequent iterates is far more varied and less understood. As before, we begin by examining the conditions necessary for (4.55) and (4.56) to occur.

4.2.1 Double Intersection of u with u_0

To show the arrangement in (4.55) is indeed possible, we look for conditions in which

$$u(a) > u_0. \tag{4.57}$$

(4.55) will then be shown as a consequence of (4.57). As before, we need to compare $u(a)$ with $u_1(a)$ and we first consider the conditions required for $u_1(a) > u_0$. Using (4.4),

$$u_0 - u_1(a) = \frac{1}{1-a^2}\int_a^1 (1-s^2)\frac{\sin\psi_1}{\sqrt{1-\sin^2\psi_1}}\,ds,$$

the integrand can now be bounded from above. For $a \le r \le \sqrt{a}$, where $\frac{\sin\psi_1}{\sqrt{1-\sin^2\psi_1}} \le 0$, note that

$$\frac{\sin\psi_1}{\sqrt{1-\sin^2\psi_1}} \le \sin\psi_1 = \frac{\cos\gamma}{1-a}\left(r - \frac{a}{r}\right). \tag{4.58}$$

On $\sqrt{a} \le r \le 1$, $\sin\psi_1$ is increasing, and for $\gamma \neq 0$:

$$\frac{\sin\psi_1}{\sqrt{1-\sin^2\psi_1}} \le \frac{\sin\psi_1}{\sqrt{1-\sin^2\psi_1(1)}} = \frac{\sin\psi_1}{\sqrt{1-\cos^2\gamma}} = \frac{\sin\psi_1}{\sin\gamma}. \tag{4.59}$$

Substituting these bounds into (4.4) gives

$$\begin{aligned} u_0 - u_1(a) &< \frac{1}{1-a^2}\left[\int_a^{\sqrt{a}} (1-s^2)\frac{\cos\gamma}{1-a}\left(s-\frac{a}{s}\right)ds \right. \\ &\quad \left. + \int_{\sqrt{a}}^1 (1-s^2)\frac{\cos\gamma}{(1-a)\sin\gamma}\left(s-\frac{a}{s}\right)ds\right] \qquad (4.60) \\ &= \frac{1}{1-a^2}\left[\frac{a\cos\gamma(a^3-2a^2-a+2+2\log a)}{4(1-a)}\right. \\ &\quad \left. + \frac{\cos\gamma(1-a^2+2a\log a)}{4\sin\gamma(1-a)}\right] \qquad (4.61) \end{aligned}$$

and since $\log a < (a-1) - \frac{1}{2}(a-1)^2 + \frac{1}{3}(a-1)^3$ on $(0,1)$,

$$\begin{aligned} u_0 - u_1(a) &< \frac{\cos\gamma}{4(1-a)(1-a^2)}\left[-\frac{5}{3}a(1-a)^3 + \frac{1}{3\sin\gamma}(3-2a)(1-a)^3\right] \qquad (4.62) \\ &= \frac{\cos\gamma(1-a)}{12(1+a)}\left[\frac{3-2a}{\sin\gamma} - 5a\right] \qquad (4.63) \end{aligned}$$

To ensure $u_1(a) > u_0$, the term in square brackets must be nonpositive:

$$\begin{aligned} \frac{3-2a}{\sin\gamma} - 5a &\le 0 \qquad (4.64) \\ \implies \quad a &\ge \frac{3}{5\sin\gamma + 2} \qquad (4.65) \end{aligned}$$

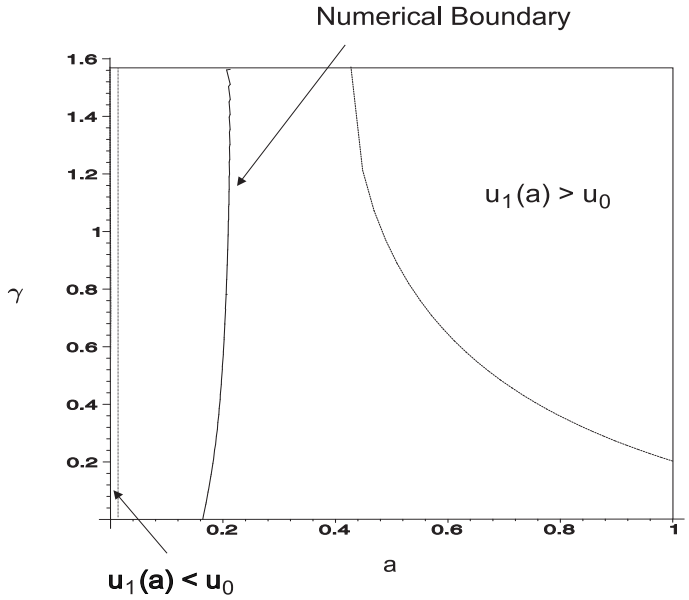

Figure 4.6: Regions of the parameter space (a, γ) where $u_1(a)$ has been shown to lie above and below u_0. A numerical approximation of the actual boundary is also included.

and physically, $a < 1$ which restricts γ to

$$\gamma > \arcsin\left(\frac{1}{5}\right) \doteq 0.2. \tag{4.66}$$

We now have $u_1(a) > u_0$ for $\gamma > \arcsin\left(\frac{1}{5}\right)$ and $a \geq \frac{3}{5\sin\gamma+2}$.

Fig. 4.6 illustrates the regions of the parameter space (a, γ) where $u_1(a)$ has been shown in this chapter to lie below and above u_0. As well, Fig. 4.7 plots $(u_0 - u_1(a))$ over the parameter space using the same numerical integration technique employed for the iterative procedure. The zero contour of this graph has also been superimposed onto Fig. 4.6, showing the approximate boundary curve between regions. Although existence of the two regions was demonstrated above, it may be possible to enlarge these sets by improving the bounds on (4.4). This provides an opportunity for further investigation.

Similar to the previous section, we are now able to find B so that $u(a)$ is forced to lie above u_0.

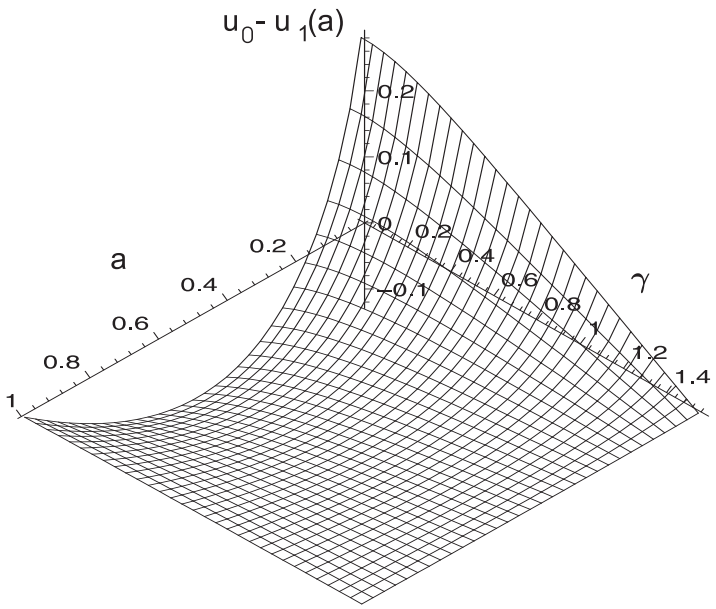

Figure 4.7: Numerical plot of $(u_0 - u_1(a))$ over the parameter space (a, γ).

Theorem 4.2.1 *For a given* $\gamma \in \left(\arcsin\left(\frac{1}{5}\right), \frac{\pi}{2}\right)$, *select* $a \geq \frac{3}{5\sin\gamma+2}$ *and*

$$B \leq \frac{\cos\gamma(1-a)^2}{6\pi}\left(5a - \frac{3-2a}{\sin\gamma}\right).$$

Under these conditions, there exist exactly two points $b_{01}, b_{02} \in (a, 1)$ *such that* $u(b_{01}) = u(b_{02}) = u_0$ *with*

$$\begin{cases} u > u_0\,, & r \in [a, b_{01}) \\ u < u_0\,, & r \in (b_{01}, b_{02}) \\ u > u_0\,, & r \in (b_{02}, 1] \end{cases}$$

Proof. Since

$$B \leq \frac{\cos\gamma(1-a)^2}{6\pi}\left(5a - \frac{3-2a}{\sin\gamma}\right) < 1 \tag{4.67}$$

(see the Appendix, Theorem A.0.12), u_1 is again defined according to Theorem 3.1.1. An analagous proof to Theorem 4.1.1 yields

$$\begin{aligned} u_0 - u(a) &\leq (u_0 - u_1(a)) + |u_1(a) - u(a)| && (4.68) \\ &< \frac{\cos\gamma(1-a)}{12(1+a)}\left(\frac{3-2a}{\sin\gamma} - 5a\right) + C(\gamma, m)B\frac{\pi}{2(1-a^2)} && (4.69) \end{aligned}$$

$$< \quad \frac{\cos\gamma(1-a)}{12(1+a)}\left(\frac{3-2a}{\sin\gamma}-5a\right)+B\frac{\pi}{2(1-a^2)} \tag{4.70}$$

and inserting the condition on B produces

$$u(a) > u_0. \tag{4.71}$$

Finally, the volume condition ensures that u and u_0 intersect, and the convexity of u, along with $u(a) < u(1)$ and (4.71) implies there exist exactly two intersection points. The configuration of (4.55) follows. ♦

4.2.2 Double Intersection of u_2 with u_0

We now aim to find conditions so that (4.56) exists. Unlike the previous section, we are unable to prove that $\sin\psi_2 < r\cos\gamma$ on $(a,1)$. Numerical experiments, however, seem to validate this bound for positive iterates. It is thus assumed that $\sin\psi_2 < r\cos\gamma$ for the following theorem.

Theorem 4.2.2 *For a given* $\gamma \in (\arcsin\left(\frac{1}{5}\right), \frac{\pi}{2})$, *select* $a \geq \frac{3}{5\sin\gamma+2}$ *and*

$$B \leq \frac{\cos\gamma(1-a)^2}{12\pi}\left(5a-\frac{3-2a}{\sin\gamma}\right).$$

Furthermore, assume $\sin\psi_2 < r\cos\gamma$ *on* $(a,1)$. *Here, there exist exactly two points* $c_{01}, c_{02} \in (a,1)$ *such that* $u_2(c_{01}) = u_2(c_{02}) = u_0$ *and*

$$\begin{cases} u_2 > u_0\,, & r \in [a, c_{01}) \\ u_2 < u_0\,, & r \in (c_{01}, c_{02}) \\ u_2 > u_0\,, & r \in (c_{02}, 1] \end{cases}$$

Proof. We use a similar proof to Theorem 4.1.3:

$$\begin{aligned} u_0 - u_2(a) &\leq (u_0 - u(a)) + |u(a) - u_2(a)| && (4.72)\\ &< \frac{\cos\gamma(1-a)}{12(1+a)}\left(\frac{3-2a}{\sin\gamma}-5a\right) \\ &\quad + B\frac{\pi}{2(1-a^2)}\left(1+B\frac{\pi}{2(1-a^2)}\right) && (4.73) \end{aligned}$$

Substituting for B gives

$$u_2(a) > u_0. \tag{4.74}$$

As well, we show that $u_2(1) > u_0$:

$$u_0 - u_2(1) \leq (u_0 - u_1(1)) + |u_1(1) - u(1)| + |u(1) - u_2(1)| \tag{4.75}$$

and since $u_1(a) < u_1(1)$ (see Appendix, Theorem A.0.13),

$$u_0 - u_2(1) < (u_0 - u_1(a)) + B\frac{\pi}{2(1-a^2)} + \left(B\frac{\pi}{2(1-a^2)}\right)^2 \tag{4.76}$$

$$< \frac{\cos\gamma(1-a)}{12(1+a)}\left(\frac{3-2a}{\sin\gamma} - 5a\right) + B\frac{\pi}{2(1-a^2)}\left(1 + B\frac{\pi}{2(1-a^2)}\right) \tag{4.77}$$

Considering the restriction on B, this results in

$$u_2(1) > u_0. \tag{4.78}$$

As before, u_2 is monotone decreasing on $[a, m_2)$ and montone increasing on $(m_2, 1]$. We use this fact along with the volume condition, (4.74) and (4.78) to reason there exist exactly two intersections between the functions, with u_0 and u_2 positioned as in (4.56).

♦

Using the theorems developed here, the double intersection case given by configurations (4.55) and (4.56) does not necessarily apply to all fluid/solid combinations. However, for those surfaces where $\gamma \in (\arcsin\left(\frac{1}{5}\right), \frac{\pi}{2})$, we may select

$$R_1 = \frac{3}{5\sin\gamma + 2}R_2 \tag{4.79}$$

with R_2 satisfying

$$B = \kappa {R_2}^2 \leq \frac{\cos\gamma(1-a)^2}{12\pi}\left(5a - \frac{3-2a}{\sin\gamma}\right). \tag{4.80}$$

and, provided[3] that $\sin\psi_2 < r\cos\gamma$ on $(a, 1)$, Theorems 4.2.1 and 4.2.2 ensure the double intersection case takes place.

[3]The inclination angle is considered in the non–dimensionalized variables.

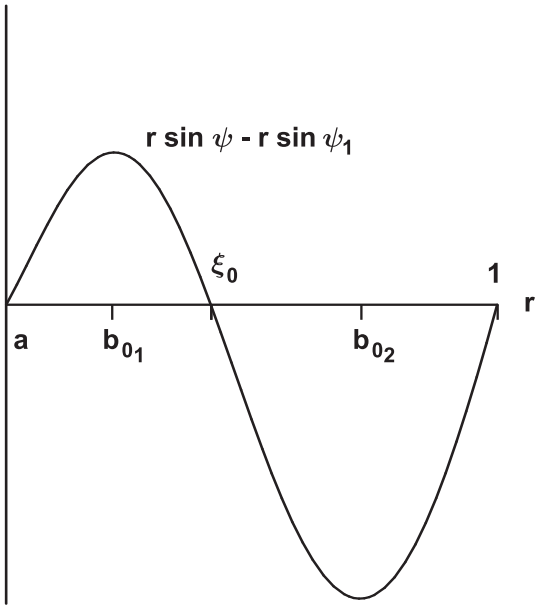

Figure 4.8: Configuration of $r\sin\psi - r\sin\psi_1$.

4.2.3 Resultant Behaviours of Double Intersections

Unlike the single intersection case which led to the iterates being organized as described in Theorem 4.1.4, the double intersection case produces a number of possible configurations. These are outlined below.

Given the arrangement of (4.55), we first examine how u_1 might behave with respect to u by considering the difference function

$$r\sin\psi - r\sin\psi_1 = B\int_a^r s(u-u_0)\,ds \tag{4.81}$$

and its derivative

$$(r\sin\psi - r\sin\psi_1)_r = Br(u-u_0). \tag{4.82}$$

In addition to (4.81) being zero at $r = a$ and $r = 1$, there exist extrema at $r = b_{01}$ and $r = b_{02}$. Since $u(a) > u_0$, (4.81) must take the form of Fig. 4.8, where there exists

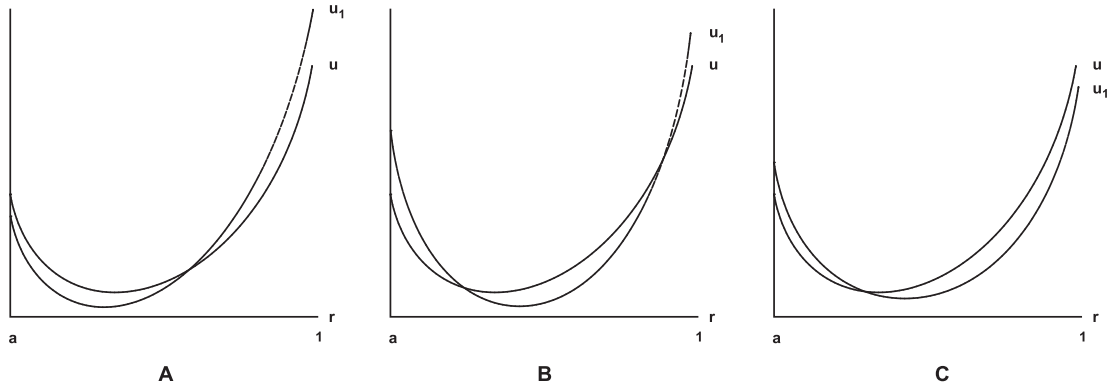

Figure 4.9: Potential configurations of u with u_1, assuming (4.55) holds.

a unique $\xi_0 \in (b_{01}, b_{02})$ such that $\psi(\xi_0) = \psi_1(\xi_0)$ with

$$\begin{cases} \psi > \psi_1\,, & r \in (a, \xi_0) \\ \psi < \psi_1\,, & r \in (\xi_0, 1) \end{cases} \tag{4.83}$$

When (4.83) is considered in conjunction with the volume condition, three configurations of u with u_1 are possible as illustrated in Fig. 4.9[4]. Using a similar analysis to the previous section, we see that if configuration A or C is attained, subsequent iterates will intersect only once with u. Specifically, for configuration A,

$$\begin{cases} u_{2n+1}(a) < u(a) < u_{2n+2}(a) \\ u_{2n+2}(1) < u(1) < u_{2n+1}(1) \end{cases} \tag{4.84}$$

or for configuration C,

$$\begin{cases} u_{2n+2}(a) < u(a) < u_{2n+1}(a) \\ u_{2n+1}(1) < u(1) < u_{2n+2}(1) \end{cases} \tag{4.85}$$

[4]Before progressing further, it should be noted that we are unable to claim $\sin\psi_n < r\cos\gamma$ for $n \geq 2$ without providing additional restrictions. Hence, Theorem 3.1.1 cannot be automatically applied to $\{u_n\}$ in the double intersection case, and existence of the iterates is not proven. However, numerical experiments suggest the iterates do exist in this scenario and we shall assume $\{u_n\}$ exhibits the properties of Theorem 3.1.1.

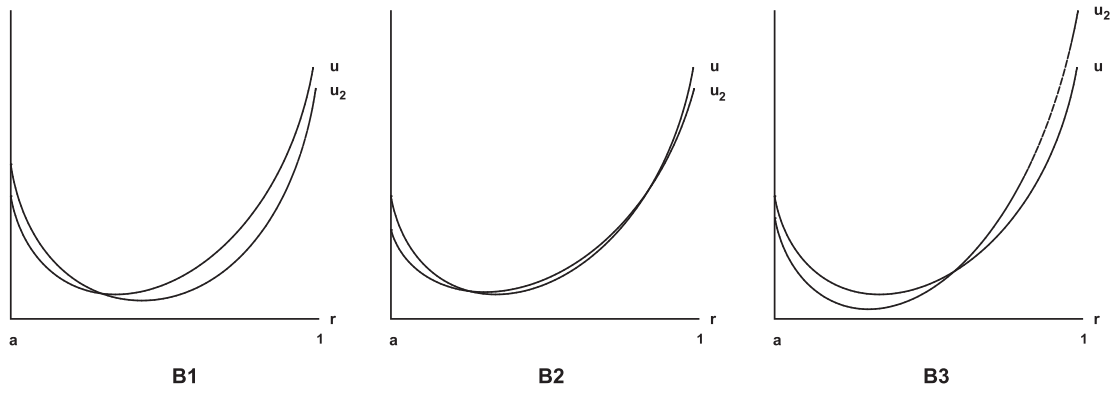

Figure 4.10: Potential configurations of u with u_2, originating from Fig. 4.9, B.

for $n \geq 0$. In configuration B, there are two points of intersection (which can be defined as b_{11} and b_{12}) and we use

$$r \sin \psi - r \sin \psi_2 = B \int_a^r s(u - u_1)\, ds \tag{4.86}$$

to show there exists a unique $\xi_1 \in (b_{11}, b_{12})$ such that $\psi(\xi_1) = \psi_2(\xi_1)$ with

$$\begin{cases} \psi < \psi_2\,, & r \in (a, \xi_1) \\ \psi > \psi_2\,, & r \in (\xi_1, 1) \end{cases} \tag{4.87}$$

At the next iterate level, configuration B thus produces three potential arrangements of u_2 with u (Fig. 4.10). A similar analysis as performed on A, B and C can be applied here.

Considering the arrangement of (4.56) separately, we can similarly comment on the behaviour of u_3 versus u_1. Again, the difference function

$$r \sin \psi_1 - r \sin \psi_3 = B \int_a^r s(u_0 - u_2)\, ds \tag{4.88}$$

implies there exists a unique $\lambda_0 \in (c_{01}, c_{02})$ such that $\psi_1(\lambda_0) = \psi_3(\lambda_0)$ with

$$\begin{cases} \psi_1 < \psi_3\,, & r \in (a, \lambda_0) \\ \psi_1 > \psi_3\,, & r \in (\lambda_0, 1) \end{cases} \tag{4.89}$$

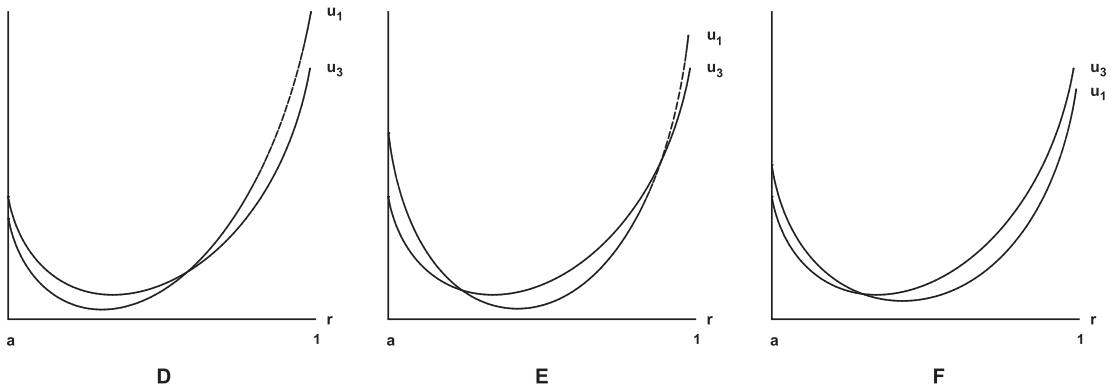

Figure 4.11: Potential configurations of u_1 with u_3, assuming (4.56) holds.

and three arrangements of u_1 with u_3 are possible, as in Fig. 4.11. Configuration D leads to the predictable behaviour

$$\begin{cases} \{u_{2n+2}(a)\} \text{ and } \{u_{2n+1}(1)\} \text{ are decreasing for } n \geq 0. \\ \{u_{2n+1}(a)\} \text{ and } \{u_{2n+2}(1)\} \text{ are increasing for } n \geq 0. \end{cases} \tag{4.90}$$

and likewise configuration F produces:

$$\begin{cases} \{u_{2n+1}(a)\} \text{ and } \{u_{2n+2}(1)\} \text{ are decreasing for } n \geq 0. \\ \{u_{2n+2}(a)\} \text{ and } \{u_{2n+1}(1)\} \text{ are increasing for } n \geq 0. \end{cases} \tag{4.91}$$

Configuration E will again split into three possible arrangements between u_2 and u_4. As one might expect, the configurations of Fig. 4.9 could concievably occur with any arrangement from Fig. 4.11, leading to a far more complex behaviour than in the single intersection case. Nevertheless, some pairings will again lead to interleaving iterates. This occurs, for example, when configuration A is paired with configuration D. Indeed, when properties (4.84) and (4.90) are matched, the interleaving properties are recovered for subsequent iterates. The same can be said of pairing configuration C with configuration F. However, if these couples were cross–matched (i.e. A–F or C–D), the combined properties would result in diverging iterates, yet this has never been

observed during any numerical experiment involving positive iterates. Further research is needed to fully understand the properties of $\{u_n\}$ over the complete parameter space.

Chapter 5

Numerical Method

5.1 Introduction

In this chapter, we propose a numerical method to estimate the iterates $\{u_n\}$ generated by the procedure introduced in Chapter 3:

$$\sin\psi_{n+1}(r) = \frac{B}{r}\int_a^r s u_n(s)\,ds - \frac{a}{r}\cos\gamma \tag{5.1}$$

$$u_{n+1}(r) = u_{n+1}(a) + \int_a^r \frac{\sin\psi_{n+1}(s)}{\sqrt{1-\sin^2\psi_{n+1}(s)}}\,ds \tag{5.2}$$

with

$$u_{n+1}(a) = \frac{2\cos\gamma}{B(1-a)} - \frac{1}{1-a^2}\int_a^1 (1-s^2)\frac{\sin\psi_{n+1}(s)}{\sqrt{1-\sin^2\psi_{n+1}(s)}}\,ds \tag{5.3}$$

and $u_0 = \frac{2\cos\gamma}{B(1-a)}$. Equations (5.1)–(5.3) suggest an iterative scheme using successive applications of numerical integration. For instance, we envisage subdividing $[a,1]$ using N grid points labelled $x_j^N, 1 \le j \le N$ (with $x_1^N = a$ and $x_N^N = 1$). Starting with

$$\sin\psi_1(r) = \frac{\cos\gamma}{1-a}\left(r - \frac{a}{r}\right) \tag{5.4}$$

(this is the highest iterate explicitly known), $u_1(a)$ could be computed using an appropriate integration technique. Following this, the integral in (5.2) would be evaluated

at each $r = x_j^N$, thus estimating u_1 over all grid points. These values could then be used in (5.1) to approximate $\sin\psi_2$ on x_j^N, and the process continues until the desired number of iterates are calculated.

Below, we suggest numerical techniques to evaluate the integrals in (5.1)–(5.3) which will include the possibility that $\gamma = 0$. Note that our investigation will be mostly concerned with

$$B < \frac{2a(1-a^2)\cos\gamma}{2(1+a)(1-a)^2\, C(\gamma, m) + a\pi\cos\gamma} \tag{5.5}$$

so that the iterates are guaranteed to be defined and continuous on $[a, 1]$. Section 5.4, however, considers some numerical experiments where B is extended beyond restriction (5.5).

5.2 IMT Method

As an additional consequence of (5.5), recall that the inclination angle of u_n will satisfy

$$-\frac{a\cos\gamma}{s} < \sin\psi_n < s\cos\gamma, \quad \text{for } s \in (a, 1) \tag{5.6}$$

with $\sin\psi_n(a) = -\cos\gamma$ and $\sin\psi_n(1) = \cos\gamma$. Consequently, the integrands of (5.2) and (5.3) are continuous on $[a, 1]$ for $\gamma \neq 0$. However for $\gamma = 0$, we use that

$$-\frac{a}{\sqrt{s^2 - a^2}} < \frac{\sin\psi_n(s)}{\sqrt{1 - \sin^2\psi_n(s)}} < \frac{s}{\sqrt{1 - s^2}}, \quad \text{for } s \in (a, 1) \tag{5.7}$$

to claim:

- the integrand in (5.2) exhibits singularities of the form $(s-a)^\alpha$ and $(1-s)^\beta$, where $\alpha = \beta = -\frac{1}{2}$.
- the integrand in (5.3) possesses a singularity of the form $(s-a)^\alpha$ (the additional factor of $(1-s^2)$ bounds the integrand at $s = 1$).

In either case, both (5.2) and (5.3) are integrable and we employ a numerical integration technique known as the IMT method[1] [10] which is designed to handle integrands with potential end point singularities. An outline of the procedure follows. Consider the integral

$$I(a,b) := \int_a^b h(x)\,dx \tag{5.8}$$

where $-\infty < a < b < \infty$, and let

$$\eta(t) = \exp\left(-\frac{c}{1-t^2}\right) \tag{5.9}$$

with $c > 0$. Introduce the change of variables

$$\begin{cases} \phi(t) = a + \frac{b-a}{\lambda}\int_{-1}^{t}\eta(u)\,du, & \text{for } t \in [-1,1] \\ \lambda = \int_{-1}^{1}\eta(u)\,du \end{cases} \tag{5.10}$$

so that (5.8) can be rewritten as

$$I(a,b) = \int_{-1}^{1} h(\phi(t))\phi'(t)\,dt. \tag{5.11}$$

Assume that h is infinitely differentiable on (a,b) and is either:

1. continuous at the end points of $[a,b]$; or
2. exhibits an algebraic singularity of the form $(x-a)^\mu$ or $(x-b)^\nu$ where μ and ν are constants greater than -1.

Given that

$$\phi'(t) = \frac{b-a}{\lambda}\exp\left(-\frac{c}{1-t^2}\right), \tag{5.12}$$

the integrand of (5.11), along with all its derivatives, will vanish at the end points of integration ([10] and [3]). The trapezoidal rule can thus be used to approximate (5.11).

[1] This is also referred to as the IMT-rule.

Specifically, if we divide the interval $[-1,1]$ using N equally spaced grid points, (5.11) is evaluated as

$$\begin{cases} I(a,b) \doteq \frac{2}{N-1}\sum_{k=2}^{N-1} w_k^N h(x_k^N) \\ x_k^N = \phi\left(\frac{2(k-1)}{N-1}-1\right), \quad w_k^N = \phi'\left(\frac{2(k-1)}{N-1}-1\right) \end{cases} \tag{5.13}$$

This algorithm has the advantage of using a single transformation to deal with end point singularities of the form contained in (5.2) and (5.3). Testing by Iri et al. [10] and de Doncker and Piessens [3] also demonstrates this procedure to be of "remarkable reliability, efficiency and accuracy" [3]. As a result, the IMT method should lend itself well to computing the integrals within (5.2) and (5.3).

To accomplish this, define $f_n(x_j^N)$ and $g_n(x_j^N), n \geq 1$ as the numerical approximations of $\sin\psi_n$ and u_n respectively (in the case of $n=1$, $f_1(x_j^N) = \sin\psi_1(x_j^N)$). If $f_n(x_j^N)$ is known, $g_n(x_1^N) \doteq u_n(a)$ can be computed according to (5.13):

$$g_n(x_1^N) = \frac{2}{N-1}\sum_{k=2}^{N-1} w_k^N \left(1-[x_k^N]^2\right)\tilde{f}_n(x_k^N) \tag{5.14}$$

where

$$\tilde{f}_n(x_k^N) = \frac{f_n(x_k^N)}{\sqrt{1-[f_n(x_k^N)]^2}}. \tag{5.15}$$

We are then able to calculate $g_n(x_j^N)$ using the appropriate partial sum of (5.13):

$$g_n(x_j^N) \tag{5.16}$$

$$= g_n(x_1^N) \tag{5.17}$$

$$+ \begin{cases} 0, & j=1 \\ \frac{1}{N-1}w_2^N f(x_2^N), & j=2 \\ \frac{1}{N-1}[w_2^N f(x_2^N) + \sum_{k=3}^{j}\left(w_{k-1}^N f(x_{k-1}^N) + w_k^N f(x_k^N)\right)], & 3 \leq j \leq N-1 \\ \frac{1}{N-1}[w_2^N f(x_2^N) + \sum_{k=3}^{N-1}\left(w_{k-1}^N f(x_{k-1}^N) + w_k^N f(x_k^N)\right) & \\ +w_{N-1}^N f(x_{N-1}^N)], & j=N \end{cases} \tag{5.18}$$

The constant c in (5.9) was selected to be 0.5 for all computations. One criticism [3] of the IMT method emphasizes that some abscissae x_j^N are clustered very close to the end

points of integration, and care must be taken to avoid interval lengths $(x_j^N - x_{j-1}^N)$ being rounded to zero. Smaller values of c lessen this clustering but simultaeously increase the error associated with the method. Using a precision of 20 digits[2], $c = 0.5$ was found experimentally to be the largest value so that rounding problems did not occur.

5.3 Undershot Trapezoidal Rule

The remaining integral found in (5.1) presents a different challenge for numerical approximation, as typified in the following example. With $g_n(x_j^N)$ now known, $f_{n+1}(x_j^N)$ must be computed for $1 \leq j \leq N$. Suppose that for values x_l^N sufficiently close to 1, the numerical algorithm employed overshoots the actual value of the integral. Depending on the severity of the overestsimation, this could result in

$$f_{n+1}(x_l^N) > 1 \tag{5.19}$$

and $g_{n+1}(x_j^N)$ would become undefined. Indeed, by employing the standard trapezoidal rule, this was found to occur for small γ, where $f_{n+1}(x_N^N) \doteq 1$ and there is an increased sensitivity to any overshooting. To avoid such problems, we present an altered version of the trapezoidal rule which should consistently undershoot the integral in (5.1). This will require that the integrand $su_n(s)$ is convex on $[a, 1]$ or, more precisely, that the set of approximate values $x_j^N \cdot g_n(x_j^N)$ will lie along a convex curve. This has yet to be shown and is only conjectured to be true. Still, preliminary tests cannot find an occurance of this method overshooting 1. We begin by dividing the abscissae $x_j^N, 2 \leq j \leq N$, into two groups and label them as

$$X_A \;=\; \{x_j^N : 2 \leq j \leq \left\lceil \frac{N}{2} \right\rceil\} \tag{5.20}$$

[2]Increasing the precision greatly affected the execution time. For an evaluation of six iterates, it was convenient to keep the calculation under one minute. All computations were performed on a Pentium 4 2.00 GHz processor.

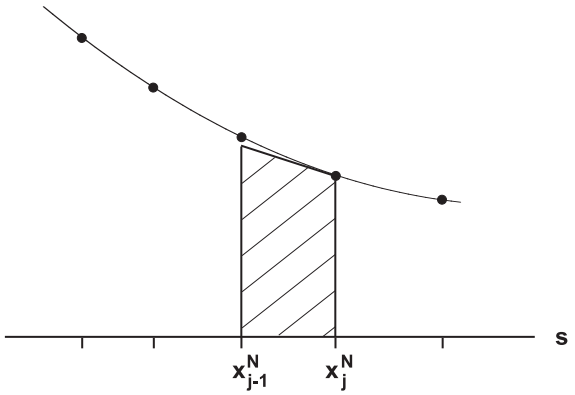

Figure 5.1: Proposed configuration of undershot trapezoid for $x_j^N \in X_A$.

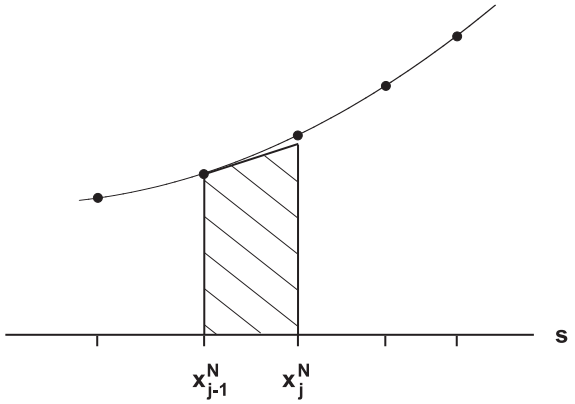

Figure 5.2: Proposed configuration of undershot trapezoid for $x_j^N \in X_B$.

$$X_B \;=\; \{x_j^N : \left\lceil \frac{N}{2} \right\rceil + 1 \le j \le N\} \tag{5.21}$$

Trapezoids are now generated as follows: for $x_j^N \in X_A$, we approximate slope[3] of the integrand at x_j^N and extend the computed tangent backward from x_j^N to x_{j-1}^N as Fig. 5.1 suggests. Provided that the associated errors are not too severe, we expect the trapezoid thus formed on the interval $[x_{j-1}^N, x_j^N]$ to lie below the approximated integrand (displayed as a dotted line in the figure). For $x_j^N \in X_B$, similar trapezoids

[3]The slope of $su_n(s)$ is given as $\frac{s \sin \psi_n(s)}{\sqrt{1-\sin^2 \psi_n(s)}} + u_n(s)$; thus, at x_j^N it is approximated as $x_j^N \cdot \tilde{f}_n(x_j^N) + g_n(x_j^N)$.

can be generated on $[x_{j-1}^N, x_j^N]$ by extending the computed tangent at x_{j-1}^N forward to x_j^N (Fig. 5.2). For each $r = x_j^N$, the integral in (5.1) should be underestimated by summing the areas of the trapezoids to this point. Hence,

$$g_n(x_j^N) = \begin{cases} -\cos\gamma, & j = 1 \\ \frac{B}{x_j^N}\sum_{k=2}^{j}\frac{x_k^N - x_{k-1}^N}{2}\left(\bar{g}_n(x_{k-1}^N) + x_k^N g_n(x_k^N)\right) - \frac{a\cos\gamma}{x_j^N}, & 2 \le j \le \left\lceil \frac{N}{2} \right\rceil \\ \frac{B}{x_j^N}\left(\sum_{k+2}^{\left\lceil \frac{N}{2} \right\rceil}\frac{x_k^N - x_{k-1}^N}{2}\left(\bar{g}_n(x_{k-1}^N) + x_k^N g_n(x_k^N)\right)\right. & \\ \left. + \sum_{k=\left\lceil \frac{N}{2} \right\rceil+1}^{j}\frac{x_k^N - x_{k-1}^N}{2}\left(x_{k-1}^N g_n(x_{k-1}^N) + \hat{g}_n(x_k^N)\right)\right) - \frac{a\cos\gamma}{x_j^N}, & \left\lceil \frac{N}{2} \right\rceil + 1 \le j \le N \end{cases}$$

where

$$\bar{g}_n(x_{k-1}^N) = x_k^N g_n(x_k^N) - \left(x_k^N \tilde{f}_n(x_k^N) + g_n(x_k^N)\right)(x_k^N - x_{k-1}^N) \tag{5.22}$$

$$\hat{g}_n(x_k^N) = x_{k-1}^N g_n(x_{k-1}^N) + \left(x_{k-1}^N \tilde{f}_n(x_{k-1}^N) + g_n(x_{k-1}^N)\right)(x_k^N - x_{k-1}^N) \tag{5.23}$$

Also, by defining the trapezoids differently in X_A and X_B, we avoid computing the slope of the integrand at the end points which will be undefined for $\gamma = 0$.

5.4 Preliminary Results

The above scheme was implemented using Maple, with a number of examples included below. Setting $N = 151$, each figure includes the first four iterates labelled as in Fig. 3.1. We first note Figs. 3.1 and 3.2 in Chapter 3 which are a result of this scheme under condition (5.5). Here, we have strong convergence such that the third and fourth iterates of $\{u_n\}$ differ at most by 8.8×10^{-5}. Figs. 5.3 and 5.4, as well as Figs. 5.5 and 5.6 provide further examples of this convergent behaviour using two extreme cases of contact angle: $\gamma = 0$ and $\gamma = \frac{\pi}{2.1}$. For $\gamma = 0$, the difference between third and fourth iterates is 2.3×10^{-4}, while for $\gamma = \frac{\pi}{2.1}$ it is 2.7×10^{-6}.

It also appears promising that the method can be applied beyond restriction (5.5). In Figs. 5.7 and 5.8, all parameters are held the same as in Figs. 5.3 and 5.4 except B is

increased to 6, far exceeding condition (5.5). Figs. 5.9 and 5.10 also have B increased to 6 from the corresponding example. In both cases, the iterates converge, albeit more slowly, with the difference between third and fourth iterates of $\{u_n\}$ recorded as 6.9×10^{-2} and 1.2×10^{-3} respectively. In fact, we are presently unable to observe diverging iterates for $u_n > 0$, but much testing is needed before the method can be deemed reliable. For instance, Iri et al. [10] provides error analysis for a single application of the IMT method, yet it is unknown how this error propagates through an indefinite number of iterations of this procedure. The same could also be said for the error associated with the undershot trapezoidal rule.

As an addendum, all figures depicting annular capillary surfaces use the sixth iterate generated by the numerical method. At this stage, subsequent iterates are visually indiscernable from one another.

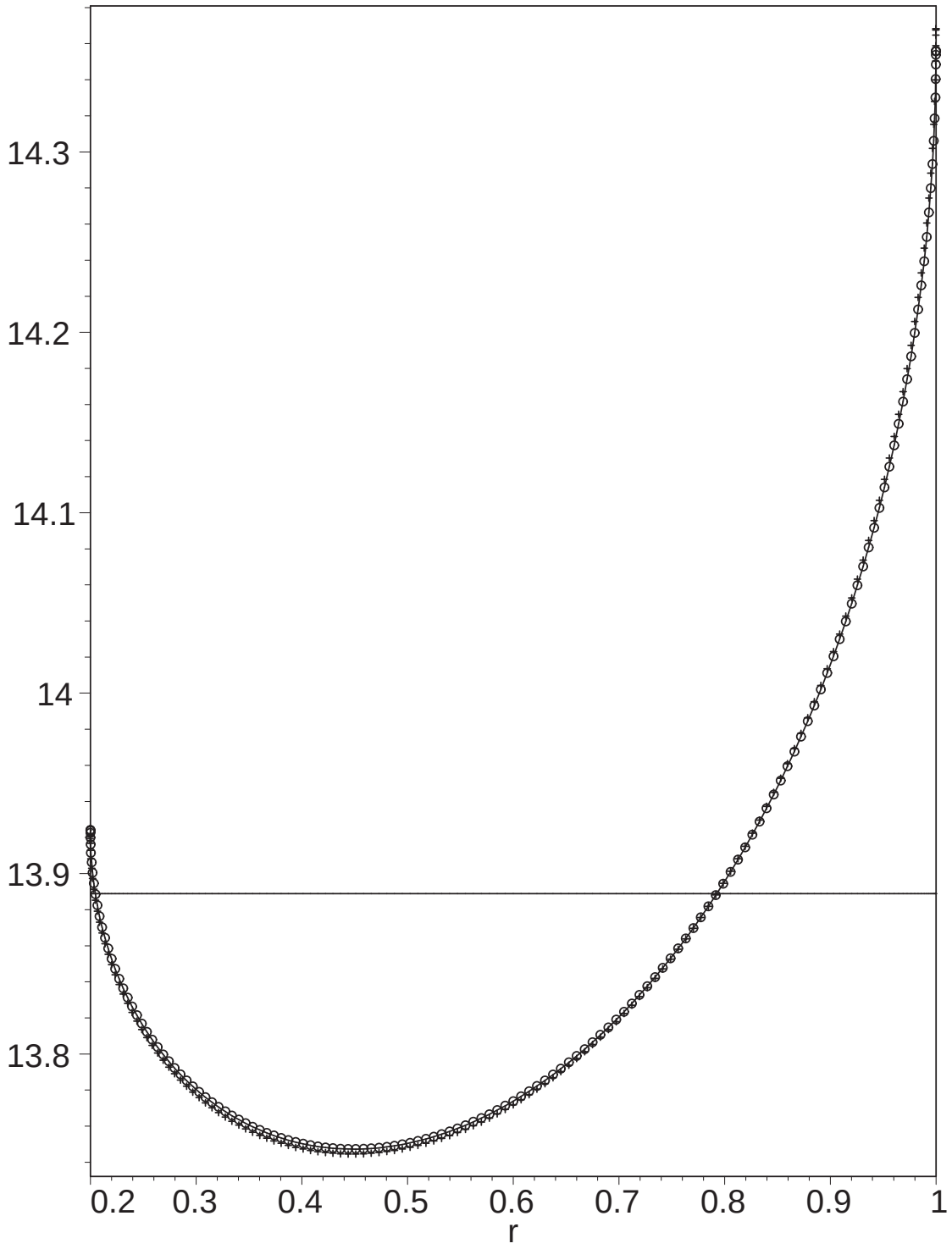

Figure 5.3: Numerical approximation of u_n vs. r for $n = 0, \ldots, 3$ with $a = 0.2$, $\gamma = 0$, $B = 0.18$. Iterates are drawn as {*solid line, cross, circle, solid curve*}.

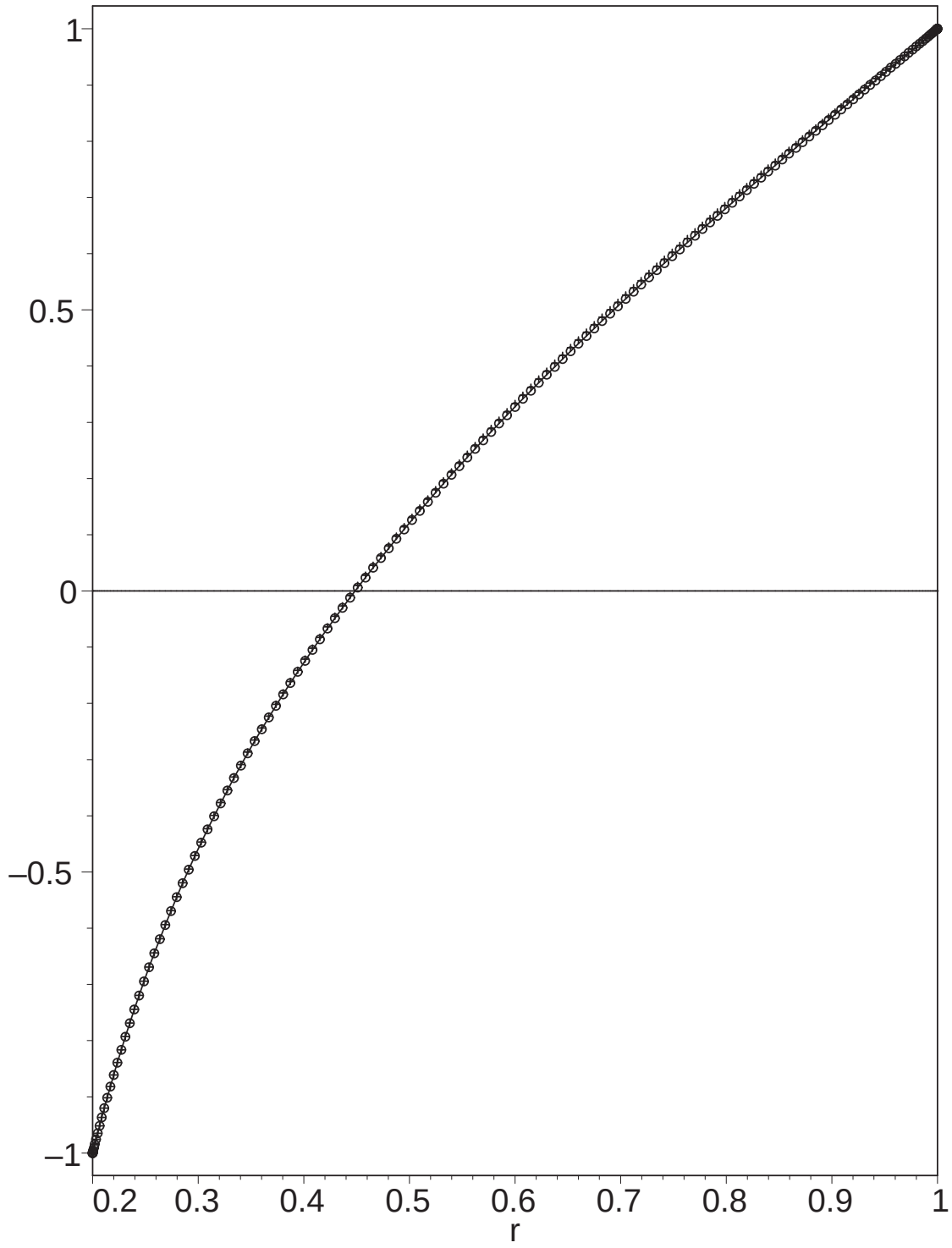

Figure 5.4: Numerical approximation of $\sin\psi_n$ vs. r for $n = 0, \ldots, 3$ with $a = 0.2$, $\gamma = 0$, $B = 0.18$. Iterates are drawn as {*solid line, cross, circle, solid curve*}.

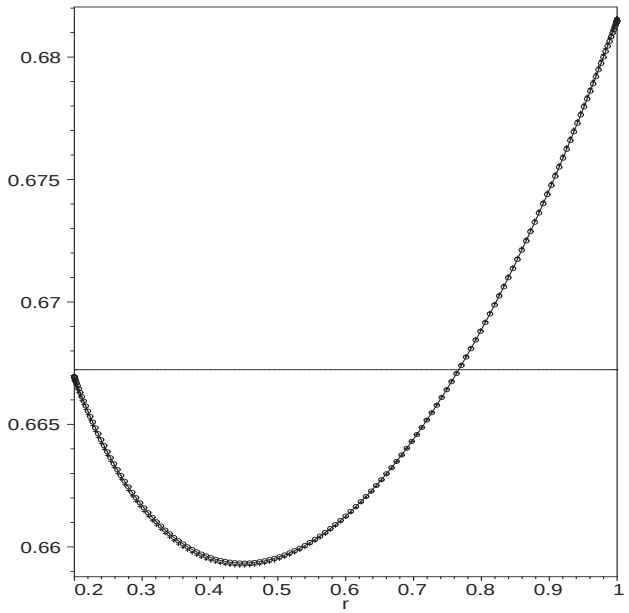

Figure 5.5: Numerical approximation of u_n vs. r for $n = 0, \ldots, 3$ with $a = 0.2$, $\gamma = \frac{\pi}{2.1}$, $B = 0.28$.

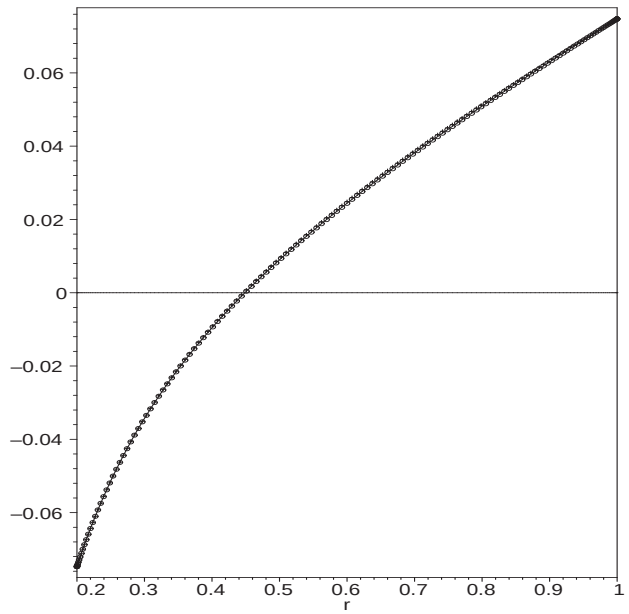

Figure 5.6: Numerical approximation of $\sin\psi_n$ vs. r for $n = 0, \ldots, 3$ with $a = 0.2$, $\gamma = \frac{\pi}{2.1}$, B = 0.28.

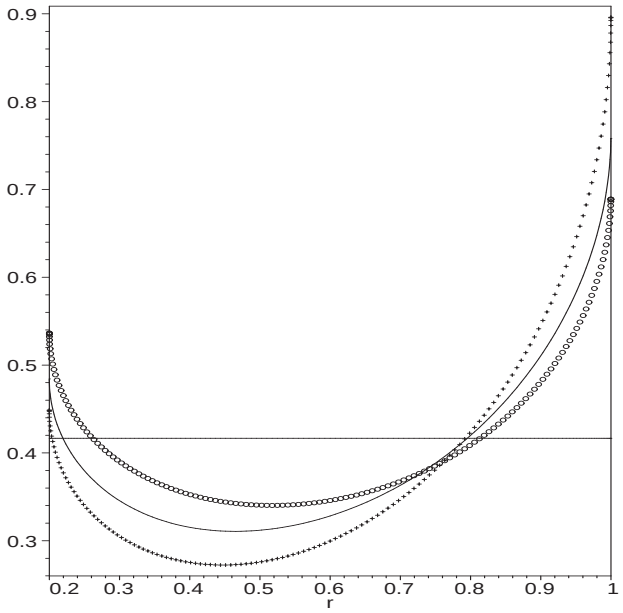

Figure 5.7: Numerical approximation of u_n vs. r for $n = 0, \ldots, 3$ with $a = 0.2$, $\gamma = 0$, $B = 6$.

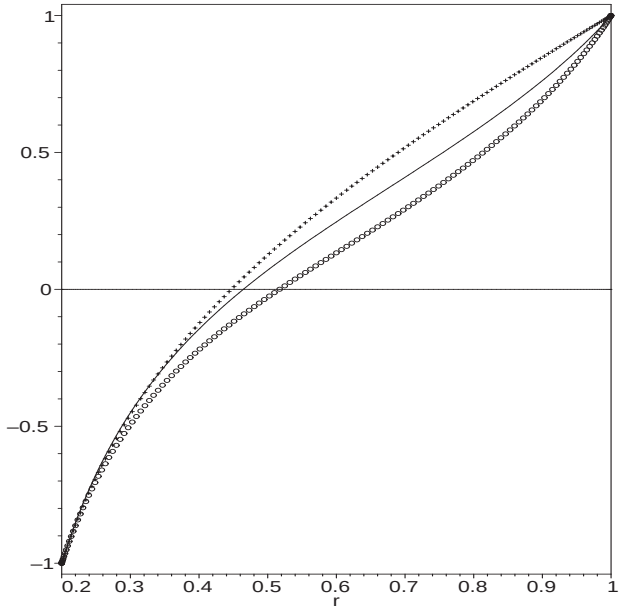

Figure 5.8: Numerical approximation of $\sin\psi_n$ vs. r for $n = 0, \ldots, 3$ with $a = 0.2$, $\gamma = 0$, $B = 6$.

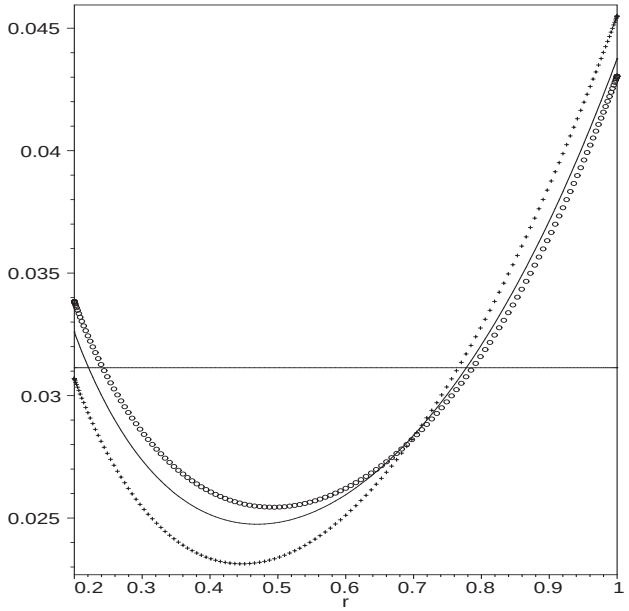

Figure 5.9: Numerical approximation of u_n vs. r for $n = 0, \ldots, 3$ with $a = 0.2$, $\gamma = \frac{\pi}{2.1}$, $B = 6$.

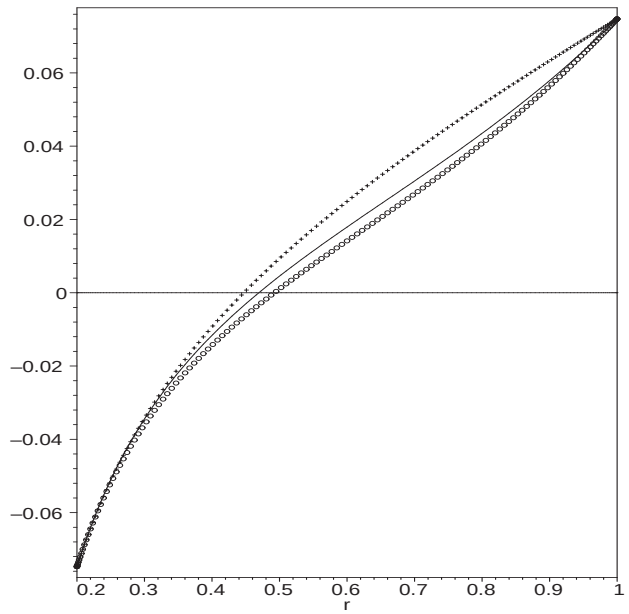

Figure 5.10: Numerical approximation of $\sin \psi_n$ vs. r for $n = 0, \ldots, 3$ with $a = 0.2$, $\gamma = \frac{\pi}{2.1}$, $B = 6$.

5.5 Maple Code

PURPOSE:

The routine calculates an approximation to the sequence of iterates {u_n}
generated by (5.1), (5.2) and (5.3).

```
> restart:
> with(plottools):
```

THE INPUT PARAMETERS:

N - number of grid points

iter - number of iterates to be generated

a - inner radius

gamma - contact angle

B - bond number

c - constant in (5.9) for IMT method

```
> N := 151:
> iter := 4:
> a := 0.3:
> unprotect(gamma):
> gamma := 0:
> B := 2:
> c := 0.5:
```

DEFINITION OF MAJOR VARIABLES:

x - abscissae between a and 1

w - set of values for d/dt(phi(t)) in (5.12)

f - set of approximate values for sin(psi_n), 1 <= n <= iter (note that the first
iterate is indexed by 1 and not 0)

g - set of approximate values for u_n, 1 <= n <= iter

l - set of points in 2D for plotting sin(psi_n)

m - set of points in 2D for plotting u_n

```
> x := array(1..N):
> w := array(1..N):
> f := array(1..N,1..iter+1):
> g := array(1..N,1..iter):
> l := array(1..iter+1):
> m := array(1..iter):
```

Function for the integrand of (5.2) and (5.3)

```
> xi := t  ->  t/sqrt(1-t^2):
```

Functions for the IMT method

```
> eta := t  ->  exp(-c/(1-t^2)):
> lambda := evalf[20](Int(eta(t),t=-1..1)):
> zeta := t  ->  a+(1-a)*t/lambda:
```

Grid size on transformed region [-1,1]

```
> h := 2/(N-1):
```

Assignment of values to abscissae x. For N = 21, 51, 101, 151, 201 values of int(eta(u), u=-1..t) on [-1,1] were pre-calculated to be imported to x using the function zeta.

```
> y := ImportVector("C:\\grid" || N):
> for i from 1 to N do
> x[i] := evalf[20](zeta(y[i])):
> end do:
```

Assignment of values to w

```
> w[1] := 0:
> w[N] := 0:
> for i from 2 to N-1 do
> w[i] := (1-a)/lambda*eta((i-1)*h-1):
> end do:
```

Assignment of sin(psi_1), u_1 and sin(psi_2) as they are known exactly.

```
> for i from 1 to N do
> f[i,1] := 0:
> g[i,1] := 2*cos(gamma)/B/(1-a):
> f[i,2] := evalf[20](cos(gamma)/(1-a)*(x[i]-a/x[i])):
> end do:
> l[1] := [[x[n], f[n,1]] $n=1..N]:
> m[1] := [[x[n], g[n,1]] $n=1..N]:
> l[2] := [[x[n], f[n,2]] $n=1..N]:
```

MAIN LOOP

- calculation of g[-,n] over abscissae x using IMT method

- calculation of f[-,n] over abscissae x using undershot trapezoidal rule

```
> for j from 2 to iter do
> alpha := evalf[20](2*cos(gamma)/(B*(1-a))
> - 1/(1-a^2)*h*(sum((1-x[n]^2)*xi(f[n,j])*w[n],n=2..N-1))):
```

```
> g[1,j] := alpha:
> g[2,j] := evalf[20](alpha + h/2*xi(f[2,j])*w[2]):
> for i from 3 to N-1 do
> g[i,j] := evalf[20](alpha + h/2*xi(f[2,j])*w[2]
> + h/2*sum(xi(f[n-1,j])*w[n-1] + xi(f[n,j])*w[n],n=3..i)):
> end do:
> g[N,j] := evalf[20](alpha + h/2*xi(f[2,j])*w[2]
> + h/2*sum(xi(f[n-1,j])*w[n-1] + xi(f[n,j])*w[n],n=3..N-1)
> + h/2*xi(f[N-1,j])*w[N-1]):
> m[j] := [[x[n], g[n,j]] $n=1..N]:
> f[1,j+1] := -cos(gamma):
> for i from 2 to ceil(N/2) do
> f[i,j+1] := evalf[20](B/x[i]*(sum((x[n]-x[n-1])/2*(x[n-1]*g[n,j]
> - x[n]*xi(f[n,j])*(x[n]-x[n-1])+x[n]*g[n,j]),n=2..i)) - a*cos(gamma)/x[i]):
> end do:
> for i from ceil(N/2)+1 to N do
> f[i,j+1] := evalf[20](B/x[i]*(sum((x[n]-x[n-1])/2*(x[n-1]*g[n,j]
> - x[n]*xi(f[n,j])*(x[n]-x[n-1])+x[n]*g[n,j]), n=2..ceil(N/2))
> + sum((x[n]-x[n-1])/2*(x[n-1]*g[n-1,j] + x[n]*g[n-1,j]
> + x[n-1]*xi(f[n-1,j])*(x[n]-x[n-1])), n=ceil(N/2)+1..i)) - a*cos(gamma)/x[i]):
> end do:
> l[j+1] := [[x[n], f[n,j+1]] $n=1..N]:
> end do:
```

Graphical output of iterates {u_n} and {sin(psi_n)}

```
> plot([m[1],m[2],m[3],m[4]], x=a..1, color=black, style=line,
> linestyle=[1,3,2,1], thickness=2):
> plot([l[1],l[2],l[3],l[4]], x=a..1,color=black, style=line,
> linestyle=[1,3,2,1], thickness=2):
```

Chapter 6

Future Work

As mentioned, capillarity research has only begun to focus on annular surfaces, and numerous (seemingly?) simple geometries have yet to be studied. Indeed, this paper touches on many subjects where extensions are clearly possible. A sample of future work is provided.

Extension 6.0.1 (Continuation of Equal Contact Angle Case) Several opportunities exist for continued research of the annular surfaces studied here (i.e. equal contact angles). Some were mentioned throughout the text and are summarized below.

1. In Chapter 2, attempts were made to determine the behaviour of u as $a \to 1$ for the case $\gamma = 0$. However, no conclusions on the asymptotics have been reached. Determining this behaviour would help to complete the qualitative properites of u.

2. Chapter 4 involved determining selections of a, γ and B where the iterates $\{u_n\}$ exhibited single or double intersection behaviour. The current bounds still appear overly restrictive and possibly could be improved.

3. Further investigation is needed to fully understand the double intersection behaviour noted in Chapter 4.

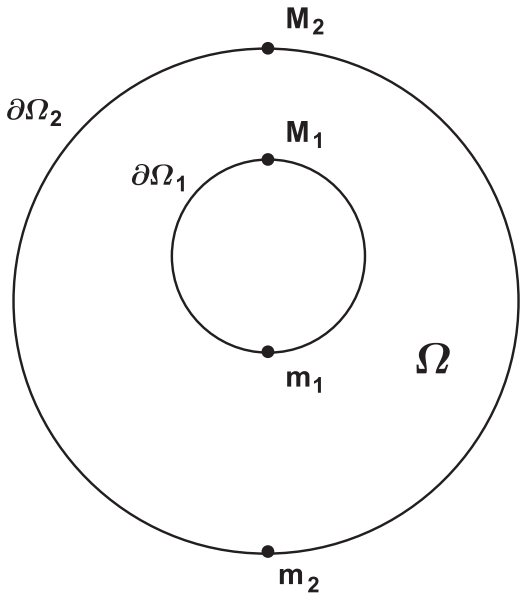

Figure 6.1: Offset annular region Ω with proposed positions of boundary extrema.

4. A formal analysis of the numerical method proposed in Chapter 5 is needed.

Extension 6.0.2 (Generalization of Contact Angles) It is expected that many of the results derived here could be generalized to solutions of the boundary value problem (1.12), where the contact angles γ_1 and γ_2 are not assumed to be equal. These generalizations may include:

1. determining conditions under which the iterative procedure of Chapter 3 (modified to accommodate arbitrary contact angles) converges to solutions of (1.12).

2. verifying that the numerical method of Chapter 5 (appropriately modified) can be applied to this case.

3. investigating if the minimum position $r = m$ maintains its monotonicity with respect to a, and whether conditions can be found so that $m \in \left(\frac{1+a}{2}, 1\right)$.

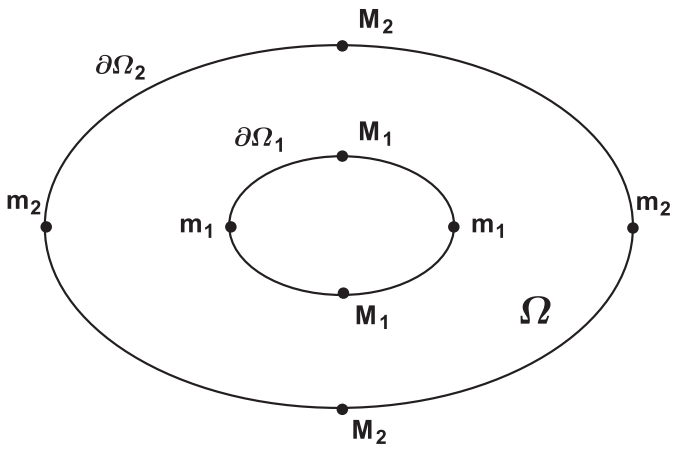

Figure 6.2: Elliptic annular region Ω with proposed positions of boundary extrema.

4. examining the conditions necessary for $u(a) < u(1)$; is it possible to have $u(a) > u(1)$?

Extension 6.0.3 (Offset Annulus) A more complex geometry is offered by the "annular" domain in which the inner boundary is off-centre from the outer boundary (Fig. 6.1). Symmetry can no longer be exploited[1], and we must return to analyzing the boundary value problem (1.6). Here, one could start by investigating the postitions of boundary extrema for the case of equal contact angles. It is conjectured that the maximum height on the inner and outer boundary will occur at the points M_1 and M_2 respectively, where the boundaries are closest and the fluid rise is likely greatest. Similary, the minimum heights are likely to occur at m_1 and m_2, where the boundaries are furthest apart.

Extension 6.0.4 (Elliptic Annulus) In this geometry, the inner and outer boundaries of the region are concentric ellipses (Fig. 6.2). Similar to Extension 6.0.3, the positions of boundary extrema can be considered. Here, symmetry requires there to

[1]Although a clever choice of coordinates may recover a form of symmetry.

exist two minimum and two maximum surface heights on each boundary. These extrema are conjectured to occur at the vertices, with the maxima M_1 and M_2 positioned at the thinnest portion of the domain and the minima m_1 and m_2 found at the widest section.

Appendix A

Additional Theorems

In the following theorems, the variables are defined as they were in the text; specifically, $0 < a < 1$, $0 \leq \gamma < \frac{\pi}{2}$ and $C(\gamma, m) = \frac{\sqrt{1-m^2\cos^2\gamma}-\sin\gamma}{\cos\gamma}$.

Theorem A.0.5 *For $a \leq r \leq 1$,*

$$\min\{r^2 - a^2, 1 - r^2\} \leq \frac{2(r^2 - a^2)(1 - r^2)}{1 - a^2}.$$

Proof. On $[a, 1]$, the functions $r^2 - a^2$ and $1 - r^2$ intersect once at $r = \sqrt{\frac{1+a^2}{2}}$. Consider the following two cases:

1. $\min\{r^2 - a^2, 1 - r^2\} = r^2 - a^2$. Here, $r \leq \sqrt{\frac{1+a^2}{2}}$ and thus

$$\begin{aligned} \frac{2(1 - r^2)}{1 - a^2} &\geq 1 && \text{(A.1)} \\ \implies \quad \frac{2(r^2 - a^2)(1 - r^2)}{1 - a^2} &\geq r^2 - a^2 && \text{(A.2)} \\ &= \min\{r^2 - a^2, 1 - r^2\} && \text{(A.3)} \end{aligned}$$

2. $\min\{r^2 - a^2, 1 - r^2\} = 1 - r^2$. Here, $r \geq \sqrt{\frac{1+a^2}{2}}$. Consequently,

$$\begin{aligned} \frac{2(r^2 - a^2)}{1 - a^2} &\geq 1 && \text{(A.4)} \\ \implies \quad \frac{2(r^2 - a^2)(1 - r^2)}{1 - a^2} &\geq 1 - r^2 && \text{(A.5)} \\ &= \min\{r^2 - a^2, 1 - r^2\} \quad \blacklozenge && \text{(A.6)} \end{aligned}$$

Theorem A.0.6 *For $a \leq r \leq 1$,*

$$\min\left\{1-\frac{a^2}{r^2}, 1-r^2\right\} \geq \left(1-\frac{a^2}{r^2}\right)(1-r^2).$$

Proof. This is straightforward when one considers that

$$0 \leq 1-\frac{a^2}{r^2} < 1 \quad \text{and} \quad 0 \leq 1-r^2 < 1, \quad \text{for } a \leq r \leq 1. \tag{A.7}$$

Hence, the product of both terms will never be greater than each term taken separately.

♦

Theorem A.0.7 *Let $f \in C^1[a,1]$ and suppose there exists a $c \in (a,1)$ such that $f(c) = 0$. Then*

$$|f(r)| \leq \int_a^1 |f'(s)|\, ds, \quad \textit{for } a \leq r \leq 1.$$

Proof. We may write

$$\begin{aligned} |f(r)| &= |f(r)-f(c)| && \text{(A.8)}\\ &= \left|\int_c^r f'(s)\, ds\right| && \text{(A.9)}\\ &\leq \int_c^r |f'(s)|\, ds && \text{(A.10)}\\ &\leq \int_a^1 |f'(s)|\, ds \quad ♦ && \text{(A.11)} \end{aligned}$$

Theorem A.0.8

$$1 < \int_a^1 \frac{r^2}{\sqrt{r^2-a^2}\sqrt{1-r^2}}\, dr < \frac{\pi}{2}$$

Proof. Introduce the change of variables $t = \sqrt{\frac{r^2-1}{a^2-1}}$ so that

$$\begin{aligned} \int_a^1 \frac{r^2}{\sqrt{r^2-a^2}\sqrt{1-r^2}}\, dr &= \int_0^1 \frac{\sqrt{1-(1-a^2)t^2}\,(1-a^2)t}{\sqrt{(1-a^2)(1-t^2)}\sqrt{(1-a^2)t^2}}\, dt && \text{(A.12)}\\ &= \int_0^1 \frac{\sqrt{1-(1-a^2)t^2}}{\sqrt{1-t^2}}\, dt && \text{(A.13)} \end{aligned}$$

(A.13) is the complete elliptic integral of the second kind with modulus $k = \sqrt{1-a^2}$. For $0 \leq t < 1$,

$$\sqrt{1-t^2} < \sqrt{1-(1-a^2)t^2} < 1 \tag{A.14}$$

$$\Longrightarrow \quad 1 < \frac{\sqrt{1-(1-a^2)t^2}}{\sqrt{1-t^2}} < \frac{1}{\sqrt{1-t^2}} \tag{A.15}$$

Integrating (A.15) from 0 to 1 and using (A.13) gives

$$1 < \int_a^1 \frac{r^2}{\sqrt{r^2-a^2}\sqrt{1-r^2}}\, dr < \frac{\pi}{2}. \quad \blacklozenge \tag{A.16}$$

Theorem A.0.9 *The condition on B in Theorem 3.2.1,*

$$B < \frac{2a(1-a^2)\cos\gamma}{2(1+a)(1-a)^2\, C(\gamma,m) + a\pi\cos\gamma},$$

implies that

$$B < \frac{2(1-a^2)}{\pi}.$$

Proof. Since $2(1+a)(1-a)^2\, C(\gamma,m) > 0$, clearly

$$\frac{a\pi\cos\gamma}{2(1+a)(1-a)^2\, C(\gamma,m) + a\pi\cos\gamma} < 1. \tag{A.17}$$

Multiplying both sides by $\frac{2(1-a^2)}{\pi}$ produces the desired result. $\blacklozenge$

Theorem A.0.10 *The condition on B in Theorem 3.2.1,*

$$B < \frac{2a(1-a^2)\cos\gamma}{2(1+a)(1-a)^2\, C(\gamma,m) + a\pi\cos\gamma},$$

implies that

$$B < \frac{2}{(1-a)\left(\frac{1}{3}\sqrt{1-a^2} + a\log\left(1+\sqrt{1-a^2}\right) - a\log a\right)}$$

which simlutaneously satisfies the hypothesis of Theorem 3.1.1 (5).

Proof. From above, we have

$$B < \frac{2a(1-a^2)\cos\gamma}{2(1+a)(1-a)^2\, C(\gamma,m) + a\pi\cos\gamma} < \frac{2(1-a^2)}{\pi} < 1 \tag{A.18}$$

For $0 < a < 1$, use the following bounds:

$$\frac{1}{3}\sqrt{1-a^2} < \frac{1}{3}\,; \quad a\log\left(1+\sqrt{1-a^2}\right) < \log 2 < 1\,; \quad a\log a \geq -\frac{1}{e} > -\frac{1}{2} \tag{A.19}$$

to arrive at

$$\frac{2}{(1-a)\left(\frac{1}{3}\sqrt{1-a^2}+a\log\left(1+\sqrt{1-a^2}\right)-a\log a\right)} > \frac{12}{11} > B \tag{A.20}$$

as required by Theorem 3.1.1 (5). ♦

Theorem A.0.11 *The condition on B in Theorem 4.1.1,*

$$B \leq \frac{2(1-a^2)\cos\gamma}{\pi}\left(\frac{1-a}{12(1+a)} - (\sqrt{a}-a)\right),$$

implies that

$$B < \frac{2}{(1-a)\left(\frac{1}{3}\sqrt{1-a^2}+a\log\left(1+\sqrt{1-a^2}\right)-a\log a\right)}$$

which simlutaneously satisfies the requirement of Theorem 3.1.1 (5).

Proof. This bound can be written as

$$B \leq \left(\frac{2}{\pi}\right)(1-a^2)(\cos\gamma)\left(\frac{1-a}{12(1+a)} - (\sqrt{a}-a)\right). \tag{A.21}$$

The first three terms are clearly less than 1. For the fourth:

$$\frac{1-a}{12(1+a)} < 1 \tag{A.22}$$

$$\implies \quad \frac{1-a}{12(1+a)} - (\sqrt{a}-a) < 1, \quad \text{for } 0 < a < 1 \tag{A.23}$$

Thus, $B < 1$ and we can arrive at the same result as (A.20). ♦

Theorem A.0.12 *The condition on B in Theorem 4.2.1,*

$$B \leq \frac{\cos\gamma(1-a)^2}{6\pi}\left(5a - \frac{3-2a}{\sin\gamma}\right),$$

implies that

$$B < \frac{2}{(1-a)\left(\frac{1}{3}\sqrt{1-a^2}+a\log\left(1+\sqrt{1-a^2}\right)-a\log a\right)}$$

which simlutaneously satisfies the requirement of Theorem 3.1.1 (5).

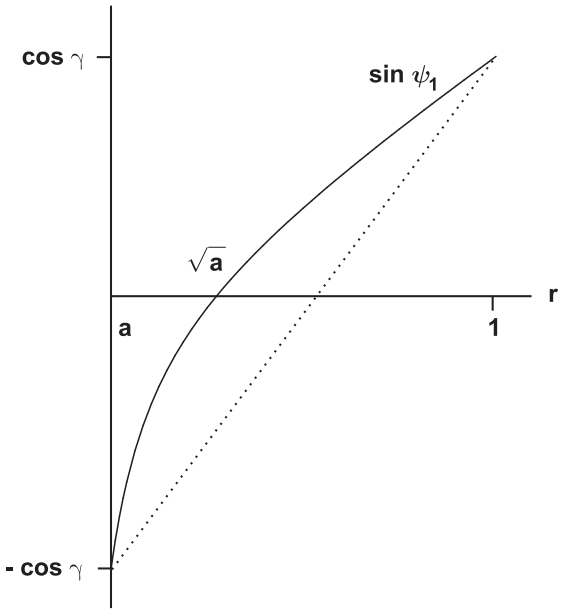

Figure A.1: Lower bound (dotted line) of $\sin\psi_1$.

Proof. We rewrite the bound as

$$(\cos\gamma)(1-a)^2\left(\frac{5a}{6\pi}-\frac{3-2a}{6\pi\sin\gamma}\right) \tag{A.24}$$

The first two terms are less than 1. In the third term:

$$\frac{5a}{6\pi} < 1 \tag{A.25}$$

$$\Longrightarrow \quad \frac{5a}{6\pi}-\frac{3-2a}{6\pi\sin\gamma} < 1 \tag{A.26}$$

Again, $B<1$ and (A.20) follows. ♦

Theorem A.0.13 *Consider the sequence of iterates $\{u_n\}$ generated by (3.25) and (3.26). For the iterate u_1, we have $u_1(a) < u_1(1)$.*

Proof. Recall that the inclination angle of u_1 is given by

$$\sin\psi_1 = \frac{\cos\gamma}{1-a}\left(r-\frac{a}{r}\right). \tag{A.27}$$

Since $\sin\psi_1$ is concave, it can be bounded from below by the linear function that connects its endpoints (see Fig. A.1):

$$\sin\psi_1 > \frac{\cos\gamma}{1-a}(2r-1-a), \quad \text{for } r \in (a,1). \tag{A.28}$$

This can be used to claim

$$\begin{aligned} u_1(1)-u_1(a) &= \int_a^1 \frac{\sin\psi_1}{\sqrt{1-\sin^2\psi_1}}\,ds && \text{(A.29)}\\ &> \int_a^1 \frac{2s-1-a}{\sqrt{\frac{(1-a)^2}{\cos^2\gamma}-(2s-1-a)^2}}\,ds && \text{(A.30)}\\ &= 0 \quad \blacklozenge && \text{(A.31)} \end{aligned}$$

Bibliography

[1] Andrew Browder. *Mathematical Analysis: An Introduction.* Springer–Verlag, New York, 1996.

[2] Kenneth R. Davidson and Allan P. Donsig. *Real Analysis with Real Applications.* Prentice Hall, Upper Saddle River, NJ, 2002.

[3] Elise De Doncker and R. Piessens. Automatic computation of integrals with singular integrand, over a finite or infinite range. *Computing.* **17** (1976), 265–279.

[4] Alan Elcrat, Tae-Eun Kim, and Ray Treinen. Annular capillary surfaces. *Arch. Math.* **82** (2004), 449–467.

[5] Robert Finn. Capillary surface interfaces. *Notices of the AMS.* **46** (1999), 770–781.

[6] Robert Finn. The contact angle in capillarity. *Phys. Fluids.* **18** (2006), 047102.

[7] Robert Finn. On the equations of capillarity. *J. Math. Fluid Mech.* **3** (2001), 139–151.

[8] Robert Finn. *Equilibrium Capillary Surfaces.* Springer-Verlag, New York, 1986.

[9] Robert Finn and Paul Concus. On capillary free surfaces in the absence of gravity. *Acta Math.* **132** (1974), 177–198.

[10] Masao Iri, Sigeiti Moriguti, and Yoshimitsu Takasawa. On a certain quadrature formula. *J. Compt. Appl. Math.* **17** (1987), 3–20.

[11] P.S. Laplace. *Celestial Mechanics, Supplements to Book X (1805/1806),* annotated English translation by N. Bowditch (1839), reprinted by Chelsea, New York, 1966.

[12] James Serrin. A symmetry problem in potential theory. *Arch. Ration. Mech.* **43** (1971), 304–318.

[13] David Siegel. Approximating symmetric capillary surfaces. *Pacific J. Math.* **224** (2006), 355–365.

[14] David Siegel. Explicit estimates of a symmetric capillary surface for small bond number. *Continuum Mechanics and its Applications,* ed. G.A.C. Graham and S.K. Malik, 497–506, Hemisphere, New York, 1989.